INERTIAL ACOUSTIC CLOAKS MADE FROM THREE ACOUSTIC FLUIDS.

BY ADAM JULIUS NAGY

A thesis submitted to the

Graduate School—New Brunswick

Rutgers, The State University of New Jersey

in partial fulfillment of the requirements

for the degree of

Master of Science

Graduate Program in Mechanical and Aerospace Engineering

Written under the direction of

Dr. Andrew N. Norris

and approved by

____

____

____

New Brunswick, New Jersey

MAY, 2011

ABSTRACT OF THE THESIS

Inertial acoustic cloaks made from three acoustic fluids.

by Adam Julius Nagy

Thesis Director: Dr. Andrew N. Norris

This thesis provides an extensive review of acoustic wave theory in one, two (polar), and three (spherical) dimensions concluding with a study of passive, non-directional cloaking. The optical theorem is derived by use of energy conservation, yielding the cross sectional scattering in two and three dimensions. A new method, the Matricant Propagator, is developed for solving the scattered pressure field in wave-object interactions. Solutions found from the Matricant Propagator method are compared with known solutions using the Global Matrix method. A review of acoustic cloaking literature is given, including numerical comparison with previously proposed cloaking models. Lastly an acoustic cloak of the inertial type, made from compressible, inviscid fluids, is proposed by layering concentric shells of only three distinct fluids. The effectiveness of the device depends upon the relative densities and compressibilities of the three fluids. Optimal results are obtained if one fluid has density equal to the background fluid, while the other two densities are much greater and much less than the background. Numerical examples display a significant reduction in scattering and were compared using multiple solution methods. It is found that use of only two unique fluids is too restrictive for cloaking, however, interesting characteristics are found where energy may be diverted such that a reduction in backscatter occurs.

Keywords: **acoustic, cloaking, passive, Matricant Propagator, metafluid, metamaterial**

Acknowledgements

I am sincerely indebted to my advisor, Professor Andrew Norris for his guidance, expertise and extraordinary patience. He is an excellent mentor and has made my experience in the graduate program tremendously rewarding. And to my family, who have always supported my endeavors. Lastly this work was completed with support from the National Science Foundation.

Dedication

Special dedication to my parents

Table of Contents

List of Tables

List of Figures

Chapter 1

Introduction

This thesis covers an extensive review of acoustics based in the realm of normal, inviscid, acoustic fluids. Solutions to the wave equation in one, two and three dimensions are summarized. Scattering solution techniques such as the Global Matrix and Matricant Propagator methods are developed and utilized. Lastly, the scattering cross-section, which identifies the amount of energy scattered occurring from object-wave interaction is discussed.

The review of acoustic wave theory forms the basis for a study of passive, non-directional acoustic cloaking. Here an acoustic cloak directs wave energy around an object such that waves incident from any direction may pass around the object through the cloaking medium. This will have the effect of hiding the object such that the effective cross-sectional scattering will ideally be zero. A region of space is thus transformed, acoustically, to a single point such that the scattering strength vanishes causing the region to become seemingly uniform. For instance if a submerged vessel underwater were to be hidden from sonar a cloak could be used to transform the region the vessel occupies to behave just as the surrounding medium. Instead of waves reverberating off the hull of the vessel they are sent around and propagate away as if the vessel were not present.

In this thesis we will only consider cloaks derived from anisotropic inertial properties defined as inertial cloaks. Simply layering different fluids defined by a unique transformation rule can create the needed anisotropicity. Further investigation reveals only three unique fluids are required for cloaking. A layering of only two unique fluids carries interesting characteristics where energy may be diverted such that a reduction in backscatter occurs.

1.1 Motivation and Literature Review

Acoustic cloaking structures have applications to a broad spectrum of fields including national defense as well as civil engineering. A cloak could be used to hide underwater vessels from sonar, create better isolated environments for laboratories, help in vibration control in blasting environments, create advanced concussion protection helmets for troops, dramatically improve seismic mitigation, and a plethora of other broader impacts that would benefit society.

Recent developments in electromagnetic cloaking have given new life in the study of acoustic cloaking. Studies in electromagnetism have found that strong anisotropic electromagnetic (EM) parameters are required for EM cloaking, [1, 2]. This class of material is referred to as a metamaterial as they do not occur in nature and must be man-made. Further studies in EM metamaterials have shown unprecedented control of wave propagation for devices such as: concentrators [3], beam splitters [4], and of course cloaks [5, 6]. These devices are created through the technique of transformation optics which is done by applying a form-invariant coordinate transform to the EM equations, deforming space in a specified manner [4]. Similarly, transformation acoustics applies a form-invariant coordinate transform to the Helmholtz equation. Work done by Cummer and Schurig [5], proposed that an acoustic material with strong mass anisotropy was needed to construct a cloaking medium. Milton et al. [7] conceptually described how spring-loaded masses could create the needed mass anisotropy, building on the work of Willis [8] who demonstrated that, for a composite material in which density varied, the effective density operator took the form of a second-order tensor. Material parameters for a two dimensional acoustic cloak were proposed by Cummer and Schurig [5] for a given transformation, however Norris [9] has shown the effective material properties of an acoustic cloak are not uniquely defined and have special relations to the transformation mapping. This finding has opened a vast range of materials for realizing acoustic cloaks. The acoustic cloak corresponds to the limiting case of a point transformed into a finite region, and it has unavoidable physical singularities associated with the extreme nature of the transformation. Different types of singularities are obtained depending on whether the transformed metamaterial is purely inertial with anisotropic density and a scalar bulk modulus, or in the other limit, purely pentamodal with isotropic inertia. The distinction is important for cloaking, for which it is known that use of only fluids with anisotropic inertia (inertial cloaks) requires infinite mass, and is therefore not a realistic path towards acoustic cloaking [9]. Despite this severe limitation, it is possible to achieve almost perfect, or near-cloaking, using layers of anisotropic fluids that approximate the transformed medium, without the singularity. Examples of this type of layering have been proposed [10, 11].

1.2 Outline of the Thesis

The thesis outline is as follows. The theory of acoustics is introduced in Chapter 2, where solutions to the wave equation are developed in one, two (polar), and three (spherical) dimensions. A further study of one dimensional acoustics is done in Chapter 3, where examples of boundaries separating semi-infinite mediums is given. We also begin developing the Matricant Propagator method. In Chapter 4, we explore anisotropic properties of cylindrically layered media, continue development of the Matricant Propagator in cylindrical coordinates and compare with the Global Matrix method. In Chapter 5 solution techniques are developed in three dimensional spherical coordinates. We begin acoustic cloaking review in Chapter 6 and numerically compare results of Torrent and Sánchez-Dehesa [10]. Chapter 7 reviews the work developed alongside this thesis in Norris and Nagy [12], where a cloaking structure comprised of only three unique fluids is developed. Finally, Chapter 8 provides a short summary of the main results of the thesis.

Chapter 2

The Acoustic Wave Equation

First we start with an examination of the wave equation.

$$\left(\nabla^2 - \frac{1}{c^2}\frac{\partial^2}{\partial t^2}\right)u(\boldsymbol{x}, t) = 0. \tag{2.1}$$

Here, ∇^2 is the Laplacian and c is the speed of wave propagation in a given medium. The method of separating variables will be employed to consider a solution consisting of a transient and steady part, starting in one dimension and working to three dimensional, spherical coordinates. As a reference on the wave equation and the separation of variables technique, Jin [13], was used for which electromagnetic fields were the interest of study.

2.1 One dimension

Starting with a one-dimensional analysis, where $u(\boldsymbol{x}, t) = u(x, t)$, we employ separation of variables such that $u(x, t) = P(x)T(t)$ and substitute into Equation (2.1) attaining

$$c^2\frac{P''(x)}{P(x)} = \frac{T''(t)}{T(t)} = \text{const.} = -\omega^2. \tag{2.2}$$

Here, ω is the angular frequency and, for an acoustic wave, P is the acoustic pressure describing local deviation from ambient. The time harmonic general solution of $T(t)$ is then $Ce^{\pm i\omega t}$, for which i is the imaginary unit, $T(t) = e^{-i\omega t}$ is taken here. This means $P(x)$ must satisfy the Helmholtz equation, namely

$$P'' + \frac{\omega^2}{c^2}P = 0. \tag{2.3}$$

The general solution for $P(x)$ is then given by $P(x) = Ae^{\pm ikx}$ for which the exponent is negative for waves traveling to the left and positive for waves traveling to the right. A is the amplitude of these waves and k is the wavenumber given by $k = \frac{\omega}{c}$.

2.2 Two dimensions, polar coordinates

In two dimensional, polar coordinates, the wave equation becomes

$$(\nabla^2 - \frac{1}{c^2}\frac{\partial^2}{\partial t^2})u(r,\theta,t) = 0. \tag{2.4}$$

Employing separation of variables, $u(r,\theta,t) = P(r)\Theta(\theta)T(t)$. This will have the same time harmonic solution for $T(t)$ and $\Theta(\theta)$ must satisfy

$$\frac{\Theta(\theta)''}{\Theta(\theta)} = \text{const.} = -n^2. \tag{2.5}$$

$\Theta(\theta)$ must be periodic such that $\Theta(\theta + 2\pi n) = \Theta(\theta)$ for n being an integer ($n = 0, 1, 2, \ldots$). A solution taken here will be $\Theta(\theta) = \sum_{n=-\infty}^{\infty} e^{in\theta}$. Now $P(r)$ must then satisfy a second order, homogeneous equation given by

$$\frac{\mathrm{d}^2 P_n}{\mathrm{d}r^2} + \frac{1}{r}\frac{\mathrm{d}P_n}{\mathrm{d}r} + (k^2 - \frac{n^2}{r^2})P_n = 0. \tag{2.6}$$

The subscript n denotes that this must hold for all values of n. The solution for P_n is found by realizing that (2.6) is Bessel's differential equation, for which the general solution for P_n can be expressed by Bessel functions of the first, J_n, second, Y_n and third, $H_n^{(1)}$, $H_n^{(2)}$ kind, with

$$P_n = \begin{cases} C_1 J_n(kr) + C_2 Y_n(kr) \\ C_3 H_n^{(1)}(kr) + C_4 H_n^{(2)}(kr) \end{cases}. \tag{2.7}$$

The method of Frobenius may be used to solve Bessel's differential equation, (2.6), as done in Greenberg [14]. Abramowitz and Stegun, [15], will be referenced in the following sections for relations regarding Bessel functions. Conservation of momentum is used to find the acoustic velocity, V, assuming constant frequency. The linearized momentum equation is written as

$$\rho\frac{\partial V}{\partial t} = -\nabla P \quad \rightarrow \quad i\omega\rho V = \nabla P. \tag{2.8}$$

We can see that the acoustic velocity is proportional to the pressure gradient as seen in Equation (2.8), for which ρ is the density. The acoustic velocity in polar coordinates for V_r and V_θ is given by

$$V_r = \frac{1}{i\omega\rho}\frac{\partial P}{\partial r}, \tag{2.9a}$$

$$V_\theta = \frac{1}{ri\omega\rho}\frac{\partial P}{\partial \theta} \rightarrow \frac{inP}{ri\omega\rho} \text{ (for mode n).} \tag{2.9b}$$

The velocity will come in handy when solving acoustic problems where solutions must satisfy continuous pressure and velocity boundary conditions.

2.3 Three dimensions, spherical coordinates

Finally the wave equation in 3D spherical coordinates is solved. We start with the three dimensional wave equation

$$(\nabla^2 - \frac{1}{c^2}\frac{\partial^2}{\partial t^2})P(x,y,z,t) = 0. \tag{2.10}$$

We next change Cartesian coordinates to spherical such that P can be expressed as $P = P(r,\theta,\phi,t)$, where $r = \sqrt{x^2+y^2+z^2}$, $\theta = \cos^{-1}\big(\frac{z}{\sqrt{x^2+y^2+z^2}}\big)$ and $\phi = \tan^{-1}\big(\frac{y}{x}\big)$. Applying these transformations to Equation (2.10), and simplifying as much as possible, the wave equation in spherical coordinates is

$$\frac{1}{c^2}\frac{\partial^2 P}{\partial t^2} = \frac{1}{r^2}\frac{\partial}{\partial r}\big(r^2\frac{\partial P}{\partial r}\big) + \frac{1}{r^2\sin(\theta)}\frac{\partial}{\partial\theta}\big[\sin(\theta)\frac{\partial P}{\partial\theta}\big] + \frac{1}{r^2\sin^2(\theta)}\frac{\partial^2 P}{\partial\phi^2}. \tag{2.11}$$

Applying separation of variables and continuing as before, the above equation may be solved for P. Let $P(r,\theta,\phi,t) = R(r)\Theta(\theta)\Phi(\phi)T(t)$. Substitution of this expression into Equation 2.11 and dividing the result by $R(r)\Theta(\theta)\Phi(\phi)T(t)$ yields

$$\frac{1}{c^2}\frac{T''}{T} = \frac{1}{r^2 R}(r^2R')' + \frac{1}{r^2\sin(\theta)}\frac{1}{\Theta}[\sin(\theta)\Theta']' + \frac{1}{r^2\sin^2(\theta)}\frac{\Phi''}{\Phi}. \tag{2.12}$$

The RHS, (right hand side), of Equation (2.12) is independent of t which makes the LHS constant. As before, we call this constant $-k^2$ where $k = \frac{\omega}{c}$, such that

$$T'' + c^2k^2T = 0. \tag{2.13}$$

The solution for T is the same as before, where $T(t) = e^{\pm i\omega t}$. Making the RHS of Equation (2.12) equal to $-k^2$ and multiplying by $r^2\sin^2(\theta)$, gives with some rearranging,

$$\frac{\Phi''}{\Phi} = -k^2r^2\sin^2(\theta) - \frac{\sin^2(\theta)}{R}(r^2R')' - \frac{\sin(\theta)}{\Theta}[\sin(\theta)\Theta']'. \tag{2.14}$$

This maneuver separated ϕ dependence from r and θ so that the LHS of Equation (2.14) can be set equal to a constant. We shall call it $-m^2$ so that Φ must satisfy

$$\Phi^{''} + m^2\Phi = 0. \tag{2.15}$$

Equation (2.15) is once again the harmonic oscillator equation, with solutions $\Phi^{\pm}(\phi) = \Phi_0 e^{\pm im\phi}$. Because continuous solutions are required as a function of ϕ, m must be restricted to integer values. $(m = 0, \pm1, \pm2, \ldots)$. If the RHS of Equation (2.14) is equal to $-m^2$ and we divide by $\sin^2(\theta)$ we have

$$\frac{1}{\sin(\theta)\Theta}[\sin(\theta)\Theta^{'}]^{'} - \frac{m^2}{\sin^2(\theta)} = -\frac{1}{R}(r^2R^{'})^{'} - k^2r^2. \tag{2.16}$$

The above equation separated θ and r dependencies. Again each side of this equation is constant and, by convention, is equal to $-l(l+1)$. The resulting differential equation for $\Theta(\theta)$ is then

$$\frac{1}{\sin(\theta)}[\sin(\theta)\Theta^{'}]^{'} + \left[l(l+1) - \frac{m^2}{\sin^2(\theta)}\right]\Theta = 0. \tag{2.17}$$

Through the change of variables $s(\theta) = \cos(\theta)$, we can think of Θ as a function of θ through the variable s with $\Theta = \Theta[s(\theta)]$ and write the derivatives of Θ as

$$\begin{aligned}
\frac{\partial\Theta}{\partial\theta} &= \frac{\partial\Theta}{\partial s}\frac{\partial s}{\partial\theta} = \frac{\partial\Theta}{\partial s}[-\sin(\theta)] = \frac{\partial\Theta}{\partial s}[-\sqrt{1-s^2}],\\
\frac{\partial^2\Theta}{\partial\theta^2} &= \frac{\partial}{\partial\theta}\left(\frac{\partial\Theta}{\partial s}\frac{\partial s}{\partial\theta}\right) = \frac{\partial^2\Theta}{\partial s^2}(1-s^2) + \frac{\partial\Theta}{\partial s}[-s].
\end{aligned}$$

Substituting the above into Equation (2.17) yields the associated Legendre equation

$$(1-s^2)\Theta^{''}(s) - 2s\Theta^{'}(s) + \left[l(l+1) - \frac{m^2}{1-s^2}\right]\Theta(s) = 0. \tag{2.18}$$

The solutions are the Legendre functions of the first and second kind denoted by $P_l^m(s)$ and $Q_l^m(s)$. However solutions associated with $Q_l^m(s)$ are not desired since these solutions diverge as $s \to \pm1$. For the $P_l^m(s)$ solutions to remain finite, l must be an integer and m must satisfy $|m| \leq 1$. For $m = 0$ (azimuthal symmetry) the solutions $P_l^0(s) \equiv P_l(s)$, these are known as the Legendre polynomials in s of order 1. Equating the RHS of Equation (2.16) to $-l(l+1)$ we attain

$$s^2R^{''}(s) + 2sR^{'}(s) + [s^2 - l(l+1)]R(s) = 0. \tag{2.19}$$

Solutions of Equation (2.19) are known as spherical Bessel functions of the first and second kind, $j_l(s)$ and $y_l(s)$, where $s = kr$. The function R is then given by

$$R_{kl}(r) = G_{kl}\ j_l(kr) + H_{kl}\ y_l(kr), \tag{2.20}$$

where indices k and l of G_{kl} and H_{kl} signify the unknown coefficients for integer l and the wave number dependency k. The final solution for $P(r, \theta, \phi, t)$ is then

$$\begin{aligned} P_{klm}(r, \theta, \phi, t) =& [G_{kl} j_l(kr) + H_{kl} y_l(kr)] \left[E_{lm} P_l^m(\cos(\theta)) + F_{lm} Q_l^m(\cos(\theta))\right] \\ & \times\ \left(C_m e^{im\phi} + D_m e^{-im\phi}\right)\left(A_k e^{ikct} + B_k e^{-ikct}\right). \end{aligned} \tag{2.21}$$

2.4 General summary

The wave equation was solved for 1D, 2D (polar) and 3D (spherical) geometries through the technique of separation of variables. This review was, in part, extensive. However, transient, unsteady, solutions such as d'Alembert's were left out. Now that solutions for the wave equation have been discussed, it is convenient to end with a discussion on how material properties might affect wave propagation through a given medium. The relationship between material properties and the sound velocity at which compressional / longitudinal waves propagate in a solid isotropic medium is given by Kinsler, [16], as

$$c = \sqrt{\frac{E(1-\nu)}{\rho(1+\nu)(1-2\nu)}} = \sqrt{\frac{K + \frac{4}{3}G}{\rho}}. \tag{2.22}$$

Here K is the bulk modulus, G is the shear modulus, E is Young's modulus, and ν is Poisson's ratio. Similarly, the shear velocity, c_S, is given by $c_S = \sqrt{\frac{G}{\rho}}$ [16]. These parameters may be found by solving the equation of motion, $\sigma_{ji,j} + F_i = \rho\frac{\partial^2 u_i}{\partial t^2}$, for a semi-infinite elastic slab where, in one case, a simple longitudinal/compressional wave is propagated through one end and in another case where a shear wave is propagated. For a fluid, the compressional wave speed is given by $c = \sqrt{\frac{K}{\rho}}$. It is easy to compare this with Equation (2.22), where G has dropped out. This occurs as a Newtonian fluid does not sustain shear forces. The next chapter will focus on the one-dimensional wave and the reflectance and transmission of such waves through boundaries separating different media.

Chapter 3

One Dimensional Semi-infinite Medium Examples

This section will consider a sequence of problems illustrating the basic concepts of one-dimensional wave propagation. In particular, we consider the amounts of reflection and transmission that occur due to a wave traveling through different media.

3.1 Simple one boundary

We start with the simplest 1-D case in which an incident wave of magnitude A_1 interacts with a boundary separating two media with different density and speed of sound. From Figure 3.1, it is seen that the reflected wave will have magnitude A_2 and the transmitted wave will have magnitude B_1. Notice that e^{ikx} refers to a wave traveling in the positive x direction while e^{-ikx} refers to a wave traveling in the negative x direction as per our definition of $T(t) = e^{-i\omega t}$. The pressure $P(x)$ and velocity $V(x)$ are given by

$$P(x) = \begin{cases} A_1 e^{ikx} + A_2 e^{-ikx}, & x < 0, \\ B_1 e^{ik_1 x}, & x > 0, \end{cases} \tag{3.1}$$

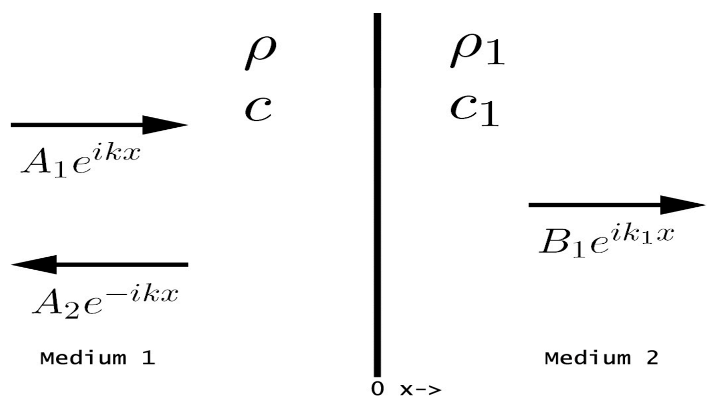

Figure 3.1: Simple one boundary diagram.

$$V(x) = \begin{cases} \frac{1}{Z}(A_1 e^{ikx} - A_2 e^{-ikx}), & x < 0, \\ \\ \frac{1}{Z_1} B_1 e^{ik_1 x}, & x > 0. \end{cases} \tag{3.2}$$

In the above equation Z is the acoustic impedance, defined as $Z = \rho c$ and $Z_1 = \rho_1 c_1$. Boundary conditions for acoustic problems require continuity of pressure and velocity and are as follows; $P(0^+) = P(0^-)$ and $V(0^+) = V(0^-)$. These conditions allow for the coefficients A_2 and B_1 to be solved in terms of the incident wave magnitude, A_1, where

$$A_2 = A_1 \frac{Z_1 - Z}{Z + Z_1}, \qquad B_1 = A_1 \frac{2Z_1}{Z + Z_1}. \tag{3.3}$$

The reflection coefficient, R, expresses the fractional amount of the incident wave that is reflected. Likewise the transmission coefficient, T, expresses the fractional amount of the incident wave that is transmitted. For this example, R and T are given by

$$R = \frac{Z_1 - Z}{Z + Z_1}, \qquad T = \frac{2Z_1}{Z + Z_1}. \tag{3.4}$$

3.2 Two boundaries: a slab

The next case we consider is that of an incident wave interacting with a slab of thickness $2h$ with acoustic properties ρ_1 and c_1. This problem will be solved using three different methods:

- Straight Forward Method : applying the interface conditions
- Symmetry / Antisymmetry : using the underlying symmetry of the problem
- Matricant (Propagator) : ODE solution.

3.2.1 A straight forward method

An incident wave of magnitude A_1 interacts with the slab as shown in Figure 3.2. The reflected wave has magnitude of A_2. The part of the incident wave that transmits through the boundary $x = -h$ will have magnitude C_1 and then at $x = h$ a reflected wave of magnitude C_2 and a transmission wave of magnitude B_1 will result. The

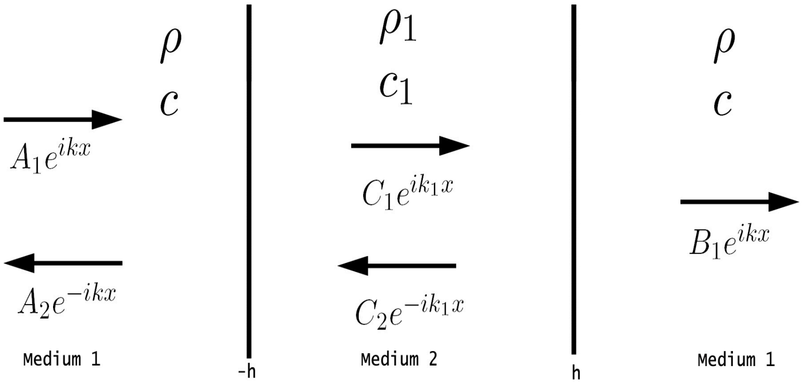

Figure 3.2: Configuration for slab wave interaction.

pressure and velocity are given by

$$P(x) = \begin{cases} A_1e^{ikx} + A_2e^{-ikx}, & x < -h, \\ C_1e^{ik_1x} + C_2e^{-ik_1x}, & -h < x < h, \\ B_1e^{ikx}, & x > h, \end{cases} \tag{3.5a}$$

$$V(x) = \begin{cases} \frac{1}{Z}(A_1e^{ikx} - A_2e^{-ikx}), & x < -h, \\ \frac{1}{Z_1}(C_1e^{ik_1x} - C_2e^{-ik_1x}), & -h < x < h, \\ \frac{1}{Z}B_1e^{ikx}, & x > h. \end{cases} \tag{3.5b}$$

Once again, the same boundary conditions are applied: $P(h^+) = P(h^-)$, $P(-h^+) = P(-h^-)$, $V(h^+) = V(h^-)$, $V(-h^+) = V(-h^-)$, which results in a system of equations to be solved with,

$$\begin{aligned} A_1e^{-ikh} + A_2e^{ikh} &= C_1e^{-ik_1h} + C_2e^{ik_1h}, \\ A_1e^{-ikh} - A_2e^{ikh} &= \frac{Z}{Z_1}(C_1e^{-ik_1h} - C_2e^{ik_1h}), \\ C_1e^{ik_1h} + C_2e^{-ik_1h} &= B_1e^{ikh}, \\ C_1e^{ik_1h} - C_2e^{-ik_1h} &= \frac{Z_1}{Z}B_1e^{ikh}. \end{aligned} \tag{3.6}$$

Answers to coefficients A_2 , C_1 , C_2 and B_1 in terms of A_1, are

$$\begin{aligned} A_2 &= -A_1 \frac{e^{-2ihk}(-1+e^{4ihk_1})(Z-Z_1)(Z+Z_1)}{e^{4ihk_1}(Z-Z_1)^2-(Z+Z_1)^2}, \\ C_1 &= -2A_1 \frac{e^{-ih(k-k_1)}Z_1(Z+Z_1)}{e^{4ihk_1}(Z-Z_1)^2-(Z+Z_1)^2}, \\ C_2 &= 2A_1 \frac{e^{-ih(k-3k_1)}Z_1(Z_1-Z)}{e^{4ihk_1}(Z-Z_1)^2-(Z+Z_1)^2}, \\ B_1 &= -4A_1 \frac{e^{-2ih(k-k_1)}ZZ_1}{e^{4ihk_1}(Z-Z_1)^2-(Z+Z_1)^2}. \end{aligned} \tag{3.7}$$

Finally the reflection and transmission coefficients can be found by using Figure 3.2 for which $R = A_2/A_1$ and $T = B_1/A_1$, yielding

$$\begin{aligned} R &= -\frac{e^{-2ihk}(-1+e^{4ihk_1})(Z-Z_1)(Z+Z_1)}{e^{4ihk_1}(Z-Z_1)^2-(Z+Z_1)^2}, \\ T &= -4\frac{e^{-2ih(k-k_1)}ZZ_1}{e^{4ihk_1}(Z-Z_1)^2-(Z+Z_1)^2}. \end{aligned} \tag{3.8}$$

3.2.2 Symmetry / Antisymmetry

Consider the two cases of symmetry and antisymmetry for which $P_S(x) = P_S(-x)$ and $P_A(x) = -P_A(-x)$, respectively. By employing these conditions on $P(x)$ from the previous example, $P_S(x)$ and $P_A(x)$ are defined by

$$P_S(x) = \begin{cases} A_1e^{ikx} + A_{2S}e^{-ikx}, & x < -h, \\ C_{1S}\cos k_1x, & -h < x < h, \\ A_1e^{-ikx} + A_{2S}e^{ikx}, & x > h, \end{cases} \tag{3.9a}$$

$$P_A(x) = \begin{cases} A_1e^{ikx} + A_{2A}e^{-ikx}, & x < -h, \\ C_{1A}\sin k_1x, & -h < x < h, \\ -A_1e^{-ikx} - A_{2A}e^{ikx}, & x > h. \end{cases} \tag{3.9b}$$

Now, when the two situations of symmetry and antisymmetry are put together, the same example is attained as seen in Figure 3.3, where

$$P(x) = \begin{cases} 2A_1e^{ikx} + A_{2S}e^{-ikx} + A_{2A}e^{-ikx}, & x < -h, \\ C_{1S}\cos k_1x + C_{1A}\sin k_1x, & -h < x < h, \\ A_{2S}e^{ikx} - A_{2A}e^{ikx}, & x > h. \end{cases} \tag{3.10}$$

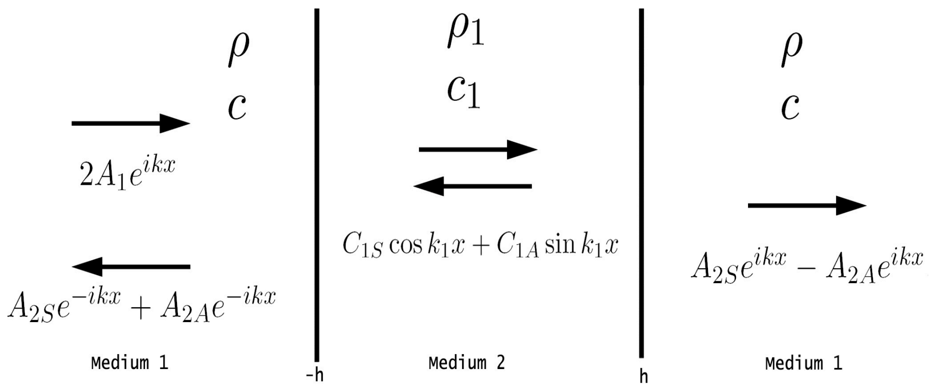

Figure 3.3: Configuration for symmetry/anti-symmetry conditions for slab wave interaction.

The system can be solved separately in terms of the symmetric and antisymmetric situations using continuity of pressure and velocity. The resulting system of equations to be solved is

$$\begin{aligned} A_1e^{ikh} + A_{2S}e^{-ikh} &= C_{1S}\cos k_1h, \\ \frac{1}{Z}(A_1e^{ikh} - A_{2S}e^{-ikh}) &= \frac{-C_{1S}}{iZ_1}\sin k_1h, \\ A_1e^{ikh} + A_{2A}e^{-ikh} &= C_{1A}\sin k_1h, \\ \frac{1}{Z}(A_1e^{ikh} - A_{2A}e^{-ikh}) &= \frac{C_{1A}}{iZ_1}\cos k_1h. \end{aligned} \tag{3.11}$$

The answers for the coefficients in terms of the incident wave magnitude, A_1 are

$$\begin{aligned} A_{2A} &= A_1e^{2ikh}[\tfrac{2\sin k_1h}{\frac{Z}{iZ_1}\cos k_1h+\sin k_1h} - 1], & C_{1A} &= \tfrac{2A_1e^{2ikh}}{\frac{Z}{iZ_1}\cos k_1h+\sin k_1h}, \\ A_{2S} &= A_1e^{2ikh}[\tfrac{2\cos k_1h}{\cos k_1h-\frac{Z}{iZ_1}\sin k_1h} - 1], & C_{1S} &= \tfrac{2A_1e^{2ikh}}{\cos k_1h-\frac{Z}{iZ_1}\sin k_1h}. \end{aligned}$$

Similarly A_{2A} and A_{2S} could have been found by applying impedance matching at one boundary such that $\frac{P(h^+)}{V(h^+)} = \frac{P(h^-)}{V(h^-)}$ since both pressure and velocity are continuous. However, C_{1A} and C_{1S} would not be found using impedance matching. From Figure 3.3, the reflection coefficient, R, will be $\frac{A_{2A}+A_{2S}}{2A_1}$ and the transmission coefficient, T, will be $\frac{A_{2S}-A_{2A}}{2A_1}$, yielding

$$R = e^{2ikh}[\frac{\sin k_1h}{\frac{Z}{iZ_1}\cos k_1h + \sin k_1h} + \frac{\cos k_1h}{\cos k_1h - \frac{Z}{iZ_1}\sin k_1h} - 1], \tag{3.12a}$$

$$T = e^{2ikh}[\frac{\sin k_1h}{\frac{Z}{iZ_1}\cos k_1h - \sin k_1h} + \frac{\cos k_1h}{\cos k_1h - \frac{Z}{iZ_1}\sin k_1h}]. \tag{3.12b}$$

These results can be shown to be identical from the previous analysis with the result in Equation (3.8).

3.2.3 The Matricant Propagator

We desire a differential equation involving the state vector, $\bar{\mathbf{U}}(x)$, describing pressure and velocity at some position, x, which we can integrate and solve from an initial position. This can be done by using the Matricant, $\boldsymbol{M}$, as described by Pease [17]. The solution of the system is in the form, $\bar{\mathbf{U}}(x) = \boldsymbol{M}\bar{\mathbf{U}}(0)$. We begin this formulation for a general case based on elastic material properties in 1-D. The stress for an elastic solid is related to the displacement in the form $\sigma = E\frac{\partial u}{\partial x}$. Pressure is related to stress by $\sigma = -P$ and the derivative of pressure is related to velocity by Equation (2.8). These relationships can be expressed in matrix form such that

$$\frac{d}{dx}\begin{pmatrix} V \\ -\sigma \end{pmatrix} = i\omega \begin{pmatrix} 0 & -\frac{1}{E} \\ \rho & 0 \end{pmatrix} \begin{pmatrix} V \\ -\sigma \end{pmatrix}. \tag{3.13}$$

From Pease [17], if the state vector $\bar{\mathbf{U}}$, which here describes pressure and velocity, can be expressed such that $\frac{d\bar{\mathbf{U}}}{dx} = \boldsymbol{Q}\bar{\mathbf{U}}$, then the Matricant can be found such that $\frac{d\boldsymbol{M}}{dx} = \boldsymbol{Q}\boldsymbol{M}$. This can be solved analytically or numerically with an ODE solver based on the complexity of the problem. The problem is then reduced to finding the system matrix, $\boldsymbol{Q}$. From Equation (3.13) we can see that,

$$\bar{\mathbf{U}} = \begin{pmatrix} V \\ -\sigma \end{pmatrix} \text{ and } \boldsymbol{Q} = i\omega \begin{pmatrix} 0 & -\frac{1}{E} \\ \rho & 0 \end{pmatrix}.$$

Note that when we take the medium to be a fluid the term $-1/E$ in the system matrix becomes $1/K$, where K is the bulk modulus, this results directly from combining the mass and momentum balance equations. Now for the slab, $\bar{\mathbf{U}}$ will be defined such that $\bar{\mathbf{U}}^{(1)}$ represents the wave traveling to the right and $\bar{\mathbf{U}}^{(2)}$ is the wave traveling to the left, such that

$$\bar{\mathbf{U}}^{(1)} = Ae^{ikx}\begin{pmatrix} 1 \\ Z \end{pmatrix}, \quad \bar{\mathbf{U}}^{(2)} = Be^{-ikx}\begin{pmatrix} 1 \\ -Z \end{pmatrix}.$$

Putting the two waves together in the vector $\bar{\mathbf{U}}$, gives

$$\bar{\mathbf{U}}(x) = \begin{pmatrix} 1 & 1 \\ Z & -Z \end{pmatrix} \begin{pmatrix} e^{ikx} & 0 \\ 0 & e^{-ikx} \end{pmatrix} \begin{pmatrix} A \\ B \end{pmatrix}. \tag{3.14}$$

Now, the Matricant can be found by solving $\bar{\mathbf{U}}(x) = \boldsymbol{M}(x)\bar{\mathbf{U}}(0)$, where

$$\bar{\mathbf{U}}(0) = \begin{pmatrix} 1 & 1 \\ Z & -Z \end{pmatrix} \begin{pmatrix} A \\ B \end{pmatrix}. \tag{3.15}$$

Multiplying $\bar{\mathbf{U}}(x) = \boldsymbol{M}(x)\bar{\mathbf{U}}(0)$ by the inverse of $\bar{\mathbf{U}}(0)$ and simplifying the resulting expression gives the Matricant as

$$\boldsymbol{M}(x) = \begin{pmatrix} \cos(kx) & \frac{i}{Z}\sin(kx) \\ Zi\sin(kx) & \cos(kx) \end{pmatrix}. \tag{3.16}$$

Alternatively we could have found $\boldsymbol{M}(x)$ by noting $\frac{d\boldsymbol{M}}{dx} = \boldsymbol{QM}$ and $\boldsymbol{M}(0) = \boldsymbol{I}$ leading to $\boldsymbol{M}(x) = e^{\boldsymbol{Q}x}$. Now, the Matricant can be used to solve the one-dimensional problem of the slab, where

$$\bar{\mathbf{U}}(h) = \boldsymbol{M}_1(2h)\bar{\mathbf{U}}(-h), \tag{3.17}$$

with $\bar{\mathbf{U}}(h)$, $\boldsymbol{M}_1(2h)$, and $\bar{\mathbf{U}}(-h)$ are defined as

$$\bar{\mathbf{U}}(h) = A_1 \begin{pmatrix} Te^{ikh} \\ ZTe^{ikh} \end{pmatrix}, \quad \boldsymbol{M}_1(2h) = \begin{pmatrix} \cos(2k_1h) & \frac{i}{Z_1}\sin(2k_1h) \\ iZ_1\sin(2k_1h) & \cos(2k_1h) \end{pmatrix},$$

$$\bar{\mathbf{U}}(-h) = A_1 \begin{pmatrix} e^{-ikh} + Re^{ikh} \\ Ze^{-ikh} - zRe^{ikh} \end{pmatrix}.$$

Multiplying and expanding Equation (3.17) gives

$$\begin{pmatrix} Te^{ikh} \\ ZTe^{ikh} \end{pmatrix} = \begin{bmatrix} \cos(2k_1h)(e^{-ikh} + Re^{ikh}) + \frac{iZ}{Z_1}\sin(2k_1h)(e^{-ikh} - Re^{ikh}) \\ iZ_1\sin(2k_1h)(e^{-ikh} + Re^{ikh}) + Z\cos(2k_1h)(e^{-ikh} - Re^{ikh}) \end{bmatrix}. \tag{3.18}$$

Solving for the reflection and transmission coefficients yields

$$R = \frac{e^{-2ikh}\sin(2k_1h)(\frac{iZ_1}{Z} - \frac{iZ}{Z_1})}{2\cos(2k_1h) - \sin(2k_1h)(\frac{iZ}{Z_1} + \frac{iZ_1}{Z})}, \tag{3.19a}$$

$$T = \cos(2k_1h)(e^{-2ikh} + R) + \frac{iZ}{Z_1}\sin(2k_1h)(e^{-2ikh} - R). \tag{3.19b}$$

A numerical demonstration was completed using Matlab for this wave-slab interaction problem. The figure below depicts frequency, ω, versus the amount of wave energy transmitted and reflected. By taking variables such as pressure and velocity at an initial point, a solution was propagated to another point in space by the Matricant. It will become apparent in the next section that the Matricant is especially useful in problems involving many separating boundaries.

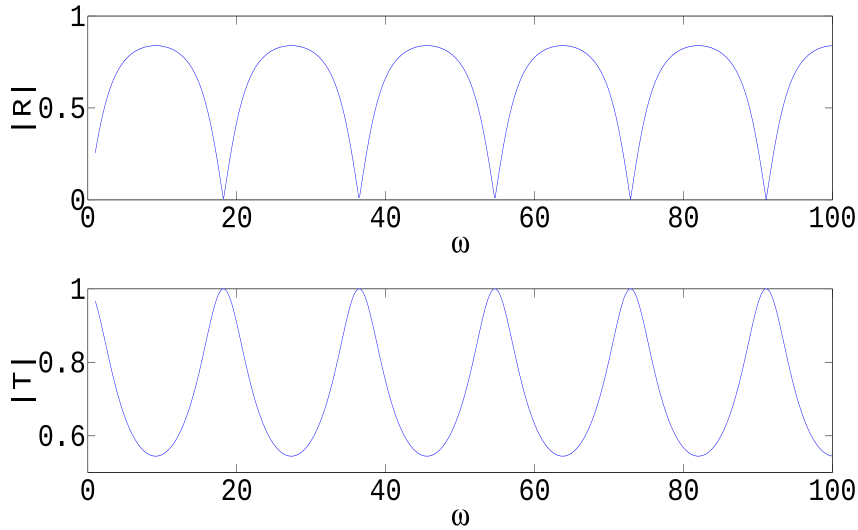

Figure 3.4: Plot of R and T vs ω for $\rho = 156\frac{\text{kg}}{\text{m}^3}$, $\rho_1 = 342\frac{\text{kg}}{\text{m}^3}$, $c = 113\frac{\text{m}}{\text{s}}$, $c_1 = 174\frac{\text{m}}{\text{s}}$, $h = 15$m, ω ranges from 1 to 100 $\frac{\text{rad}}{\text{s}}$

3.3 Using the Matricant to solve general slabs

To show how powerful the Matricant propagator method is, we will next use it to solve for an array of slabs. When used in conjunction with numeric solving programs such as Matlab, the Matricant proves to be very useful.

3.3.1 Periodic slabs

In the next example a system in which an incident wave interacts with a series of five periodic slabs of properties ρ_1 and c_1, spaced apart by distance h_1, as shown in Figure 3.5, will be solved. Setting up the problem using the Matricant, we have

$$\begin{aligned}[\mathbf{U}(5(h_1+h))] = \quad & ([\boldsymbol{M}_1(h_1)][\boldsymbol{M}(h)][\boldsymbol{M}_1(h_1)][\boldsymbol{M}(h)][\boldsymbol{M}_1(h_1)][\boldsymbol{M}(h)][\boldsymbol{M}_1(h_1)][\boldsymbol{M}(h)] \\ & \times[\boldsymbol{M}_1(h_1)][\boldsymbol{M}(h)])[\boldsymbol{U}(0)],\end{aligned}$$

where

$$\mathbf{U}[5(h_1+h)] = \begin{pmatrix} Te^{5ik(h_1+h)} \\ ZTe^{5ik(h_1+h)} \end{pmatrix}, \qquad \mathbf{U}(0) = \begin{pmatrix} 1+R \\ Z(1-R) \end{pmatrix},$$

$$\boldsymbol{M}_1(h_1) = \begin{pmatrix} \cos k_1h_1 & \frac{i}{Z_1}\sin k_1h_1 \\ iZ_1\sin k_1h_1 & \cos k_1h_1 \end{pmatrix}, \qquad \boldsymbol{M}(h) = \begin{pmatrix} \cos kh & \frac{i}{Z}\sin kh \\ iZ\sin kh & \cos kh \end{pmatrix}.$$

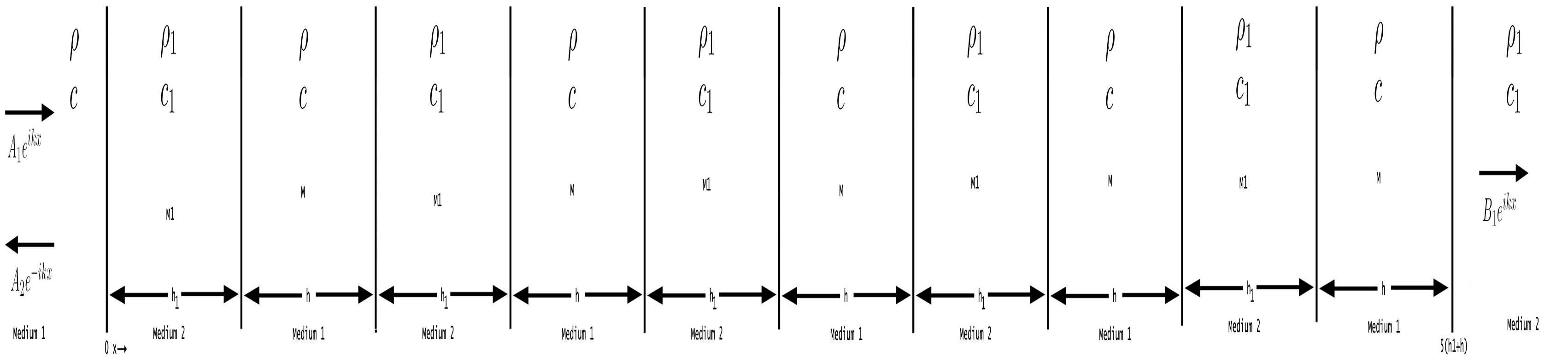

Figure 3.5: General case of periodic slabs.

The system may then be solved numerically using Matlab with given ρ, c, h, ρ_1, c_1, h_1 and ω. Alternatively this problem can be solved by creating a system of equations,

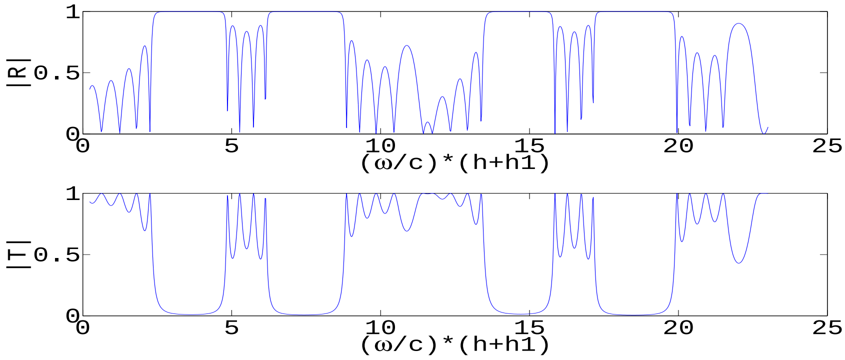

Figure 3.6: Plot generated by the Matlab code for Reflection and Transmission coefficients, $\rho = 156\frac{\text{kg}}{\text{m}^3}$, $c = 113\frac{\text{m}}{\text{s}}$, $h = 15$m, $\rho_1 = 342\frac{\text{kg}}{\text{m}^3}$, $c_1 = 174\frac{\text{m}}{\text{s}}$, $h_1 = 11$m and ω ranges from 1 to 100 $\frac{\text{rad}}{\text{s}}$ in steps of 0.1.

matching pressure and velocity at each boundary and solving. When this system of equations is arranged into a matrix and solved it is referred to as the global matrix method which will be discussed for problems involving concentric cylinders later on.

3.3.2 Systems in which properties vary smoothly

Equation (3.13) may be used to solve for a slab for which properties vary smoothly. When using the Matricant, a solution is propagated forward through a finely discretized thickness such that the properties may vary from layer to layer. Alternatively analytic solutions may also be found for simple enough problems. In general,

$$\frac{d\boldsymbol{M}}{dx} = \boldsymbol{Q}(x)\boldsymbol{M}, \qquad \boldsymbol{M}(0) = I, \qquad \boldsymbol{Q}(x) = i\omega \begin{pmatrix} 0 & \frac{1}{E(x)} \\ \rho(x) & 0 \end{pmatrix}. \tag{3.20}$$

We next use the Matricant to solve a one-dimensional problem in which the density, ρ, and Young's modulus, E, are continuous functions of x. Consider $E(x) = 50 + 10x$ Pa and $\rho(x) = 50 - 5x\ \frac{\text{kg}}{\text{m}^3}$. The Matricant, $\mathbf{M}$(x), will be solved for numerically using the ODE solver in Matlab with the equation $\frac{d\boldsymbol{M}}{dx} = \boldsymbol{Q}(x)\boldsymbol{M}$. For $\omega = 50$ rad/s, the Matricant evaluated at $x = 1$ is

$$\boldsymbol{M}(1) = \begin{pmatrix} -0.8113 & 0 + 0.0110i \\ 0 + 28.6364i & -0.8436 \end{pmatrix}.$$

The answer from the ODE solver in Matlab can be checked by using Equation (3.16) and approximating ρ and E as constant over small dx. By taking the step dx to be 10^{-6}, Matlab yields

$$\boldsymbol{M}(1) = \begin{pmatrix} -0.8113 & 0 + 0.0110i \\ 0 + 28.6365i & -0.8436 \end{pmatrix}.$$

As before $\bar{\mathbf{U}}(x)$ can be solved by using $\bar{\mathbf{U}}(x) = \boldsymbol{M}(x)\bar{\mathbf{U}}(0)$.

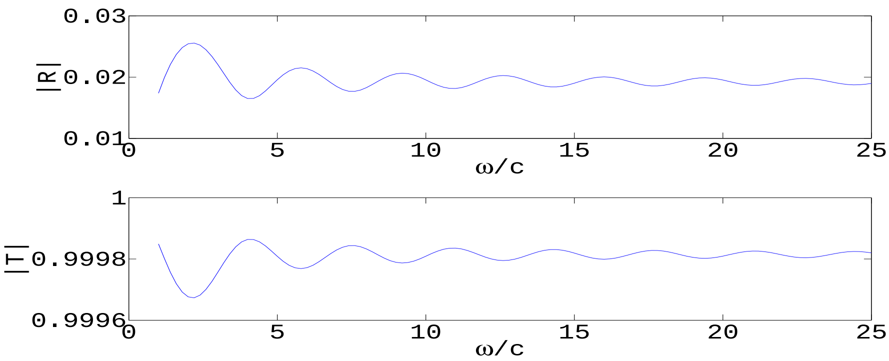

Figure 3.7: Plot of the Reflection and Transmission vs. $\frac{\omega}{c}$ for ω ranging from 1 to 25 $\frac{\text{rad}}{\text{s}}$ using $\rho(x) = 50 - 5x \ \frac{\text{kg}}{\text{m}^3}$ and $E(x) = 50 + 10x$ Pa for a slab starting at $x = 0$ to $x = 1$ m.

3.4 Energy conservation

From the original one-dimensional problem of the slab, a relationship between the reflection and transmission coefficients will yield the one-dimensional optical theorem which can be derived by an energy balance of the system. In 1-D, the transmitted

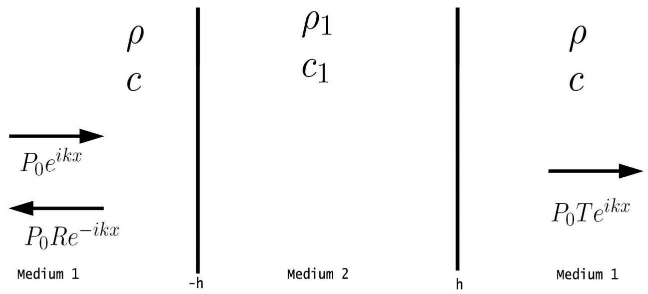

part of the solution can be rewritten such that

$$P_0Te^{ikx} = P_0e^{ikx}(1 + T'), \qquad T' = T - 1.$$

In the above equation, R and T' contribute to the scattered field which is equal to the total field less the incident. We then may write $|R|^2 + |T' + 1|^2 = 1$, such that $|R|^2 + (T' + 1)(T'^* + 1) = 1$ where $|z|^2 = zz^*$, and * denotes the complex conjugate. The final result is then,

$$|R|^2 + |T'|^2 = -2\mathrm{Re}(T'). \tag{3.21}$$

Similar formulations will be studied in two and three dimensions in order to determine a numeric value on the amount of scattering that occurs, given by the scattering cross section.

3.5 Summary

One-dimensional acoustic problems were studied in which several techniques were used to solve the same problem. An important result of this one-dimensional study was displaying that if the impedance, Z, of two media matched the entire wave transmits through. In other words, the reflection coefficient becomes zero and the transmission coefficient becomes one for this case. Techniques such as the Matricant propagator and matching coefficients were developed and used to solve semi-infinite boundary problems.

These techniques will be further developed in two and three dimensions in the following chapters.

Chapter 4

2D Acoustic Wave Theory

Here we continue the discussion from Section 2.2 and solve simple scattering problems involving infinitely long cylinders. We also continue the development on the Matricant propagator technique from the previous chapter into the two-dimensional realm. This chapter finishes with a discussion concerning the amount of energy scattered by a target in order to quantify the scattering strength.

4.1 Transforming the incident plane wave to polar coordinates

From before, the incident plane wave was given as Ce^{ikx}. In polar coordinates the parameter x turns into $r\cos\theta$. This can be transformed into a series involving Bessel functions by using the complex Fourier series where

$$f(x) = \sum_{n=-\infty}^{\infty} C_n e^{inx}, \quad C_n = \frac{1}{2\pi}\int_{-\pi}^{\pi} f(x)e^{-inx}dx.$$

Using the Complex Fourier series for our function $e^{ir\cos(\theta)}$, results in

$$e^{ir\cos(\theta)} = \sum_{n=-\infty}^{\infty} C_n e^{in\theta}, \quad C_n = \frac{1}{2\pi}\int_{-\pi}^{\pi} e^{ir\cos(\theta)}e^{-in\theta}d\theta.$$

Using Bessel's first integral, C_n can be simplified in terms of a Bessel function where Bessel's first integral is given by [15], with

$$J_n(r) = \frac{1}{2\pi i^n}\int_{0}^{2\pi} e^{ir\cos(\theta)}e^{in\theta}, \quad C_n = i^n J_n(r).$$

Putting everything together

$$e^{ir\cos(\theta)} = \sum_{n=-\infty}^{\infty} i^n J_n(r)e^{in\theta}. \tag{4.1}$$

Alternatively this series could be found such that n ranges from 0 to ∞ instead of $-\infty$ to ∞. By using the Cosine Fourier Series for $e^{ir\cos(\theta)}$ and using another version of

Bessel's first integral where $J_n(r) = \frac{i^{-n}}{\pi}\int_0^{\pi} e^{ir\cos(\theta)}\cos(n\theta)d\theta$. Then $e^{ir\cos(\theta)}$ may be written as

$$e^{ir\cos(\theta)} = J_0(r) + 2\sum_{n=1}^{\infty} i^n J_n(r)\cos(n\theta). \tag{4.2}$$

4.2 Scattering from a cylinder

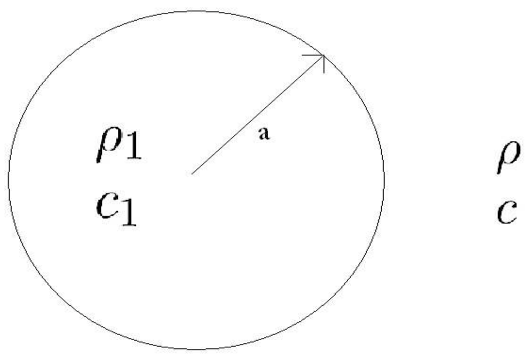

Consider the case for which the order of Bessel's differential equation is zero. That is $n = 0$ from Equation (2.6). Then,

$$r^2 P_0'' + rP_0' + ((kr)^2 - 0)P_0 = 0,$$

the pressure is then defined by Equation (2.7) such that

$$P(r) = \begin{cases} A_1 H_0^{(2)}(kr) + A_2 H_0^{(1)}(kr), & r > a, \\ B_1 J_0(k_1 r) + B_2 Y_0(k_1 r), & 0 < r < a. \end{cases}$$

However $\lim_{r\to 0} Y_0(r) = -\infty$, which means $B_2 = 0$. Using continuity conditions such that $P(a^+) = P(a^-)$ and $V_r(a^+) = V_r(a^-)$,

$$B_1 = -\frac{A_1\left(H_{-1}^{(2)}(ka) - \frac{H_0^{(2)}(ka)H_{-1}^{(1)}(ka)}{H_0^{(1)}(ka)}\right)}{\frac{Z}{Z_1}J_1(k_1 a) + \frac{J_0(k_1 a)H_{-1}^{(1)}(ka)}{H_0^{(1)}(ka)}}, \tag{4.3a}$$

$$A_2 = -A_1\left[\frac{J_0(k_1 a)\left(H_{-1}^{(2)}(ka) - \frac{H_0^{(2)}(ka)H_{-1}^{(1)}(ka)}{H_0^{(1)}(ka)}\right)}{\frac{Z}{Z_1}H_0^{(1)}(ka)J_1(k_1 a) + J_0(k_1 a)H_{-1}^{(1)}(ka)} + \frac{H_0^{(2)}(ka)}{H_0^{(1)}(ka)}\right], \tag{4.3b}$$

where A_1 is the magnitude of the incident wave, A_2 is the magnitude of the outgoing wave, and B_1 is the magnitude of the standing wave inside the cylinder. The next problem is to find the pressure distribution caused by an incident plane wave on a cylinder of radius a for all n. From Equation (4.1), the incident wave can be found in polar coordinates as

$$P_{incident} = P_0 e^{ikx} = P_0 e^{ikr\cos(\theta)} = P_0 \sum_{n=-\infty}^{\infty} i^n J_n(kr) e^{in\theta}, \quad r > a. \tag{4.4}$$

By the Sommerfeld condition, the energy radiated from the source must scatter to infinity and no energy from infinity may be radiated to the field. See Ihlenburg [18]. This simplifies the $P_{scattered}$ equation such that it is only dependent on $H_n^{(1)}(kr)$, which represents outgoing waves. The function $H_n^{(2)}(kr)$ represents incoming waves, which by the Sommerfeld condition, should not be present. The scattering solution is then

$$P_{scattered} = P_0 \sum_{n=-\infty}^{\infty} A_n H_n^{(1)}(kr) e^{in\theta}, \quad r > a, \tag{4.5}$$

and the field inside the cylinder is

$$P_{in} = \sum_{n=-\infty}^{\infty} B_n J_n(k_1 r) e^{in\theta}, \quad r < a. \tag{4.6}$$

Combining solutions for $r > a$ and $r < a$ the total field inside and outside is given by

$$P(r,\theta) = \sum_{n=-\infty}^{\infty} e^{in\theta} \times \begin{cases} \left(i^n P_0 J_n(kr) + A_n H_n^{(1)}(kr)\right), & r > a, \\ B_n J_n(k_1 r), & r < a, \end{cases} \tag{4.7a}$$

$$V_r(r,\theta) = -i \sum_{n=-\infty}^{\infty} e^{in\theta} \times \begin{cases} Z^{-1}\left(i^n P_0 J_n'(kr) + A_n H_n^{'(1)}(kr)\right), & r > a, \\ Z_1^{-1} B_n J_n'(k_1 r), & r < a. \end{cases} \tag{4.7b}$$

Imposing continuous pressure and velocity boundary conditions at $r = a$, as done in the previous chapter, the solution for the scattering coefficients A_n and B_n are

$$A_n = \frac{i^n J_n(ka)}{H_n^{(1)}(ka)} \frac{\left[\frac{J_n'(k_1 a)}{Z_1 J_n(k_1 a)} - \frac{J_n'(ka)}{Z J_n(ka)}\right]}{\left[\frac{H_n^{'(1)}(ka)}{Z H_n^{(1)}(ka)} - \frac{J_n'(k_1 a)}{Z_1 J_n(k_1 a)}\right]}, \tag{4.8}$$

$$B_n = \frac{P_0 i^n J_n(ka)}{J_n(k_1 a)} \left[1 + \frac{\left[\frac{J_n'(k_1 a)}{Z_1 J_n(k_1 a)} - \frac{J_n'(ka)}{Z J_n(ka)}\right]}{\left[\frac{H_n^{'(1)}(ka)}{Z H_n^{(1)}(ka)} - \frac{J_n'(k_1 a)}{Z_1 J_n(k_1 a)}\right]}\right]. \tag{4.9}$$

A_n could also have been found by using the impedance matching method where we want to solve the equation $\frac{P(a^+)}{V(a^+)} = \frac{P(a^-)}{V(a^-)}$ such that

$$\frac{iZ[i^n J_n(ka) + A_n H_n^{(1)}(ka)]}{[i^n J_n'(ka) + A_n H_n^{'(1)}(ka)]} = iZ_1 \frac{J_n(k_1 a)}{J_n'(k_1 a)}. \tag{4.10}$$

Solving Equation (4.10) for A_n,

$$A_n = \frac{i^n [J_n(ka) - \frac{Z_1}{Z} \frac{J_n(k_1 a)}{J_n'(k_1 a)} J_n'(ka)]}{[\frac{Z_1}{Z} \frac{J_n(k_1 a)}{J_n'(k_1 a)} H_n^{'(1)}(ka) - H_n^{(1)}(ka)]} = \frac{i^n J_n(ka)}{H_n^{(1)}(ka)} \frac{[\frac{J_n'(k_1 a)}{Z_1 J_n(k_1 a)} - \frac{J_n'(ka)}{Z J_n(ka)}]}{[\frac{H_n^{'(1)}(ka)}{Z H_n^{(1)}(ka)} - \frac{J_n'(k_1 a)}{Z_1 J_n(k_1 a)}]},$$

which is exactly the same as Equation (4.8). Notice that B_n, the coefficient solution for the inner cylinder, is not found by the impedance matching method. This also occurred in the previous chapter where the solution inside the slab could not be determined by this method. This occurs as these coefficients are divided out of the solution, for instance the right hand side of Equation (4.10) does not contain the B_n coefficients.

Limiting boundary conditions

For the case of a pressure release cylinder, where the quantity $Z_1 = \rho_1 c_1 \longrightarrow 0$,

$$A_{n,pres.rel.} = -i^n \frac{J_n(ka)}{H_n^{(1)}(ka)}, \quad B_{n,pres.rel.} = \frac{2P_0 i^n J_n(ka)}{J_n(k_1 a)}. \tag{4.11}$$

For the case of a rigid cylinder, where $Z_1 \longrightarrow \infty$,

$$A_{n,rigid} = -i^n \frac{J_n'(ka)}{H_n^{'(1)}(ka)}, \quad B_{n,rigid} = \frac{P_0 i^n}{J_n(k_1 a)} [J_n(ka) - \frac{J_n'(ka) H_n^{(1)}(ka)}{H_n^{'(1)}(ka)}]. \tag{4.12}$$

Using the Wronskian to simplify $B_{n,rigid}$, where the Wronskian relationship is given in [15], gives

$$W = J_v(z) Y_v'(z) - Y_v(z) J_v'(z) = Y_v(z) J_{v+1}(z) - J_v(z) Y_{v+1}(z) = \frac{2\pi}{z},$$

$$B_{n,rigid} = \frac{2\pi P_0 i^{n+1}}{ka J_n(k_1 a) H_n^{'(1)}(ka)}. \tag{4.13}$$

Of all objects, rigid targets tend to produce the highest level of backscattering, scattering opposite the direction of wave motion, as will be shown later in Section 4.6.1. For this reason, rigid targets will represent the object surrounded by the cloaking medium in later discussion on cloaking theory. We end this section with a figure displaying the pressure distribution of cylinder-wave interaction, for given fluid properties.

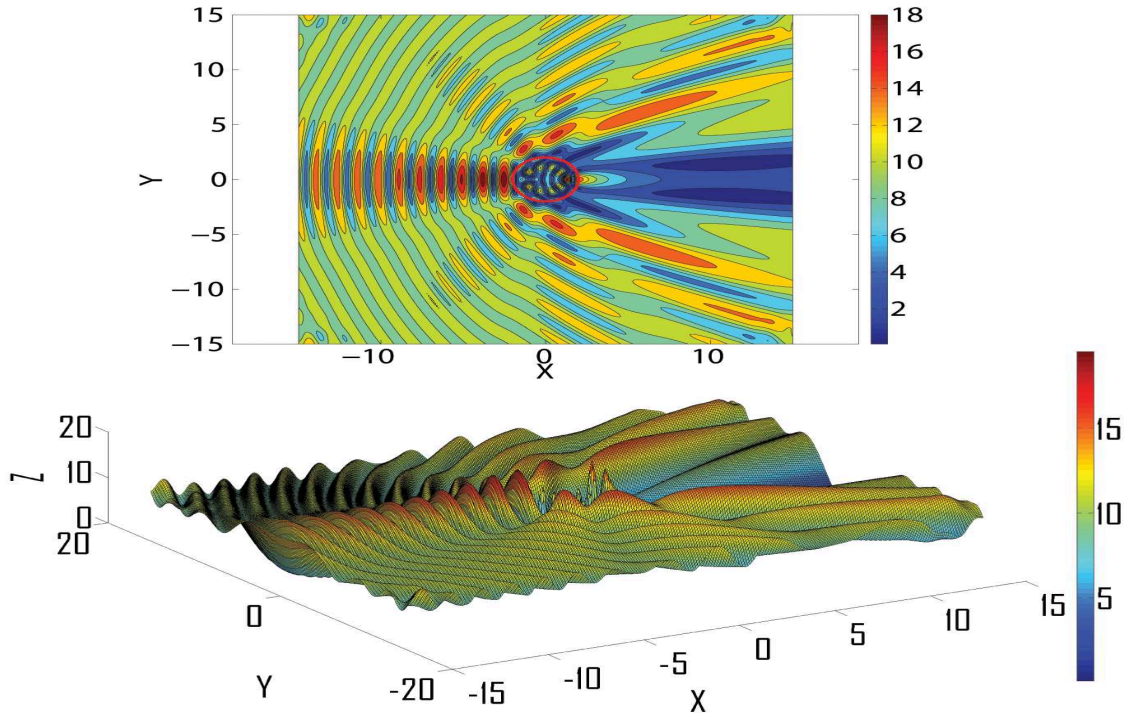

Figure 4.1: Contour and surface plots using Equations (4.8) and (4.9) for $a = 2$m, cylinder radius, n ranges from -50 to 50 , the resolution is 0.1 m controlled by [x,y] = meshgrid([-15:.1:15]), $\rho = 10\frac{\text{kg}}{\text{m}^3}$, $c = 15\frac{\text{m}}{\text{s}}$, $\rho_1 = 5\frac{\text{kg}}{\text{m}^3}$, $c_1 = 7\frac{\text{m}}{\text{s}}$, magnitude of incoming wave, $P_0 = 10$ Pa, $\omega = \frac{5c}{a}\frac{\text{rad}}{\text{s}}$

4.3 Using the Matricant

From Equations (2.9a) and (2.9b) the Matricant can be found to solve for cylindrical geometries. Rewriting these equations in matrix form,

$$i\omega\rho \begin{pmatrix} V_r \\ V_\theta \end{pmatrix} = \begin{pmatrix} \frac{\partial}{\partial r}P \\ \frac{inP}{r} \end{pmatrix}. \tag{4.14}$$

Next, we can eliminate V_θ to get two equations dependent on P and V_r only. This can be done by using the mass balance equation, $i\omega P = K\nabla.\underline{V}$, where K is the bulk modulus, $\underline{V} = -i\omega\underline{u}$ and $\nabla.\underline{V}$ is given in polar coordinates by,

$$\nabla.\underline{V} = \frac{1}{r}\frac{\partial}{\partial r}(rV_r) + \frac{1}{r}\frac{\partial}{\partial\theta}V_\theta = \frac{1}{r}\frac{\partial}{\partial r}(rV_r) + \frac{inV_\theta}{r}. \tag{4.15}$$

Eliminating V_θ by using the mass balance equation such that, $\frac{i\omega}{K}P = \frac{1}{r}\frac{\partial}{\partial r}(rV_r) + \frac{inV_\theta}{r}$ gets us $\frac{\partial}{\partial r}(rV_r) = \frac{i\omega}{r}P[\frac{r^2}{K} - \frac{n^2}{\omega^2\rho}]$. The system matrix, $\boldsymbol{Q}$, can now be found, as in Section

3.2.3, by writing the derivative of the state vector in terms of itself, where

$$\frac{\mathrm{d}}{\mathrm{d}r}\begin{pmatrix} P \\ rV_r \end{pmatrix} = \frac{i\omega}{r}\begin{pmatrix} 0 & \rho \\ \frac{r^2}{K} - \frac{n^2}{\omega^2\rho} & 0 \end{pmatrix}\begin{pmatrix} P \\ rV_r \end{pmatrix}. \tag{4.16}$$

The quantities P and rV_r may now be solved and propagated forward by solving $\frac{\mathrm{d}\boldsymbol{M}}{\mathrm{d}r} = \boldsymbol{Q}(r)\boldsymbol{M}$ for $\boldsymbol{M}$. Thus,

$$\boldsymbol{Q}(r) = \frac{i\omega}{r}\begin{pmatrix} 0 & \rho \\ \frac{r^2}{K} - \frac{n^2}{\omega^2\rho} & 0 \end{pmatrix}. \tag{4.17}$$

Solutions for P and rV_r may now be found in the form

$$\begin{pmatrix} P \\ rV_r \end{pmatrix}_{r=a} = \begin{pmatrix} M_{11} & M_{12} \\ M_{21} & M_{22} \end{pmatrix}_{a,b}\begin{pmatrix} P \\ rV_r \end{pmatrix}_{r=b}. \tag{4.18}$$

4.3.1 Using Matlab to compute the Matricant

Using Equation (4.16), a Matlab code was written and a check performed using Equation (2.7). As done in Section 3.3.2, the ODE solver will be used to solve for the Matricant, again

$$\frac{d\boldsymbol{M}}{dr} = \boldsymbol{Q}(r)\boldsymbol{M}, \quad \boldsymbol{M}(0) = \boldsymbol{I}, \quad \boldsymbol{Q}(r) = \frac{i\omega}{r}\begin{pmatrix} 0 & \rho \\ \frac{r^2}{K} - \frac{n^2}{\omega^2\rho} & 0 \end{pmatrix}. \tag{4.19}$$

As a check we can use Equation (2.7), where $P(r) = AJ_n(kr) + BY_n(kr)$ and $rV(r) = \frac{r}{iZ}(AJ_n^{'}(kr) + BY_n^{'}(kr))$. In this way we can find $\boldsymbol{M}$ as done before in Section 3.2.3. Hence,

$$\bar{U}(r) = \begin{pmatrix} P \\ rV_r \end{pmatrix} = \begin{pmatrix} J_n(kr) & Y_n(kr) \\ \frac{r}{iZ}J_n^{'}(kr) & \frac{r}{iZ}Y_n^{'}(kr) \end{pmatrix}\begin{pmatrix} A \\ B \end{pmatrix},$$

where $\bar{U}(r) = \boldsymbol{M}(r)\bar{U}(r_{min})$ and $\boldsymbol{M}(r) = \bar{U}(r)\bar{U}(r_{min})^{-1}$. $\boldsymbol{M}(r)$ is then

$$\boldsymbol{M}(r) = \begin{pmatrix} J_n(kr) & Y_n(kr) \\ \frac{r}{iZ}J_n^{'}(kr) & \frac{r}{iZ}Y_n^{'}(kr) \end{pmatrix}\begin{pmatrix} J_n(kr_{min}) & Y_n(kr_{min}) \\ \frac{r}{iZ}J_n^{'}(kr_{min}) & \frac{r}{iZ}Y_n^{'}(kr_{min}) \end{pmatrix}^{-1}. \tag{4.20}$$

To make the problem more interesting, consider the bulk modulus, K, and the density, ρ, to be continuous functions of r. Since we are considering a fluid medium, we use the speed of sound, $c = \sqrt{\frac{K}{\rho}}$. A Matlab code was written and attached in the appendix where D.1 contains the main code, D.2 contains the function used for finding the Matricant, and D.3 contains the check performed between the exact and ODE solver values for $\boldsymbol{M}$.

4.4 Concentric cylinders

Having described the Matricant we now consider the global matrix method and compare how to find the scattering coefficients for the two methods. Setup: An incident wave interacts with concentric cylinders for which the surrounding medium properties are ρ_0 and c_0. The properties of the outer cylinder are ρ_1 and c_1 and the properties of the most inner cylinder are ρ_2 and c_2. This two dimensional example is comparable to the slab example from Section 3.2.

4.4.1 Global Matrix method

The solution for pressure for $r_2 > r \geq 0$ has to be finite at $r = 0$. Since $\lim_{r\to 0} Y_0(r) \to -\infty$, only solutions involving J_n will exist for $r_2 > r \geq 0$. In the intermediate layer $r_1 > r > r_2$ both types of radial solutions are possible. In the exterior $r > r_1$ the incident wave is assumed, and the scattered solution must be an outgoing wave (one that has energy going out, not in), which are represented by $H_n^{(1)}(kr)$, assuming $e^{-i\omega t}$. For two concentric cylinders the pressure and velocity is

$$P(r,\theta) = \sum_{n=-\infty}^{\infty} i^n e^{in\theta} \times \begin{cases} P_0 J_n(k_0 r) + C_{0n} H_n^{(1)}(k_0 r), & r > r_1, \\ C_{1n} J_n(k_1 r) + D_{1n} Y_n(k_1 r), & r_1 > r > r_2, \\ C_{2n} J_n(k_2 r), & r_2 > r \geq 0, \end{cases} \tag{4.21a}$$

$$V_r(r,\theta) = -i \sum_{n=-\infty}^{\infty} i^n e^{in\theta} \times \begin{cases} Z_0^{-1}\big(P_0 J_n'(k_0 r) + C_{0n} H_n^{(1)'}(k_0 r)\big), & r > r_1, \\ Z_1^{-1}\big(C_{1n} J_n'(k_1 r) + D_{1n} Y_n'(k_1 r)\big), & r_1 > r > r_2, \\ Z_2^{-1} C_{2n} J_n'(k_2 r), & r_2 > r \geq 0. \end{cases} \tag{4.21b}$$

Matching pressure and velocity at the r_1 interface,

$$C_{1n} J_n(k_1 r_1) + D_{1n} Y_n(k_1 r_1) = P_0 J_n(k_0 r_1) + C_{0n} H_n^{(1)}(k_0 r_1), \tag{4.22a}$$

$$Z_1^{-1}\big(C_{1n} J_n'(k_1 r_1) + D_{1n} Y_n'(k_1 r_1)\big) = Z_0^{-1}\big(P_0 J_n'(k_0 r_1) + C_{0n} H_n^{(1)'}(k_0 r_1)\big). \tag{4.22b}$$

Similarly, matching for the r_2 interface,

$$C_{1n}J_n(k_1r_2) + D_{1n}Y_n(k_1r_2) = C_{2n}J_n(k_2r_2), \tag{4.23a}$$

$$Z_1^{-1}\big(C_{1n}J_n'(k_1r_2) + D_{1n}Y_n'(k_1r_2)\big) = Z_2^{-1}C_{2n}J_n'(k_2r_2). \tag{4.23b}$$

Rewriting these equations in matrix form:

$$\begin{pmatrix} H_n^{(1)}(k_0r_1) & -J_n(k_1r_1) & -Y_n(k_1r_1) & 0 \\ -Z_0^{-1}H_n^{'(1)}(k_0r_1) & Z_1^{-1}J_n'(k_1r_1) & Z_1^{-1}Y_n'(k_1r_1) & 0 \\ 0 & J_n(k_1r_2) & Y_n(k_1r_2) & -J_n(k_2r_2) \\ 0 & -Z_1^{-1}J_n'(k_1r_2) & -Z_1^{-1}Y_n'(k_1r_2) & Z_2^{-1}J_n'(k_2r_2) \end{pmatrix} \begin{pmatrix} C_{0n} \\ C_{1n} \\ D_{1n} \\ C_{2n} \end{pmatrix} = \begin{pmatrix} -P_0J_n(k_0r_1) \\ Z_0^{-1}P_0J_n'(k_0r_1) \\ 0 \\ 0 \end{pmatrix}. \tag{4.24}$$

Similarly this method can be applied to any number of concentric cylinders for which the size of the matrix will be on the order of (two times the number of layers) by (two times the number of layers). A Matlab code was written for the general case of any number of concentric cylinders and was compared to the Matricant method as described in the next section.

4.4.2 Using the Matricant

From Equation (4.16), the Matricant was found for a single cylinder. For concentric cylinders it can be used given the impedance, ratio of pressure and velocity at the inner most radius. Using Equations (4.21a) and (4.21b) for $r_2 > r \geq 0$ and solving $M_{(r_1,r_2)}$ using an ODE solver in Matlab, the impedance at $r = r_1$ will be

$$Z_1 = \frac{M_{(r_1,r_2),11}J_n(k_2r_2) + M_{(r_1,r_2),12}\frac{r_2}{iZ_2}J_n'(k_2r_2)}{M_{(r_1,r_2),21}J_n(k_2r_2) + M_{(r_1,r_2),22}\frac{r_2}{iZ_2}J_n'(k_2r_2)}. \tag{4.25}$$

Then the scattering coefficient for $r > r_1$ is found by manipulating (4.22a) such that the scattering coefficient, C_{0n} may be written as

$$C_{0n} = P_0\frac{J_n(k_1r_1) - \frac{Z_1}{iZ_0}J_n'(k_1r_1)}{\frac{Z_1}{iZ_0}H_n^{'(1)}(k_1r_1) - H_n^{(1)}(k_1r_1)}, \tag{4.26}$$

where $Z_0 = \rho_0 c_0$. The Matlab code which compares these two methods will be discussed later in which both methods are used to duplicate the results of Torrent and Sánchez-Dehesa, [10]. It will first be necessary to understand how layered fluids may act as a single medium with anisotropic properties.

4.5 Homogenized cylindrically layered media

In the limit in which the wavelength is much larger than the spacing between many concentric cylinders, the wave responds as if the medium had a single effective bulk modulus and an anisotropic density. Here we discuss the formulation of the effective medium properties by the characteristic properties of the individual fluids.

4.5.1 Effective properties

Consider a series of concentric cylinders in which cylindrical shells consist of properties ρ_1, ρ_2, c_1 and c_2, where each shell alternates from medium 1 to medium 2. Now, this layered media may be thought of as a single cylinder with effective bulk modulus, K_{eff} and inertial properties differing in the θ and r directions. From [8], a composite medium in which density varies is thought of as having an effective density operator that takes the form of a second-order tensor. Writing the momentum balance equation, we may find how this effective density behaves,

$$\boldsymbol{\rho}\frac{\partial \boldsymbol{v}}{\partial t} = -\nabla p \quad \Rightarrow \quad \begin{pmatrix} \rho_r & 0 \\ 0 & \rho_\theta \end{pmatrix} \frac{\partial \boldsymbol{v}}{\partial t} = -\nabla p. \tag{4.27}$$

The homogenized properties are defined by averages as

$$K_{eff} = \langle K^{-1} \rangle^{-1} = \Big(\frac{\phi_1}{K_1} + \frac{\phi_2}{K_2}\Big)^{-1}, \tag{4.28a}$$

$$\rho_r = \langle \rho \rangle = \phi_1 \rho_1 + \phi_2 \rho_2, \tag{4.28b}$$

$$\rho_\theta = \langle \rho^{-1} \rangle^{-1} = \Big(\frac{\phi_1}{\rho_1} + \frac{\phi_2}{\rho_2}\Big)^{-1}, \tag{4.28c}$$

with $K_j = \rho_j c_j^2$, as usual, and volume fractions $\phi_j \geq 0$, $j = 1, 2$, and $\phi_1 + \phi_2 = 1$. This same formulation will be introduced later using three fluid shells in order to create a medium that will behave as a cloak.

4.5.2 Solutions using effective properties

Eliminating the velocity, a single equation results for the time-harmonic pressure with

$$\frac{K_{eff}}{r\rho_r}\frac{\partial}{\partial r}\big(r\frac{\partial P}{\partial r}\big) + \big(\omega^2 - \frac{n^2 K_{eff}}{r^2\rho_\theta}\big)P = 0, \tag{4.29}$$

which is Bessel's differential equation but now for non-integer order N. Rewriting Equation (4.29), attains

$$r^2 P'' + rP' + \big(k^2r^2 - N^2\big)P = 0, \quad \text{with } k = \omega\sqrt{\frac{\rho_r}{K_{eff}}}, \quad N = n\sqrt{\frac{\rho_r}{\rho_\theta}}. \tag{4.30}$$

This corresponds to solutions we have seen before, implying the pressure and radial velocity may be written as

$$P(r,\theta) = \sum_{n=0}^{\infty}\varepsilon_n i^n \cos n\theta \times \begin{cases} \big(P_0 J_n(k_0 r) + A_n H_n^{(1)}(k_0 r)\big), & r > a, \\ B_n J_N(kr), & r < a, \end{cases} \tag{4.31a}$$

$$V_r(r,\theta) = -i\sum_{n=0}^{\infty}\varepsilon_n i^n \cos n\theta \times \begin{cases} Z^{-1}\big(P_0 J_n'(k_0 r) + A_n H_n^{'(1)}(k_0 r)\big), & r > a, \\ Z_r^{-1} B_n J_N'(kr), & r < a. \end{cases} \tag{4.31b}$$

where $Z_r = \sqrt{K_{eff}\rho_r}$, and $\varepsilon_n = 1$ for $n = 0$, $\varepsilon_n = 2$ for $n > 0$. Note that the sum is strictly on positive values of n. Unlike the case for a normal fluid, where the Bessel functions are all of integer order, in this case the sum for the interior pressure must be written using only positive n since Bessel functions of the form $J_{-N}(kr)$ are not regular at $r = 0$ if N is positive but non-integral. In other words, only the functions $J_N(kr)$ for $N > 0$ provide the basis for representing the pressure in the neighborhood of $r = 0$, where it must remain finite.

4.5.3 Layer properties for given homogenized medium

Suppose we wanted to design a medium with given properties ρ_r, ρ_θ, K_{eff}, along with ρ_1, c_1. We may then find the properties and volume fractions of the second fluid needed to create this medium. ϕ_2, ρ_2, c_2 can be found by inverting (4.28a), resulting in

$$\phi_2 = \left((1 - \frac{\rho_r}{\rho_1})^{-1} + (1 - \frac{\rho_1}{\rho_\theta})^{-1} \right)^{-1}, \tag{4.32a}$$

$$\rho_2 = \left(\frac{\rho_r - \rho_1}{\rho_\theta - \rho_1} \right) \rho_\theta, \tag{4.32b}$$

$$K_2 = \left(K_1^{-1} + \frac{K_{eff}^{-1} - K_1^{-1}}{\phi_2} \right)^{-1}. \tag{4.32c}$$

The values of ρ_r and ρ_θ are not completely free. In addition to the requirement that they are positive, we also have

$$\langle \rho \rangle \langle \rho^{-1} \rangle - 1 = \phi_1 \phi_2 \left(\sqrt{\frac{\rho_1}{\rho_2}} - \sqrt{\frac{\rho_2}{\rho_1}} \right)^2 \geq 0. \tag{4.33}$$

This implies $\rho_r \geq \rho_\theta$, with equality only if the cylinder is completely uniform, which is not of interest. Therefore, $0 < \rho_\theta < \rho_r$ in general. In addition, in order to get a positive but finite K_2, the effective bulk modulus must satisfy $0 < K_{eff} < \frac{K_1}{1-\phi_2}$. As long as these constraints are satisfied, we can generate a layered medium that approximates the properties of the homogenized cylinder.

4.5.4 Alternative Matricant

From balance of momentum using Equation (4.27),

$$i\omega \begin{pmatrix} \rho_r & 0 \\ 0 & \rho_\theta \end{pmatrix} \begin{pmatrix} V_r \\ V_\theta \end{pmatrix} = \begin{pmatrix} \frac{\mathrm{d}}{\mathrm{d}r} P \\ \frac{in}{r} P \end{pmatrix}. \tag{4.34}$$

Inverting the above equation, we find that $V_\theta = \frac{n}{r\omega\rho_\theta} P$ and $\frac{\mathrm{d}}{\mathrm{d}r} P = i\omega\rho_r V_r$. Using the balance of mass Equation (4.15), we have $i\omega P = K \nabla . \underline{V}$, where $\nabla . \underline{V} = \frac{1}{r} \frac{\mathrm{d}}{\mathrm{d}r}(r V_r) + \frac{in}{r} V_\theta$. With some manipulation of pressure and velocity, the system matrix $\boldsymbol{Q}$ may be found, where

$$\frac{i\omega}{K} P = \frac{\mathrm{d}}{\mathrm{d}r} V_r + \frac{V_r}{r} + \frac{in}{r} V_\theta = \frac{\mathrm{d}}{\mathrm{d}r} V_r + \frac{V_r}{r} + \frac{in^2}{r^2 \omega \rho_\theta} P, \tag{4.35a}$$

$$\frac{\mathrm{d}}{\mathrm{d}r} V_r = P \left[\frac{i\omega}{K} - \frac{in^2}{r^2 \omega \rho_\theta} \right] - \frac{V_r}{r}. \tag{4.35b}$$

Now that the derivative of P and V_r with respect to r have been found, $\boldsymbol{Q}$ may be written such that

$$\frac{\mathrm{d}}{\mathrm{d}r} \begin{pmatrix} P \\ V_r \end{pmatrix} = \boldsymbol{Q} \begin{pmatrix} P \\ V_r \end{pmatrix}, \quad \text{where} \quad \boldsymbol{Q} = \begin{pmatrix} 0 & i\omega\rho_r \\ \frac{i\omega}{K} - \frac{in^2}{r^2 \omega \rho_\theta} & -\frac{1}{r} \end{pmatrix}. \tag{4.36}$$

Using the same method as before, the Matricant, $\boldsymbol{M}$, may be found, using an ODE solver for $\frac{\mathrm{d}\boldsymbol{M}}{\mathrm{d}r} = \boldsymbol{QM}$.

4.6 Far field response

By using the Method of Steepest Descent the behavior of the Bessel functions can be found for $x >> 1$. We may then apply this result to the wave solutions for large values of kr. Hence,

$$\int_A^B \mathbf{X}(z) e^{rf(z)} dz = \sqrt{\frac{2\pi}{r}} \frac{e^{rf(z_0)}}{[-f''(z_0)]^{1/2}} [1 + \boldsymbol{o}(1)].$$

Evaluating the Hankel function for large r,

$$H_n^{(1)}(r) = \frac{e^{i\pi n/2}}{\pi} \int_{C_1} e^{ir\cos z} e^{inz} dz = \frac{e^{i\pi n/2}}{\pi} \int_{C_1} e^{rf(z)} \mathbf{X}(z) dz,$$

where $\mathbf{X}(z) = e^{inz}$, $f(z) = i\cos z$, $f'(z) = -i\sin z$, $f''(z) = -i\cos z$. The critical points (saddle points) are found by finding $f'(z) = 0$ which correspond to $z = 0, \pm\pi, \pm 2\pi, \ldots$ The integration limits of $H_n^{(1)}(r)$ in the complex z-plane are found from Figure 4.2. Figure 4.2 shows that the most direct path of steepest descent intersects the critical

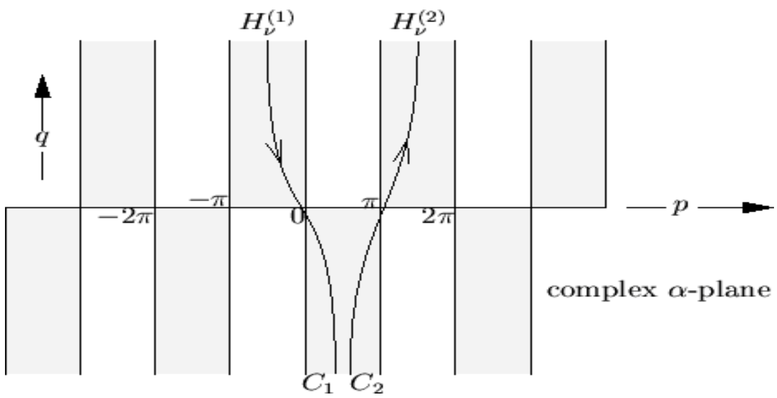

Figure 4.2: Contour integration paths C_1 and C_2 for the two Hankel functions $H_n^{(1)}$ and $H_n^{(2)}$. Source: http://www.math.ohio-state.edu/ gerlach/math/BVtypset/node121.html

point $z_0 = 0$. The phase angle, ϕ, of the integration path $z - z_0 = \tau e^{i\phi}$ is determined by the condition $(z - z_0)^2 f''(z_0) = -\tau^2 |f''(z_0)|$ such that $e^{2i\phi} e^{-i\pi/2} = -1 = e^{\pm i\pi}$, so $e^{i\phi} = e^{-i\pi/4}$. So, for large r the asymptotic expansion of the Hankel function is

$$H_n^{(1)}(r) = \frac{e^{-i\pi n/2}}{\pi} \sqrt{\frac{2\pi}{r}} e^{ir} e^{-i\pi/4} [1 + \boldsymbol{O}(\frac{1}{r})]. \tag{4.37}$$

4.6.1 Far field scattering response

Consider the scattered pressure when kr becomes very large, ($kr >> 1$). $P_{scattered}$ was defined in Equation (4.5), using the series expansion

$$H_n^{(1)}(kr) \longrightarrow a_n \frac{e^{ikr}}{\sqrt{kr}}[1 + \boldsymbol{O}(\frac{1}{kr})],$$

where, from Equation (4.37), $a_n = e^{\frac{-i\pi}{4}} e^{\frac{-in\pi}{2}} \sqrt{\frac{2}{\pi}}$. Now, $P_{scattered}$ can be broken up into functions, $f(\theta)$, and $g(r)$, as follows:

$$\frac{P_{scattered}}{P_0} = g(r)f(\theta), \tag{4.38}$$

where,

$$g(r) = \frac{e^{ikr}}{\sqrt{kr}}, \qquad f(\theta) = e^{\frac{-i\pi}{4}} \sqrt{\frac{2}{\pi}} \sum_{n=-\infty}^{\infty} A_n e^{in(\theta - \frac{\pi}{2})}. \tag{4.39}$$

Using A_n as defined in Equation (4.8), a polar plot can be created describing the amount of scattering as a function of θ, as done in Figure 4.3. The upper image in Figure

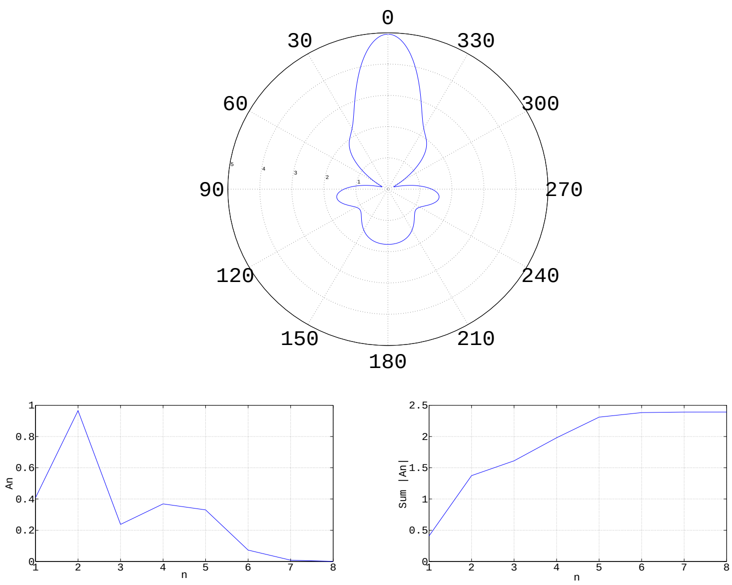

Figure 4.3: Polar plot for rigid cylinder using equation (4.12) for $a = 1$, cylinder radius, n ranges from -10 to 10 , $\rho = 1$, $c = 100$, magnitude of incoming wave, $P_0 = 10$, $\omega = \frac{3.4c}{a}$. The bottom two figures show the convergence of the A_n coefficients.

4.3 compares well with Figure 9 of [19], showing the direction of far field scattering as a function of θ as well as the convergence of the scattering coefficients, A_n, as a function of n. Next by finding the scattering coefficients, A_n, such that they depend on solid material properties, which unlike fluids will include shear waves, more figures from Faran [19] may be compared to. This is done by using Equation (4.40) from [20],

$$\hat{Z_\perp} = \frac{Z_\perp}{C_{66}} = 2\begin{bmatrix} 1 & in \\ -in & 1 \end{bmatrix} + (k_2a)^2\begin{bmatrix} k_1a\frac{J_n'(k_1a)}{J_n(k_1a)} & -in \\ in & k_2a\frac{J_n'(k_2a)}{J_n(k_2a)} \end{bmatrix}^{-1}, \tag{4.40}$$

where the impedance, pressure divided by velocity, of Equation (4.40) is given by

$$\hat{z} = \frac{Z_2}{k_2a}\frac{\det(\hat{Z_\perp})}{\hat{Z_{\perp 22}}}.$$

Now, by matching the impedance at the interface in this case between a solid cylinder and a fluid at radius $r = a$, the next equation may be solved to find A_n and a polar plot may be produced to compare with Faran [19], where

$$\frac{Z_2}{k_2a}\frac{\det(\hat{Z_\perp})}{\hat{Z_{\perp 22}}} = \frac{Z_3(i^nJ_n(k_3a) + A_nH_n^{(1)}(k_3a))}{i^nJ_n'(k_3a) + A_nH_n^{'(1)}(k_3a)},$$

rewritting shows that A_n is,

$$A_n = \frac{i^n(\hat{z}J_n'(k_3a) - Z_3J_n(k_3a))}{Z_3H_n^{(1)}(k_3a) - \hat{z}H_n^{'(1)}(k_3a)}. \tag{4.41}$$

Figure 4.4 compares with Figure 3 from Faran [19] for which the target is a brass cylinder surrounded by water.

4.7 Energy conservation

In the two-dimensional case, the energy balance requires that the total energy flux averaged over one period must be zero. The energy flux is found by multiplying pressure and velocity, where the intensity is a measure of the time-averaged energy flux. Using the period $\frac{2\pi}{\omega}$ we write

$$\int \mathrm{dS}\; n.(\underline{V}P) = r_0\int_0^{2\pi} \mathrm{d}\theta\; V_rP, \quad r = r_0 > a. \tag{4.42}$$

Next the real parts of pressure and velocity are written and multiplied to find the energy flux.

$$\mathrm{Re}(P(r,\theta)e^{-i\omega t}) = \frac{1}{2}[P(r,\theta)e^{-i\omega t} + P^*(r,\theta)e^{i\omega t}], \tag{4.43a}$$

$$\mathrm{Re}(V(r,\theta)e^{-i\omega t}) = \frac{1}{2}[V(r,\theta)e^{-i\omega t} + V^*(r,\theta)e^{i\omega t}], \tag{4.43b}$$

$$F = \mathrm{Re}(Pe^{-i\omega t})\mathrm{Re}(Ve^{-i\omega t}) = \frac{1}{4}[PVe^{-2i\omega t} + P^*\mathrm{V}^*e^{2i\omega t} + (PV^* + P^*V)]. \tag{4.43c}$$

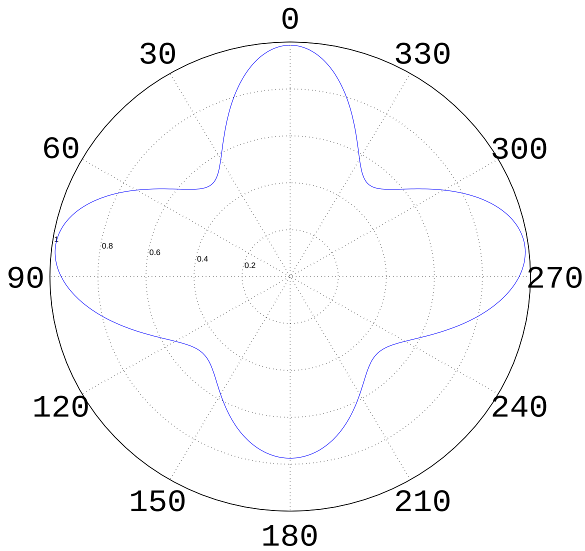

Figure 4.4: Scattering pattern for brass cylinder .0322 inches in diameter at frequency 1.00 mc/sec. Young's modulus is $10.1 * 10^{11}$ dynes/cm^2. $x_3 = 1.7, x_1 = 0.6$, where x_* is $k_* a$, Poisson's ratio is $\frac{1}{3}$ and $\rho_1 = 8.5$ g/cm^3.

Taking the average over one period,

$$\int_0^{\frac{2\pi}{\omega}} F \,\mathrm{dt} = \frac{\pi}{2\omega}(PV^* + P^*V), \quad \text{since} \quad \int_0^{2\pi} e^{ix}\mathrm{dx} = 0, \tag{4.44}$$

where $PV^* + P^*V = 2\mathrm{Re}(P^*V)$. Next we use energy conservation such that

$$\frac{\partial}{\partial t}(\frac{1}{2}\rho_0 v^2 + \frac{\rho^2}{2\rho_0 c^2}) + \nabla.F = 0, \tag{4.45a}$$

$$\int_0^{\frac{2\pi}{\omega}} \mathrm{dt}\nabla.F = 0. \tag{4.45b}$$

The above requires that the intensity integrated over all angles, θ, be zero,

$$\int_0^{2\pi} \mathrm{Re}(P^*V_{,r}) \,\mathrm{d}\theta = 0. \tag{4.46}$$

We separate the above into three parts for convenience such that

$$\int_0^{2\pi} \mathrm{Re}(P^*_{sc}V_{sc,r})\mathrm{d}\theta + \int_0^{2\pi} \mathrm{Re}(P^*_{inc}V_{inc,r})\mathrm{d}\theta + \int_0^{2\pi} \mathrm{Re}(P^*_{inc}V_{sc,r} + P^*_{sc}V_{inc,r})\mathrm{d}\theta = 0. \tag{4.47}$$

By considering values for large kr and noting the flux of incident waves over a closed surface is zero the middle term drops out. We find a relationship for the A_n coefficients which is derived in detail in the appendix, Section A, where:

$$\frac{4|P_0|^2}{r\omega\rho}[\sum_{n=-\infty}^{\infty} |A_n|^2 + \sum_{n=-\infty}^{\infty} \mathrm{Re}(A_n e^{-\frac{in\pi}{2}})] = 0. \tag{4.48}$$

$$\sum_{n=-\infty}^{\infty} |A_n|^2 = -\sum_{n=-\infty}^{\infty} \mathrm{Re}(A_n e^{-\frac{in\pi}{2}}). \tag{4.49}$$

This is a useful relationship since it can be applied to check the A_n coefficients.

The scattering cross-section is a ratio between the time averaged rate at which energy of the incident wave crosses a unit area normal to wave propagation (3D) or unit length normal (2D) and the time averaged rate at which energy is scattered by the target over one period. In the limit of optics, where the wavelength approaches zero and the object is taken as rigid, the scattering cross-section of a sphere of radius, r, is simply $\sigma_{sc} = \pi r^2$ so that in 2D the scattering length is simply $2r$. These results can be used as a check in acoustics for small wavelengths with relatively rigid and large objects. The scattering cross-section, σ_{sc}, is found in acoustics by integration of the absolute value squared of Equation (4.39) such that

$$\sigma_{sc} = \frac{1}{2}\int_0^{2\pi} |f(\theta)|^2 \mathrm{d}\theta. \tag{4.50}$$

Using Equation (4.49) and simplifying as much as possible, the total scattering cross-section, σ_{sc}, in 2D will be

$$\sigma_{sc} \equiv \sum_{n=-\infty}^{\infty} -2\mathrm{Re}(A_n e^{-\frac{in\pi}{2}}) \equiv \sum_{n=-\infty}^{\infty} 2|A_n|^2. \tag{4.51}$$

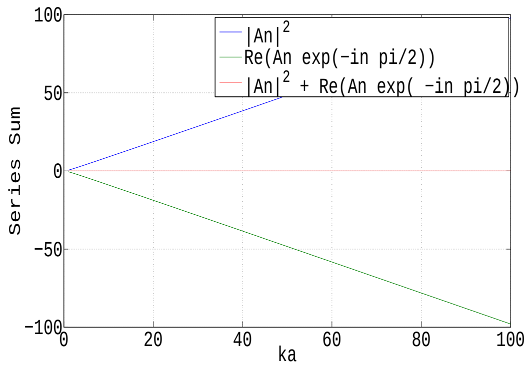

Figure 4.5: Numerical check of the optical theorem using $A_{n,rigid}$.

4.8 Conclusion

In this chapter we have developed acoustic scattering solutions from plane wave interaction with infinitely long cylinders. Solutions techniques such as the Matricant

Propagator and Global Matrix methods were formulated and examples shown. Development of cylindrically layered media and the effective properties of such a material was discussed and will allow for a study of inertial cloaking structures. This chapter has laid the foundation for us to consider cylindrical acoustic cloaks which will be discussed later on. Next, however, we will discuss these solution techniques for three-dimensional, spherical coordinates.

Chapter 5

3D Acoustic Wave Theory

Continuing the development into three-dimensional, spherical coordinates from Section 2.3, we find the solution for scattering from a single as well as concentric spheres. The Matricant is further developed into spherical coordinates using properties of each spherical shell, with density, ρ_i and speed of sound, c_i, as well as for radial properties, ρ_r, ρ_θ and K_{eff}, for homogenized concentric spheres continuing development from Section 4.5.4. Lastly, energy conservation yields the far field scattering solution as a function of θ, as well as relations for the scattering cross section, σ_{sc}. This is the last chapter before we delve into acoustic cloaking theory.

5.1 Scattering from a sphere

In spherical coordinates, z transforms into $r\cos\theta$. Referring back to Section 4.1, we use the complex Fourier series and then use Abramowitz and Stegun [15] to find the solution of the incident wave in terms of spherical Bessel functions and Legendre polynomials.

$$e^{ikz} = P_{incident} = \sum_{n=0}^{\infty} i^n(2n+1)j_n(k_0 r)P_n(\cos\theta), \tag{5.1}$$

where $P_n(\cos\theta)$ is the nth degree Legendre polynomial. Next, the scattered solution is similar to the solution found for cylindrical coordinates, where we leave out solutions involving $h_n^{(2)}(kr)$, as these waves would represent energy scattered from infinity to the field, which by the Sommerfeld condition, are not present. We therefore have

$$P_{scattered} = \sum_{n=0}^{\infty} A_n h_n^{(1)}(k_0 r)P_n(\cos\theta). \tag{5.2}$$

Similarly, solutions for $0 \leq r < a$ require that the coefficient for $y_n(kr)$ must be zero since $y_n(r \to 0) \to \infty$. The total pressure solution for a plane wave incident on a sphere of radius, a, is then given by

$$P(r,\theta)=\sum_{n=0}^{\infty}P_n(\cos\theta)\begin{cases} i^n(2n+1)j_n(k_0r)+A_nh_n^{(1)}(k_0r), & r>a,\\ B_nj_n(kr), & 0\le r<a.\end{cases}$$

By using the linearized momentum equation the radial and angular velocities may be found where $i\omega\rho\underline{V}=\nabla P$, $V_r=\frac{1}{i\omega\rho}\frac{\partial P}{\partial r}$, $V_\theta=\frac{1}{ri\omega\rho}\frac{\partial P}{\partial\theta}$, $V_\phi=\frac{1}{r\sin\theta}\frac{\partial P}{\partial\phi}=0$. We can then write out the solutions for V_r and V_θ as functions of r and θ. Hence,

$$V_r(r,\theta)=-i\sum_{n=0}^{\infty}P_n(\cos\theta)\begin{cases} Z_0^{-1}\left[i^n(2n+1)j_n'(k_0r)+A_nh_n^{(1)'}(k_0r)\right], & r>a,\\ Z^{-1}B_nj_n'(kr), & 0\le r<a,\end{cases} \tag{5.3}$$

$$V_\theta(r,\theta)=\sum_{n=0}^{\infty}\frac{n\cos\theta P_n(\cos\theta)-nP_{n-1}(\cos\theta)}{ri\omega\rho\sin\theta}\begin{cases} i^n(2n+1)j_n(k_0r)+A_nh_n^{(1)}(k_0r), & r>a,\\ B_nj_n(kr), & 0\le r<a.\end{cases}$$

The coefficients A_n and B_n are found by making pressure and velocity continuous at the boundary $r=a$. Thus,

$$B_n=\frac{i^n(2n+1)\left[j_n'(k_0a)-\frac{j_n(k_0a)h_n^{(1)'}(k_0a)}{h_n^{(1)}(k_0a)}\right]}{\frac{Z_0}{Z}j_n'(ka)-\frac{j_n(ka)h_n^{(1)'}(k_0a)}{h_n^{(1)}(k_0a)}}, \tag{5.4a}$$

$$A_n=\frac{B_nj_n(ka)}{h_n^{(1)}(k_0a)}-\frac{i^n(2n+1)j_n(k_0a)}{h_n^{(1)}(k_0a)}. \tag{5.4b}$$

With these coefficients found, the scattering solution is complete for a plane wave incident on a sphere. Relationships between the spherical Bessel functions and Bessel functions are given below from [15]. These are important for programming numerical solutions, as Matlab does not contain the spherical functions but does include the Bessel functions as used in the previous chapter.

$$j_n(x)=\sqrt{\frac{\pi}{2x}}J_{n+\frac{1}{2}}(x), \tag{5.5a}$$

$$y_n(x)=\sqrt{\frac{\pi}{2x}}Y_{n+\frac{1}{2}}(x), \tag{5.5b}$$

$$h_n^{(1)}(x)=\sqrt{\frac{\pi}{2x}}H^{(1)}_{n+\frac{1}{2}}(x), \tag{5.5c}$$

$$\frac{\partial}{\partial x} j_n(x) = \sqrt{\frac{\pi}{2x}}\left(\frac{J_{n-\frac{1}{2}}(x) - J_{n+\frac{3}{2}}(x)}{2}\right) - \frac{1}{2}\sqrt{\frac{\pi}{2}} x^{-3/2} J_{n+\frac{1}{2}}(x), \tag{5.6a}$$

$$\frac{\partial}{\partial x} y_n(x) = \sqrt{\frac{\pi}{2x}}\left(\frac{Y_{n-\frac{1}{2}}(x) - Y_{n+\frac{3}{2}}(x)}{2}\right) - \frac{1}{2}\sqrt{\frac{\pi}{2}} x^{-3/2} Y_{n+\frac{1}{2}}(x), \tag{5.6b}$$

$$\frac{\partial}{\partial x} h_n^{(1)}(x) = \sqrt{\frac{\pi}{2x}}\left(\frac{H^{(1)}_{n-\frac{1}{2}}(x) - H^{(1)}_{n+\frac{3}{2}}(x)}{2}\right) - \frac{1}{2}\sqrt{\frac{\pi}{2}} x^{-3/2} H^{(1)}_{n+\frac{1}{2}}(x). \tag{5.6c}$$

In general, these functions have the property $\frac{d}{dz} f_n(z) = \frac{n}{z} f_n(z) - f_{n+1}(z)$.

5.2 Matricant in 3D: spherical coordinates

By using mass and momentum balance, the derivatives of pressure and velocity may be found with respect to pressure and velocity. Starting with the mass balance equation, $i\omega P = K\nabla.\underline{\mathrm{V}}$, where in spherical coordinates the divergence of velocity is

$$\nabla.\underline{\mathrm{V}} = \frac{1}{r^2}\frac{\partial}{\partial r}(r^2 V_r) + \frac{1}{r\sin\theta}\frac{\partial}{\partial \phi} V_\phi + \frac{1}{r\sin\theta}\frac{\partial}{\partial \theta}(V_\theta \sin\theta). \tag{5.7}$$

With some manipulations we find the derivative of the quantity $r^2 V_r$ with respect to r, in terms of P and V_r. Thus,

$$\frac{r^2 i\omega P}{K} = \frac{\partial}{\partial r}(r^2 V_r) + \frac{1}{i\omega\rho\sin\theta}\frac{\partial}{\partial\theta}(\frac{\partial P}{\partial \theta}\sin\theta), \tag{5.8a}$$

$$\frac{\partial}{\partial r}(r^2 V_r) = \frac{r^2 i\omega P}{K} - \frac{1}{i\omega\rho\sin\theta}\frac{\partial}{\partial\theta}(\sin\theta\frac{\partial P}{\partial \theta}), \tag{5.8b}$$

$$\frac{\mathrm{d}}{\mathrm{d}r}(r^2 V_r) = (\frac{i\omega r^2}{K} + \frac{n(n+1)}{i\omega\rho})P, \tag{5.8c}$$

where the last equation, (5.8c) comes from the Legendre differential equation of the form

$$\frac{1}{\sin(\theta)}[\sin(\theta)\Theta']' + \left[l(l+1) - \frac{m^2}{\sin^2(\theta)}\right]\Theta = 0, \tag{5.9}$$

with $m = 0$, for azimuthal symmetry. From Equation (5.3), the derivative of pressure is found such that we may write the matrix equation,

$$\frac{\mathrm{d}}{\mathrm{d}r}\begin{pmatrix} P \\ r^2 V_r \end{pmatrix} = i\omega \begin{pmatrix} 0 & \frac{\rho}{r^2} \\ \frac{r^2}{K} - \frac{n(n+1)}{\rho\omega^2} & 0 \end{pmatrix}\begin{pmatrix} P \\ r^2 V_r \end{pmatrix}. \tag{5.10}$$

This is now in a form where $\boldsymbol{Q} = i\omega \begin{pmatrix} 0 & \frac{\rho}{r^2} \\ \frac{r^2}{K} - \frac{n(n+1)}{\rho\omega^2} & 0 \end{pmatrix}$, and we may proceed as in Section 4.3 to find $\boldsymbol{M}$.

5.2.1 Alternative Matricant

An alternative form of $\boldsymbol{Q}$ depends on the choice of the state vector. In the previous section the state vector was given by $\begin{pmatrix} P \\ r^2V_r \end{pmatrix}$. Here we derive the Matricant using the effective radial properties, where the state vector is now $\begin{pmatrix} P \\ V_r \end{pmatrix}$. From balance of momentum,

$$i\omega \begin{pmatrix} \rho_r & 0 \\ 0 & \rho_\theta \end{pmatrix} \begin{pmatrix} V_r \\ V_\theta \end{pmatrix} = \begin{pmatrix} \frac{\partial}{\partial r}P \\ \frac{in}{r}P \end{pmatrix}. \tag{5.11}$$

This means $V_\theta = \frac{n}{r\omega\rho_\theta}P$ and $\frac{\partial}{\partial r}P = i\omega\rho_r V_r$. Using the above equation and the balance of mass equation, $i\omega P = K\nabla.\underline{V}$, the derivative of V_r is found with respect to r

$$\frac{i\omega}{K}P = \frac{\partial}{\partial r}V_r + \frac{V_r}{r} + \frac{in}{r}V_\theta = \frac{\partial}{\partial r}V_r + \frac{V_r}{r} + \frac{in^2}{r^2\omega\rho_\theta}P, \tag{5.12a}$$

$$\frac{\partial}{\partial r}V_r = P\left[\frac{i\omega}{K} - \frac{in^2}{r^2\omega\rho_\theta}\right] - \frac{V_r}{r}. \tag{5.12b}$$

Rewriting the equations in matrix form, we have

$$\frac{\partial}{\partial r}\begin{pmatrix} P \\ V_r \end{pmatrix} = \begin{pmatrix} 0 & i\omega\rho_r \\ \frac{i\omega}{K} - \frac{in^2}{r^2\omega\rho_\theta} & -\frac{1}{r} \end{pmatrix} \begin{pmatrix} P \\ V_r \end{pmatrix}, \tag{5.13}$$

where we can see that

$$\boldsymbol{Q} = \begin{pmatrix} 0 & i\omega\rho_r \\ \frac{i\omega}{K} - \frac{in^2}{r^2\omega\rho_\theta} & -\frac{1}{r} \end{pmatrix}. \tag{5.14}$$

Again, referring back to Section 4.3, $\boldsymbol{M}$ may be found by integration of $\frac{d\boldsymbol{M}}{dr} = \boldsymbol{QM}$.

5.3 Concentric spheres general solution

Very similar to the development of Section 4.4.1, the solution for a plane wave incident on concentric spheres takes the form

$$P(r,\theta) = \sum_{n=0}^{\infty} P_n(\cos\theta) \begin{cases} P_0 i^n (2n+1) j_n(k_0 r) + C_{0n} h_n^{(1)}(k_0 r), & r > r_1, \\ C_{1n} j_n(k_1 r) + D_{1n} y_n(k_1 r), & r_1 > r > r_2, \\ C_{2n} jn(k_2 r), & r_2 > r \geq 0, \end{cases}$$

$$V_r(r,\theta) = -i \sum_{n=0}^{\infty} P_n(\cos\theta) \begin{cases} Z_0^{-1}\left[P_0 i^n (2n+1) j_n'(k_0 r) + C_{0n} h_n^{(1)'}(k_0 r)\right], & r > r_1, \\ Z_1^{-1}\left(C_{1n} j_n'(k_1 r) + D_{1n} y_n'(k_1 r)\right), & r_1 > r > r_2, \\ Z_2^{-1} C_{2n} j_n'(k_2 r), & r_2 > r \geq 0, \end{cases}$$

where a sphere of properties, ρ_2, c_2 and radius r_2 is surrounded by another sphere of properties ρ_1, c_1 and radius r_1, all contained in an infinite medium of properties ρ_0 and c_0. Notice that, as before, so long as the radius does not go to zero solutions involving $y_n(k_i r)$ exist. By matching pressure and velocity as done before, this system of equations can be turned into a matrix equation, where

$$\begin{pmatrix} h_n^{(1)}(k_0 r_1) & -j_n(k_1 r_1) & -y_n(k_1 r_1) & 0 \\ -Z_0^{-1} h_n^{'(1)}(k_0 r_1) & Z_1^{-1} j_n'(k_1 r_1) & Z_1^{-1} y_n'(k_1 r_1) & 0 \\ 0 & j_n(k_1 r_2) & y_n(k_1 r_2) & -j_n(k_2 r_2) \\ 0 & -Z_1^{-1} j_n'(k_1 r_2) & -Z_1^{-1} y_n'(k_1 r_2) & Z_2^{-1} j_n'(k_2 r_2) \end{pmatrix} \begin{pmatrix} C_{0n} \\ C_{1n} \\ D_{1n} \\ C_{2n} \end{pmatrix} = \begin{pmatrix} -P_0 i^n (2n+1) j_n(k_0 r_1) \\ Z_0^{-1} P_0 i^n (2n+1) j_n'(k_0 r_1) \\ 0 \\ 0 \end{pmatrix}. \tag{5.16}$$

Matricant

Using Equation (5.10), we may find $\boldsymbol{M}$ by integrating $\frac{\mathrm{d}\boldsymbol{M}}{\mathrm{d}r} = \boldsymbol{Q}(r)\boldsymbol{M}$, with $\boldsymbol{M}(0) = \boldsymbol{I}$, where,

$$\frac{\mathrm{d}\boldsymbol{M}}{\mathrm{d}r} = \begin{pmatrix} Q_{1,1}M_{1,1} + Q_{1,2}M_{2,1} & Q_{1,1}M_{1,2} + Q_{1,2}M_{2,2} \\ Q_{2,1}M_{1,1} + Q_{2,2}M_{2,1} & Q_{2,1}M_{1,2} + Q_{2,2}M_{2,2} \end{pmatrix}. \tag{5.17}$$

$\boldsymbol{M}$ is found using an ODE solver to go from the r_2 to r_1 boundary, and then equating

$$\boldsymbol{M}\begin{pmatrix} C_{2n}j_nk_2r_2 \\ \frac{C_{2n}r_2^2}{iZ_2}j_n'(k_2r_2) \end{pmatrix} = \begin{pmatrix} M_{1,1}C_{2n}j_n(k_2r_2) + M_{1,2}\frac{C_{2n}r_2^2}{iZ_2}j_n'(k_2r_2) \\ M_{2,1}C_{2n}j_n(k_2r_2) + M_{2,2}\frac{C_{2n}r_2^2}{iZ_2}j_n'(k_2r_2) \end{pmatrix} = \begin{pmatrix} P(r_1) \\ r_1^2V_r(r_1) \end{pmatrix}. \tag{5.18}$$

Now we may find the scattering coefficient for $r > r_1$ by finding the impedance Z_b at $r = r_1$, where

$$Z_b = \frac{iZ_0\left[P_0 i^n(2n+1)j_n(k_0r_1) + C_{0n}h_n^{(1)}(k_0r_1)\right]}{P_0 i^n(2n+1)j_n'(k_0r_1) + C_{0n}h_n^{(1)'}(k_0r_1)}. \tag{5.19}$$

Inverting the above equation and finding the scattering coefficient gives

$$C_{0n} = \frac{P_0 i^n(2n+1)\left[iZ_0j_n(k_0r_1) - Z_bj_n'(k_0r_1)\right]}{Z_bh_n^{(1)'}(k_0r_1) - iZ_0h_n^{(1)}(k_0r_1)}. \tag{5.20}$$

5.4 Far field response and energy conservation

Far field scattering amplitude may be found by taking Equation (5.2) and finding the response as $r \to \infty$. The spherical Bessel function, $h_n^{(1)}(kr)$, response for $r \to \infty$, may be found by using the method of steepest descent this results in the relation below.

$$\lim_{kr\to\infty} h_n^{(1)}(kr) \approx -i\frac{e^{ikr}}{kr}(-i)^n = -i\frac{e^{i(kr-n\pi/2)}}{kr}. \tag{5.21}$$

Now, the far field scattering amplitude may be represented by a function of $g(r)$ and $f(\theta)$ where each is given by the following:

$$P_{sc} = g(r)f(\theta), \qquad g(r) = \frac{e^{ikr}}{kr}, \qquad f(\theta) = -i\sum_{n=0}^{\infty} A_nP_n(\cos\theta)e^{-in\pi/2}. \tag{5.22}$$

The energy balance requires that the total energy flux averaged over one period must be zero. This is done by integrating the real parts of pressure multiplied by velocity and using a period equal to $\frac{2\pi}{\omega}$. Hence,

$$F = \mathrm{Re}(Pe^{-i\omega t})\mathrm{Re}(Ve^{-i\omega t}) = \frac{1}{4}[PVe^{-2i\omega t} + P^*V^*e^{2i\omega t} + P^*V + PV^*], \tag{5.23}$$

Next, we take the average over one period and note that any integral over one period of a periodic function such as e^{ix} is zero. This leaves us with

$$\int_0^{\frac{2\pi}{\omega}} F\mathrm{d}t = \frac{\pi}{2\omega}(P^*V + PV^*) = \frac{\pi}{\omega}\mathrm{Re}(P^*V). \tag{5.24}$$

Next, by integrating over ϕ and θ, we will find a conserved quantity and find the optical theorem for a plane wave incident on a sphere, since the energy balance requires the net flux to be zero. Equating $\int_0^\pi \int_0^{2\pi} \mathrm{Re}(P^* V_r) \sin\theta \mathrm{d}\phi \mathrm{d}\theta = 0$, yields

$$\int_0^{pi} \int_0^{2\pi} (\mathrm{Re}(P_{sc}^* V_{sc,r}) + \mathrm{Re}(P_{inc}^* V_{inc,r}) + \mathrm{Re}(P_{inc}^* V_{sc,r} + P_{sc}^* V_{inc,r})) \sin\theta \mathrm{d}\phi \mathrm{d}\theta = 0. \quad (5.25)$$

A detailed solution of this integral is located in the appendix, Section B. The end result of Equation (5.25) is the optical theorem for a plane wave incident on a sphere, for which the forward scattering is related to the scattering coefficients by the relation

$$\mathrm{Im}(f(0)) = \sum_{n=0}^{\infty} \frac{|A_n|^2}{2n+1}. \quad (5.26)$$

Again, the cross sectional scattering takes the form

$$\sigma_{sc} = \int_0^{2\pi} \int_0^{2\pi} |f(\theta)|^2 \mathrm{d}\theta \mathrm{d}\phi. \quad (5.27)$$

5.5 Conclusion

Scattering from spheres has much in common with its two dimensional counterpart for cylinders. The Matricant and Global Matrix solution methods have been developed in spherical coordinates. Although examples were not shown, the following chapters will go over many numeric results using both methods. Now, having reviewed acoustic wave theory in two-dimensional polar, and three-dimensional spherical coordinates, we may begin to examine and review cloaking theory in the next chapter with respect to cylinders and spheres.

Chapter 6

Acoustic Cloaking Review

Acoustic cloaking is achieved through transformation acoustics in which a coordinate transformation makes it possible for one region of fluid to acoustically mimic another. Fluids with this property are known as metafluids. The range of possible acoustic metafluids has been derived [21], and includes fluids with anisotropic inertia and pentamode materials. For an acoustic cloak, the transformation considers the limiting case of a point transformed into a finite region, requiring materials that are radically anisotropic with unavoidable singularities associated with material properties. Different singularities are found depending on whether the transformed metafluid is purely pentamodal, or purely inertial. A pentamodal material is a special type of anisotropic elastic medium in which the shear modulus is zero. Perfect inertial cloaks, those created with fluids of anisotropic inertia only, in which the scattered field is zero have been found to require infinite mass [9]. Considering almost perfect cloaks, Torrent and Sánchez-Dehesa [10] and Scandrett et al. [11] have proposed construction techniques of such mediums.

6.1 Torrent and Sánchez-Dehesa model and numerical results

Torrent and Sánchez-Dehesa [10] proposed a two-dimensional inertial cloak in which two fluid shells of equally thin, radially symmetric fluids surrounded an object. The cylindrical layering of the shells yields an effective medium as discussed before with anisotropic density and scalar bulk modulus. A possible cloaking medium proposed by Cummer and Schurig [5] defined the effective medium properties and were then used to define the local properties of the two fluid shells through local averaging equations. This results in a layering of several hundred unique fluids which makes the creation of such a cloak challenging.

6.1.1 Effective medium

As in Section 4.5.1, this cylindrically layered medium will result in a effective density operator and scalar bulk modulus. In general, the effective fluid will be defined by a scalar compressibility C_{eff} and an anisotropic inertia with radial density ρ_r, and circumferential density ρ_θ. Compressibility is defined as the inverse of the bulk modulus, $C = K^{-1}$. The parameters of the effective fluid are defined by homogenization of the stratified medium as in [22],

$$\begin{pmatrix} \rho_r \\ \rho_\theta^{-1} \\ C_{eff} \end{pmatrix} = \begin{pmatrix} \langle \rho \rangle \\ \langle \rho^{-1} \rangle \\ \langle C \rangle \end{pmatrix}, \tag{6.1}$$

where, $\langle \cdot \rangle$ is the local average over the volume fractions of the layered fluids. For the structure proposed by Torrent and Sánchez [10] the local averaging yields the effective properties, such that the averaged quantities are given by,

$$\rho_r = \frac{1}{2}(\rho_1 + \rho_2), \tag{6.2a}$$

$$\rho_\theta = [\frac{1}{2}(\rho_1^{-1} + \rho_2^{-1})]^{-1}, \tag{6.2b}$$

$$K_{eff} = [\frac{1}{2}(K_1^{-1} + K_2^{-1})]^{-1}. \tag{6.2c}$$

A linear transformation proposed by Cummer and Schurig [5] was then used in which the effective properties are defined by the inner, r_0 and outer, r_{out} radii of the cloaking medium, such that an object of radius r_0 may then be cloaked by such a material. With,

$$\rho_r = \frac{r}{r - r_0}, \quad \rho_\theta = \frac{r - r_0}{r}, \tag{6.3a}$$

$$K_{eff} = (\frac{r_{out} - r_0}{r_{out}})^2 \frac{r}{r - r_0}, \tag{6.3b}$$

where the quantities ρ_r, ρ_θ, and K_{eff} have been normalized to the background fluid properties. Using Equations (6.2) and (6.3), Torrent and Sánchez-Dehesa proposed that the properties $\{\rho_j, K_j\}$, $j = 1, 2$ of the two fluid shells have the form,

$$\rho_1(r) = \frac{r}{r - r_0} + \sqrt{\frac{2r_0}{r - r_0}}, \tag{6.4a}$$

$$\rho_2(r) = \frac{r - r_0}{r + \sqrt{2r_0(r - r_0)}}, \tag{6.4b}$$

$$c_1(r) = c_2(r) = \frac{r_{out} - r_0}{r_{out}} \frac{r}{r - r_0}. \tag{6.4c}$$

In order to achieve this equivalence it is necessary that the device have a large number of distinct fluids: 100 and 400 for the two numerical examples reported by Torrent and Sánchez-Dehesa [10]. It is now convenient to replicate these numerical examples using the Global Matrix and Matricant Propagator methods. The next section shows that the two methods result in the same answer. More importantly, it shows that the cylindrical layering of these fluids does indeed create an effective medium with properties as described by Cummer and Schurig [5].

6.2 Numerical comparison

The Matlab code is given in the appendix, Section D.4, where $r_0 = 1$, $r_{out} = 1/2$ and the inner cylinder (object that is being cloaked) is taken as hard, by numerically inserting large values for density and speed of sound. Next we can plot the scattering solutions for the two different methods. Comparing the difference of the scattering coefficient A_n, describing the amplitude of the scattered pressure for $r > r_{out}$ for a given mode n, between the two methods is done below where the difference between the two answers is on the order of 10^{-12}. Clearly these two methods yield equivalent answers.

Matlab Code: 6.1: Comparison of scattering coefficient A_n for Global Matrix and Matricant methods.

```
>>An'-Anm'

ans =

   1.0e-012 *

   -0.0123 - 0.9246i
```

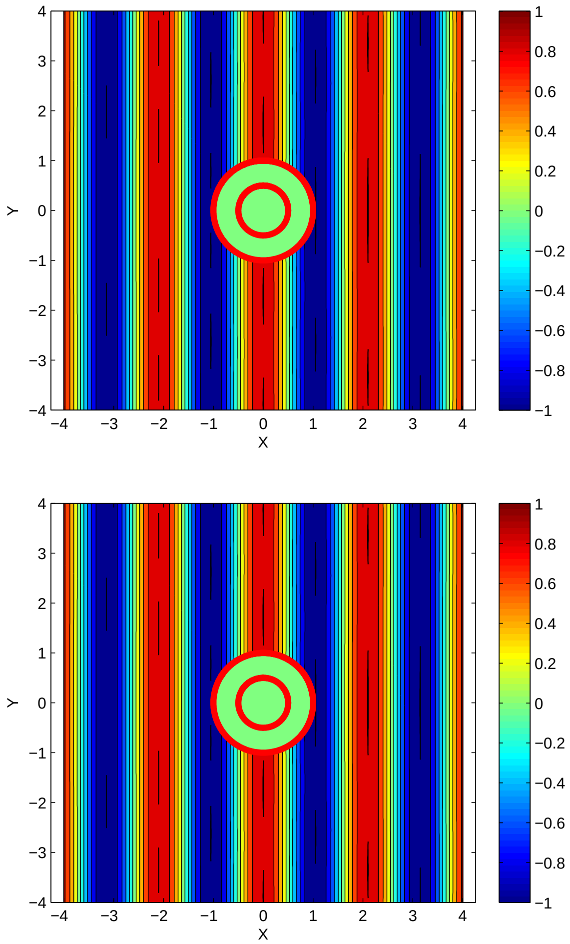

Figure 6.1: Scattering solutions for pressure, Top: Global Matrix Method. Bottom: Matricant Propagator Method

8	0.0011 − 0.4668 i
9	0.0019 − 0.1300 i
10	−0.0003 − 0.0227 i
11	0.0000 − 0.0019 i
12	0.0000 − 0.0001 i
13	−0.0000 − 0.0000 i
14	0.0000 − 0.0000 i
15	−0.0000 − 0.0000 i

The two methods agree with a significant amount of accuracy. Noting that the scattering strength is proportional to $\sum |A_n|^2$, the sum of the absolute value of the scattering coefficients squared is then $\sum |A_n|^2 \approx 2.9184 * 10^{-5}$ for the cloaked object.

Lastly, considering the same cylinder of radius 1/2, without the cloaking medium yields $\sum |A_n|^2 \approx 0.7734$. This shows that a significant amount of scattering has been reduced by this layered cloaking medium.

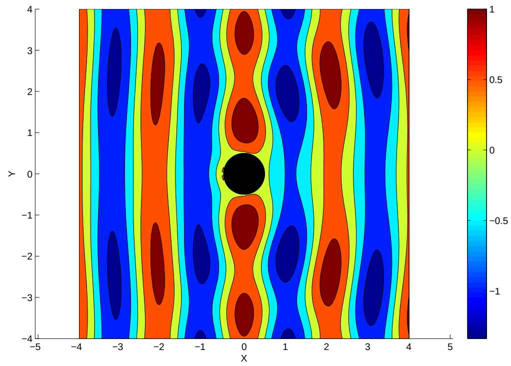

Figure 6.2: Scattering solution for pressure using hard cylinder of radius, 1/2 (no cloaking medium used).

6.3 Conclusion

The numerical demonstration has proven the Matricant Propagator and Global Matrix methods agree with significant accuracy. The layered medium does indeed create an anisotropic medium described by the equations of Cummer and Schurig [5]. Considering feasibility in manufacturing, this cloaking medium will require 400 unique fluids. In the next chapter we consider developing a theory in which we may find the fewest number of individual fluids required to create such a medium.

Chapter 7

Determination of Fewest Distinct Fluids For Inertial Cloaking

This chapter includes the work done in Norris and Nagy [12], which was researched alongside the construction of this thesis. The purpose is to demonstrate that almost perfect inertial cloaks can be achieved using layers comprised of only three acoustic fluids. Similar to Torrent and Sánchez-Dehesa [10], the idea is to make a finely layered shell that surrounds an object, however we only allow the use of N distinct fluids. Instead of prescribing the thickness of each layer, the thickness is allowed to vary as a function of r. Transformation formulas from [9] then imply unique values for the relative concentrations of the N fluids as functions of r, in cylindrical and spherical configurations.

7.1 Setup

Considering radially symmetric configurations, cylindrical in 2D and spherical in 3D, a metafluid shell occupies $0 < r_0 \leq r \leq r_{out}$, where r_0 is the radius of the object to be cloaked. A uniform acoustic medium with density and sound speed ρ_{out}, c_{out}, in $r > r_{out}$ surrounds the structure. The shell is made from N distinct fluids, finely stratified compared to the incident wavelength, that results in an effective material with smoothly varying properties as seen in [10]. Here we are interested in finding the smallest number, N, of distinct fluids to create a metafluid capable of cloaking. Of course $N = 1$ fluid does not result in any effective anisotropic medium as described by the local averages back in Section 6.1.1. We therefore concentrate on the cases $N = 2$ and $N = 3$. We set $r_{out} = 1$, $c_{out} = 1$ and $\rho_{out} = 1$, this chooses units for length, time and mass, respectively and lets us consider non-dimensional quantities.

The N distinct fluids are defined by their mass densities, $\rho_1, \ldots, \rho_N$, and compressibilities $C_1, \ldots, C_N$. Compressibility, C, is defined as the inverse of the bulk modulus, $C_i = K_i^{-1}$ where K_i is the bulk modulus. Wave speeds are defined by $c_i = \sqrt{K_i/\rho_i}$, and the impedances are $Z_i = \sqrt{K_i \rho_i}$, $i = 1, \ldots, N$. Later we will use the quantity $S_i = \rho_i C_i$, or $S_i = c_i^{-2}$, and we may identify $\sqrt{S_i}$ as acoustic slowness in fluid i.

7.1.1 Transformative properties

Referring to Equation (6.1), the local averaging has the form

$$\langle x \rangle = \sum_{i=1}^{N} \phi_i x_i, \quad \text{with } \langle 1 \rangle = 1, \tag{7.1}$$

where it is assumed that volume fractions of fluid i, written as ϕ_i, will be a function of r, $\phi_i = \phi_i(r)$, so that the averages (6.1) define parameters $\rho_r(r)$, $\rho_\theta(r)$, and $C_{eff}(r)$. This type of homogenized medium was proven to occur with cylindrically layered shells as seen in the comparison with Torrent and Sánchez [10].

The acoustic cloak corresponds to transformations from the current (physical) domain to the mimicked one in which the limiting case of a point is mapped to a finite region. This makes the shell appear acoustically as if it is a larger shell of fluid with uniform properties equal to the exterior fluid. The key is a transformation function, $r \to R = R(r)$, such that the range of R exceeds its domain, i.e., the inverse mapping $R \to r$ physically contracts space. To be specific, the outer boundary is mapped to itself, $r = R = 1$, and the inner boundary $r = r_0$ is mapped to $R = R_0$, with $0 < R_0 = R(r_0) < r_0$. The perfect acoustic cloak is defined by $R_0 = 0$. The transformed material has properties ρ_{rT}, $\rho_{\theta T}$, and $C_{eff,T}$, with values uniquely defined by the transformation in $d-$dimensions given by [9] as

$$\begin{pmatrix} \rho_{rT} \\ \rho_{\theta T}^{-1} \\ C_{eff,T} \end{pmatrix} = R' \begin{pmatrix} (r/R)^{d-1} \\ (r/R)^{3-d} \\ (r/R)^{1-d} \end{pmatrix}, \quad d = 2 \text{ or } 3, \tag{7.2}$$

where $R' = \mathrm{d}\, R / \mathrm{d}\, r$.

The connection between the homogenized material (6.1) and the acoustically transformed material (7.2) is now made explicit by requiring $\rho_{rT} = \rho_r$, $\rho_{\theta T} = \rho_\theta$ and

$C_{eff,T} = C_{eff}$ (and we drop the subscript T). Our objective is to find families of transformation functions $R = R(r)$, $\phi_i = \phi_i(r)$ for which this equivalence can be achieved. It depends, of course, on the choices of material properties $\{\rho_i, C_i\}$, $i = 1, \ldots, N$, and not all combinations will work. Among the requirements is that the transformation function is one-to-one, and that the volume fractions are all between zero and unity. We therefore require that $\boldsymbol{\phi} \in \Phi_N$ where $\boldsymbol{\phi}$ is the $N-$dimensional vector of volume fractions, and Φ_N the $N-1$ dimensional surface on which it must lie,

$$\Phi_N = \{\phi_i \geq 0,\ \sum_i \phi_i = 1,\ i = 1, \ldots, N\}. \tag{7.3}$$

In order to gain some understanding of the problem we start with the simpler case $N = 2$ and then move on to consider $N = 3$.

7.2 The two-fluid material

Here we consider the use of $N = 2$ fluids. Interesting metafluid structures made from only two fluids were investigated, where acoustic wave energy may be diverted from the backscatter direction. We find that the use of only two fluids is too restrictive and an additional parameter is required for cloaking to occur. A layering of two unique fluids is considered where the compressibility of one of the fluids is allowed to vary as a function of r, which can be achieved by adding small concentrations of bubbles. We call this the two and a half fluid material.

7.2.1 Algebraic formulation

The first two relations in (6.1), for $d = 2$ dimensions, and the identity (7.1), are written in matrix form as

$$\begin{pmatrix} 1 & 1 & 0 \\ \rho_1 & \rho_2 & -\rho_r \\ \frac{1}{\rho_1} & \frac{1}{\rho_2} & -\rho_\theta^{-1} \end{pmatrix} \begin{pmatrix} \phi_1 \\ \phi_2 \\ 1 \end{pmatrix} = \begin{pmatrix} 1 \\ 0 \\ 0 \end{pmatrix}. \tag{7.4}$$

Inverting the above equation, the concentrations, ϕ_i, are

$$\phi_1 = \frac{\rho_r - \rho_2}{\rho_1 - \rho_2}, \qquad \phi_2 = \frac{\rho_1 - \rho_r}{\rho_1 - \rho_2}, \tag{7.5}$$

and the densities ρ_r, ρ_θ are related by

$$\rho_r + \rho_1\rho_2\rho_\theta^{-1} = \rho_1 + \rho_2. \tag{7.6}$$

The effective compressibility, which follows from (7.5) and the third relation in (6.1), satisfies

$$(\rho_1 - \rho_2)C_{eff} + (C_2 - C_1)\rho_r = \rho_1 C_2 - \rho_2 C_1. \tag{7.7}$$

Equation (7.5) provides relations for the volume fractions in terms of the radial inertia ρ_r. One can also interpret Equations (7.6) and (7.7) as defining ρ_θ and C_{eff}, respectively, in terms of ρ_r. Therefore, all parameters in the two-fluid material can be defined by a single quantity, in this case ρ_r.

However, in order to relate the two-fluid material to a transformation it is necessary that there exists a function R which satisfies the three differential identities (7.2). Substitution of these into Equations (7.6) and (7.7) gives a pair of equations which can be considered as algebraic equations in two unknowns: R' and R/r. Solutions for both of these quantities can be found in terms of the two-fluid properties ρ_1, ρ_2, C_1, C_2, but the solutions are not of practical interest. The reason is that the constant values of R' and R/r that are found, say $R' = a$, $R/r = b$, must be equal, leading to trivial cases. The main conclusion of the study of the $N = 2$ case is that the 2-fluid material is overly restrictive for construction of an acoustic cloak, and we need to introduce more degrees of freedom. Before considering $N = 3$ we note some possible useful properties of the 2-fluid shells.

7.2.2 A special case of a uniform two-fluid material

While it is not possible for the 2-fluid material to reproduce a transformation material suitable for cloaking, it is possible to make some interesting uniform fluids with anisotropic inertia. The idea is to seek constant values of ρ_r, ρ_θ and C_{eff} which also match to the exterior fluid in $r > 1$. This requires that $R = 1$ at $r = 1$. Enforcement of (7.2) then requires the three parameters in the left vector be equal to R'. Substituting into Equation (7.6) yields

$$\rho_r = \rho_\theta^{-1} = C_{eff} = \rho_{r3}, \tag{7.8}$$

where

$$\rho_{ri} = \frac{\rho_j + \rho_k}{1 + \rho_j \rho_k} \quad (i \neq j \neq k \neq i). \tag{7.9}$$

The volume fractions follow from (7.5) as

$$\phi_1 = \rho_1 \rho_{r3} \left(\frac{1 - \rho_2^2}{\rho_1^2 - \rho_2^2} \right), \quad \phi_2 = \rho_2 \rho_{r3} \left(\frac{1 - \rho_1^2}{\rho_2^2 - \rho_1^2} \right), \tag{7.10}$$

which are both positive if and only if $(1-\rho_1)(1-\rho_2) < 0$. The one remaining condition, that for the compressibility, implies using (7.7) and (7.8) and the condition that the two compressibilities must be related such that

$$C_1 \rho_1 (1 - \rho_2^2) + C_2 \rho_2 (\rho_1^2 - 1) = \rho_1^2 - \rho_2^2. \tag{7.11}$$

The anisotropic fluid (7.8) is defined by the parameter $\rho_{r3} = \rho_{r3}(\rho_1, \rho_2)$, and is composed of volume fractions $\phi_i = \phi_i(\rho_1, \rho_2)$ of fluid $i = 1, 2$. Denote any pair satisfying the relation (7.11) as $C_i = C_i(\rho_1, \rho_2)$, $i = 1, 2$. It is interesting to note that these functions are invariant under the interchange $\{\rho_1, \rho_2, \phi_1, \phi_2, C_1, C_2\} \to \{\rho_2^{-1}, \rho_1^{-1}, \phi_2, \phi_1, C_2, C_1\}$.

Examples

If, for instance, $C_1\rho_1 = C_2\rho_2$ then (7.11) implies that $C_1\rho_1 = C_2\rho_2 = 1$. Both fluids have the same wave speed as the background fluid. They differ only in their impedances, which in this case are $z_i = \rho_i = C_i^{-1}$, $i = 1, 2$.

Conversely, if $C_1/\rho_1 = C_2/\rho_2$ then (7.11) implies that $C_1/\rho_1 = C_2/\rho_2 = 1$. The two fluids have the same acoustic impedance as the background fluid, and differ only in their wave speeds, which are $c_i = \rho_i^{-1} = C_i^{-1}$, $i = 1, 2$.

Interesting properties of two fluid mediums

Using Equation (7.8) we may investigate interesting properties of an inertial medium described by a single parameter ρ_r. Utilizing Equations (4.31a), (4.31b), and (4.36), we may now compare solutions using anisotropic properties where, (4.31a), (4.31b) are used to construct a global matrix method and (4.36) is used to find Matricant propagator solutions. The Matlab code in the appendix D.6 considers a rigid object of radius,

$r_0 = 1/2$, surrounded by a medium described by Equation (7.8), where $\rho_r = 20$ and outer radius $r_{out} = 1$. This structure is then immersed in a fluid of $\rho_0 = 1$ and $c_0 = 1$.

Running the Matlab code in the appendix, Section D.6, allows us to compare answers for the scattering coefficients, A_n. The code uses the global matrix and Matricant propagator methods, using the effective properties, ρ_r, ρ_θ and C_{eff} from Equations (4.31a), (4.31b), and (4.36).

Comparing results for the two methods,

```
>> Anm'-An'
ans =
   1.0e-004 *
    0.2860 - 0.3445i
   -0.1803 - 0.4213i
    0.0844 + 0.4155i
   -0.3400 - 0.0901i
    0.1649 - 0.2453i
    0.0772 - 0.0746i
    0.0000 + 0.0000i
    0.0000 + 0.0000i
```

Also, comparing scattering strength measured by $\sum |A_n|^2$, found by the two methods,

```
>> sum(abs(An).^2)
ans =
     3.7391

>> sum(abs(Anm).^2)
ans =
     3.7391

>> sum(abs(A_r).^2)
ans =
     2.4967
```

where An, in the above command prompt, was found using the global matrix method and Anm was found using the Matricant, A_r is the scattering coefficients caused by a rigid cylinder of radius, $r_0 = 1/2$. Unfortunately this medium increased the scattering. However we find that a significant amount of energy has been directed away from the backscattering direction. Using Equation (4.39) polar plots were created, as shown in Figure 7.1. Lastly, this medium can be achieved by layering shells described by Equations (7.9) and (7.10), where for $\rho_r = 20$ a possible combination of two fluid layering may be $\rho_1 = .01$, $\rho_2 = 24.9875$ where the volume fractions of the layered shells for fluid i will have the ratio $\phi_1 = .19968$ and $\phi_2 = .80032$. From Figure 7.1 the rigid cylinder causes a significant amount of backscatter. However, using a two fluid medium with the property of $\rho_r = 20$ and defined by Equation (7.8) a large amount of energy has been directed away from the backscatter direction.

7.2.3 Two and a half fluids

We consider the 2D case, for which $(r/R)R' = \rho_r$, from Equation $(7.2)_1$. It follows from $(7.6)_2$, i.e. $\rho_r = \rho_\theta^{-1}$, that $\rho_r = \rho_{r3}$, a constant. Taking into account the boundary condition $R(1) = 1$, the unique mapping is

$$R(r) = r^{\rho_{r3}}. \tag{7.12}$$

Equation (7.7) combined with $(7.2)_3$ then implies

$$(1 - \rho_2^2)S_1 + (\rho_1^2 - 1)S_2 = (\rho_1^2 - \rho_2^2)r^{2(\rho_{r3}-1)}. \tag{7.13}$$

This cannot be satisfied if the fluids have properties independent of r. If we still require that the densities are fixed, but the compressibilities could vary with r, then (7.13) suggests that a mapping can be realized if one or both S_1, S_2 are such that the equality holds for some range of r. It is well known that adding a small concentration of bubbles to a liquid results in an increase in the compressibility without significant change in the effective density.

Since $(\rho_1 - 1)(\rho_3 - 1)$ must be negative, we take, with no loss in generality, $\rho_1 > 1 > \rho_3$. A large value of ρ_{r3} is achieved if $\rho_1 \gg 1$, $\rho_3 \ll 1$, in which case (7.13) becomes

$$\rho_1^{-2}S_1 + S_2 \approx r^{2(\rho_{r3}-1)}. \tag{7.14}$$

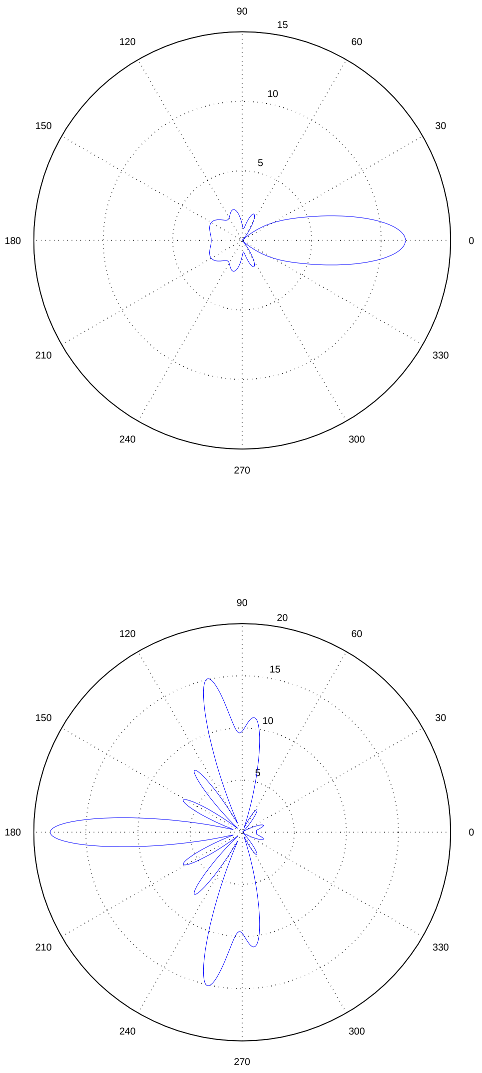

Figure 7.1: The top figure is the far field scattering caused by a rigid cylinder of $r_0 = 1/2$, the bottom is of the same rigid cylinder wrapped in a medium described by equation (7.8) where $\rho_r = 20$ and $r_{out} = 1$.

7.3 The three-fluid material

We now consider $N = 3$ fluid configurations. The extra fluid adds a significant amount of freedom in that we do not expect $\rho_r = \rho_\theta^{-1} = C_{eff}$. Also the volume fractions will not be constrained to single values. Instead, we expect to have $\phi_i = \phi_i(r)$.

7.3.1 Algebraic formulation

We again start with the first two relations in (6.1) and the identity $(7.1)_2$, which may be written in matrix form as

$$\begin{pmatrix} 1 & 1 & 1 \\ \rho_1 & \rho_2 & \rho_3 \\ \rho_1^{-1} & \rho_2^{-1} & \rho_3^{-1} \end{pmatrix} \begin{pmatrix} \phi_1 \\ \phi_2 \\ \phi_3 \end{pmatrix} = \begin{pmatrix} 1 \\ \rho_r \\ \rho_\theta^{-1} \end{pmatrix}. \tag{7.15}$$

Inverting the above equation to find the 3-vector of volume fractions in terms of ρ_r and ρ_θ^{-1} and substituting into the third relation in (6.1) yields an expression for C_{eff} in terms of ρ_r and ρ_θ^{-1}. Thus,

$$\boldsymbol{\phi} = \boldsymbol{f}_0 + \rho_r \boldsymbol{f}_1 + \rho_\theta^{-1} \boldsymbol{f}_2, \tag{7.16a}$$

$$C_{eff} = \alpha + \beta_1 \rho_r + \beta_2 \rho_\theta^{-1}, \tag{7.16b}$$

where the 3-vectors in (7.16a) are

$$\boldsymbol{\phi} = \begin{pmatrix} \phi_1 \\ \phi_2 \\ \phi_3 \end{pmatrix}, \quad \boldsymbol{f}_0 = D \begin{pmatrix} \frac{\rho_2}{\rho_3} - \frac{\rho_3}{\rho_2} \\ \frac{\rho_3}{\rho_1} - \frac{\rho_1}{\rho_3} \\ \frac{\rho_1}{\rho_2} - \frac{\rho_2}{\rho_1} \end{pmatrix}, \quad \boldsymbol{f}_1 = D \begin{pmatrix} \frac{1}{\rho_2} - \frac{1}{\rho_3} \\ \frac{1}{\rho_3} - \frac{1}{\rho_1} \\ \frac{1}{\rho_1} - \frac{1}{\rho_2} \end{pmatrix}, \quad \boldsymbol{f}_2 = D \begin{pmatrix} \rho_3 - \rho_2 \\ \rho_1 - \rho_3 \\ \rho_2 - \rho_1 \end{pmatrix}, \tag{7.17}$$

with $D = \rho_1\rho_2\rho_3/[(\rho_1 - \rho_2)(\rho_2 - \rho_3)(\rho_3 - \rho_1)]$, and the scalars α, β_1 and β_2 in (7.16b) are

$$\alpha = \boldsymbol{C}^T \boldsymbol{f}_0, \quad \beta_1 = \boldsymbol{C}^T \boldsymbol{f}_1, \quad \beta_2 = \boldsymbol{C}^T \boldsymbol{f}_2, \tag{7.18}$$

with $\boldsymbol{C}^T = (C_1, C_2, C_3)$.

7.3.2 The transformation function

The transformation function $r \to R(r)$ is manipulated into a differential equation and solved in terms of α, β_1, and β_2. Using Equation (7.2) to eliminate C_{eff}, ρ_r and ρ_θ^{-1}

from (7.16b) yields,

$$\Big(\frac{R}{r}\Big)^{d-1}R' = \alpha + \left(\beta_1\Big(\frac{r}{R}\Big)^{d-1} + \beta_2\Big(\frac{r}{R}\Big)^{3-d}\right)R', \tag{7.19}$$

where $d = 2$ or 3 is the spatial dimension. Rewriting results in

$$\frac{\mathrm{d}\,R}{\mathrm{d}\,r} = \alpha \begin{cases} \big(\frac{R}{r} - \beta\frac{r}{R}\big)^{-1}, & 2D, \\ \big(\frac{R^2}{r^2} - \beta_1\frac{r^2}{R^2} - \beta_2\big)^{-1}, & 3D, \end{cases} \tag{7.20}$$

subject to the boundary condition $R(1) = 1$, such that the outer radius is mapped to itself. We define the parameters β, λ, and μ, here as:

$$\beta = \beta_1 + \beta_2 \quad \lambda = \alpha + \beta, \quad \mu = -\frac{\beta}{\alpha}, \tag{7.21}$$

which will be useful in solving (7.20).

2D solution

Considering the 2D Equation $(7.20)_1$, let $x = r^2$, $X = R^2$, then Equation $(7.20)_1$ becomes

$$X\frac{\mathrm{d}\,x}{\mathrm{d}\,X} + \frac{\beta}{\alpha}x = \frac{X}{\alpha}, \qquad x(1) = 1. \tag{7.22}$$

Integrating yields

$$r = \left(\frac{R^2 + (\lambda - 1)R^{2\mu}}{\lambda}\right)^{1/2}. \tag{7.23}$$

The 2D transformation function is therefore completely defined by the two parameters λ and μ.

3D solution

The 3D Equation $(7.20)_2$ becomes, with the change of variable $s = \frac{r}{R}$,

$$\frac{1}{R}\frac{\mathrm{d}\,R}{\mathrm{d}\,s} = \frac{-\alpha s^2}{\beta_1 s^4 + \alpha s^3 + \beta_2 s^2 - 1} = \sum_{i=1}^{4}\frac{\gamma_i}{s - s_i}, \quad R(1) = 1, \tag{7.24}$$

where the four roots s_i and the coefficients γ_i, $i = 1, 2, 3, 4$, are defined by

$$\beta_1\prod_{j=1}^{4}(s - s_j) = \beta_1 s^4 + \alpha s^3 + \beta_2 s^2 - 1, \quad \gamma_i = \frac{-\alpha s_i^2}{\beta_1\prod_{j\neq i}(s_i - s_j)}. \tag{7.25}$$

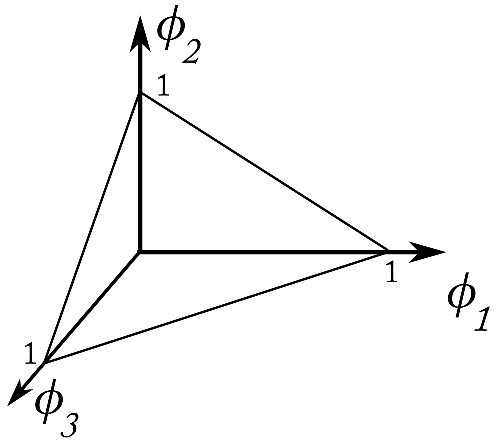

Figure 7.2: The range of $\boldsymbol{\phi}$ for the 3-fluid.

Note that $\sum_i \gamma_i = 0$, $\sum_i s_i = -\alpha/\beta_1$, $\sum_i \gamma_i s_i = -\alpha/\beta_1$, $\sum_i \gamma_i s_i^2 = (\alpha/\beta_1)^2$. Integration of (7.24) yields

$$R = \prod_{i=1}^{4} \left(\frac{\frac{r}{R} - s_i}{1 - s_i} \right)^{\gamma_i}. \tag{7.26}$$

This provides an implicit formula for R and r in terms of the three parameters α, β_1 and β_2. Using the fact that $1 \leq s \leq s_0$, where s_0 is defined in the next subsection, Equation (7.26) gives R as a function of s, from which $r = sR$ is obtained.

7.3.3 The inner radii r_0 and R_0

It follows from continuity of the solution of the differential equation (7.20) that the values of the inner radii r_0 and R_0 should correspond to a point on the edge of the triangular region Φ_3. See Figure 7.2. The actual radial values can be determined by starting with (7.15), using ρ_r and ρ_θ as defined in (7.2), and keeping the parameter $s = \frac{r}{R}$ to express ϕ_i of (7.16a) in the form

$$\phi_i = \frac{\rho_i \left[(s^{d-1} + \rho_j \rho_k s^{3-d}) R' - (\rho_j + \rho_k) \right]}{(\rho_i - \rho_j)(\rho_i - \rho_k)}, \tag{7.27}$$

where $i \neq j \neq k \neq i$. Replacing R' by (7.20) and setting (7.27) to zero implies an algebraic (polynomial) equation for s. In principle there are three possible solutions, corresponding to each of $\phi_i = 0$, $i = 1, 2, 3$. However, in practice for a given set of 3-fluids only one is important, and we choose the 3-fluid properties so that it is the root for $\phi_2 = 0$. We consider first $d = 2$.

In the 2D cylindrical configuration the equation $\phi_2 = 0$ is a quadratic in s with a single positive root greater than unity (corresponding to $r_0 > R_0$), combined with (7.23) we can find both R_0 and r_0 in explicit form as

$$R_0 = \left\{(\lambda - 1)\left(\frac{\rho_{r2}^{-1} - \mu}{1 - \rho_{r2}^{-1}}\right)\right\}^{\frac{1}{2(1-\mu)}}, \tag{7.28a}$$

$$r_0 = \left\{\lambda\left(\frac{\rho_{r2}^{-1} - \mu}{1 - \mu}\right)\right\}^{-\frac{1}{2}} R_0, \tag{7.28b}$$

where ρ_{r2} follows from the definition (7.9).

For the 3D spherical case the equation $\phi_2 = 0$ becomes a biquadratic in s with a single positive root. We find

$$R_0 = \prod_{i=1}^{4} \left(\frac{s_0 - s_i}{1 - s_i}\right)^{\gamma_i}, \quad r_0 = s_0 R_0, \tag{7.29}$$

where s_0 is the smallest positive root greater than unity of

$$s^4[\alpha + \beta_1(\rho_1 + \rho_3)] + s^2[\alpha\rho_1\rho_3 + \beta_2(\rho_1 + \rho_3)] - (\rho_1 + \rho_3) = 0. \tag{7.30}$$

7.3.4 Total mass and average density

The total mass m of the 3-fluid shell is the integral of local average of the density, $\langle\rho\rangle$. Therefore, m follows from Equation (6.1) as the volumetric integral of $\rho_r(r)$. Substituting from $(7.2)_1$ and using (7.20), the integral can be expressed in closed form for the 2D case, and reduced to an integral in $s = r/R$ for the 3D case. We find

$$m = \begin{cases} \frac{\pi}{\lambda}\{1 - R_0^2 + \frac{(\lambda-1)}{\mu}(1 - R_0^{2\mu})\}, & 2D, \\ 4\pi\frac{\alpha}{\beta_1}\int\limits_1^{s_0} s^6 \prod\limits_{i=1}^{4} \frac{\left(s-s_i\right)^{3\gamma_i-1}}{\left(1-s_i\right)^{3\gamma_i}}\,\mathrm{d}\,s, & 3D, \end{cases} \tag{7.31}$$

from which the average density in the shell, $\bar{\rho} = 3m/[\pi(d+1)(1 - r_0^d)]$, can be found. The average density for 2D becomes, after some simplification,

$$\bar{\rho} = \frac{1}{\mu} - \frac{1}{\beta}\left(\frac{1 - R_0^2}{1 - r_0^2}\right), \quad 2D. \tag{7.32}$$

7.3.5 Summary

We have shown that the three-fluid shell is uniquely related to a possible transformation function in both 2- and 3-dimensions. The connection is still somewhat tentative, since

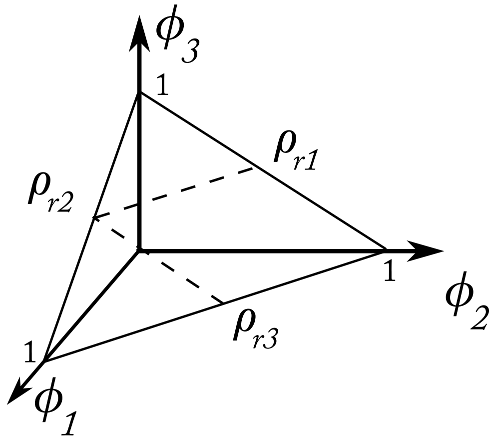

Figure 7.3: The range of $\boldsymbol{\phi}$ for the 3-fluid in the cylindrical configuration. The dashed lines show the possible straight line paths. In practice, the path begins at some point inside the triangular region ($r = R = 1$) and ends at $\phi_2 = 0$ ($r = r_0, R = R_0$).

we must confirm that the function is physically realistic. This requires, among other things, that the volume fractions are all positive and between zero and unity, i.e. that $\boldsymbol{\phi} \in \Phi_3$ where the equilateral triangle surface Φ_3 is defined by (7.3). We will consider numerical examples in a following section. Next we will consider how to go about choosing three fluid possibilities for which the transformation occurs.

7.4 Three fluid analysis

Beginning with the density implications, Equation (7.16a) reduces, using $\rho_r\rho_\theta = 1$, to give

$$\phi_i = \frac{\rho_i(\rho_j + \rho_k)(\rho_r - \rho_{ri})}{\rho_{ri}(\rho_i - \rho_j)(\rho_i - \rho_k)}, \quad i \neq j \neq k \neq i, \tag{7.33}$$

where the critical values of ρ_r are given by (7.9). Based upon the above equation, we note that

$$\phi_i\big|_{\rho_r=\rho_{ri}} = 0, \quad \phi_j\big|_{\rho_r=\rho_{ri}} = \rho_j\rho_{ri}\left(\frac{1-\rho_k^2}{\rho_j^2 - \rho_k^2}\right), \tag{7.34}$$

where $i \neq j \neq k \neq i$. The points defined by (7.34) are the intersections of the line (7.33) with the planes $\boldsymbol{e}_i \cdot \boldsymbol{\phi} = 0$. In order to have some $\boldsymbol{\phi} \in \Phi_3$ at least one of the intersections must lie on the boundary of Φ_3. Consider ρ_{ri} of (7.9), then ϕ_j and ϕ_k must both be positive, which occurs if and only if one of (ρ_j, ρ_k) is larger than, and the other is less than, unity. This gives an important condition, that at least one of the three densities is larger than unity and at least one must be less than unity. We introduce the density values ρ_p, ρ_m, $\{p \neq m\} \in \{1, 3\}$, such that

$$(\rho_2 - 1)(\rho_p - 1) > 0, \quad (\rho_2 - 1)(\rho_m - 1) < 0, \tag{7.35}$$

with $2 \neq p \neq m \neq 2$. We note some other properties of the critical values of the densities:

$$\rho_{ri} - \rho_{rj} = \rho_{ri}\rho_{rj}\frac{(\rho_j - \rho_i)(1 - \rho_k^2)}{(\rho_i + \rho_k)(\rho_j + \rho_k)}, \tag{7.36a}$$

$$\rho_{ri} - 1 = -\rho_{ri}\frac{(\rho_{rj} - 1)(1 - \rho_{rk})}{\rho_{rj} + \rho_{rk}}, \tag{7.36b}$$

where $i \neq j \neq k \neq i$. These imply, respectively, that $\rho_{r2} > \rho_{rp} > \rho_{rm}$, and $\rho_{r2} > 1$, $\rho_{rp} > 1$ and $\rho_{rm} < 1$. Combining these with the previous inequalities, we surmise the ordering $\rho_{r2} > \rho_{rp} > 1 > \rho_{rm}$. Thus, for instance, if $\rho_2 > 1$, then the possible range of ρ_r is $\rho_{r1} \leq \rho_r \leq \rho_{r2}$. If $\rho_2 < 1$ then it is $\rho_{r3} \leq \rho_r \leq \rho_{r2}$. Any value of ρ_r in the range $\rho_{rp} \leq \rho_r \leq \rho_{r2}$ therefore yields a triple of concentration values satisfying $\boldsymbol{\phi} \in \Phi_3$. At the upper (lower) value, $\rho_r = \rho_{r2}$ $(= \rho_{rp})$, the concentration $\boldsymbol{\phi}$ lies on the boundary of the triangle with $\phi_2 = 0$ $(\phi_p = 0)$. But these limiting values are not necessarily achieved. Thus, at $r = R = 1$ the differential equality (7.20) implies that $\rho_r = \alpha/(1 - \beta)$. This is the practical lower bound on the range of ρ_r.

Sensitivity

The reachable range of ρ_r is, from (7.20), $\rho_{rp} < \rho_r < \rho_{rp} + \Delta\rho_r$ where

$$\Delta\rho_r \equiv \rho_{r2} - \rho_{rp} = \frac{(\rho_p - \rho_2)(1 - \rho_m^2)}{(1 + \rho_2\rho_m)(1 + \rho_p\rho_m)}. \tag{7.37}$$

Hence,

$$\begin{aligned}
\frac{\partial\Delta\rho_r}{\partial\rho_2} &= -\frac{(1 - \rho_m^2)}{(1 + \rho_2\rho_m)^2}, \\
\frac{\partial\Delta\rho_r}{\partial\rho_p} &= \frac{(1 - \rho_m^2)}{(1 + \rho_p\rho_m)^2}, \\
\frac{\partial\Delta\rho_r}{\partial\rho_m} &= -\frac{(\rho_p - \rho_2)(1 + \rho_m^2)(\rho_2 + \rho_p + 2\rho_2\rho_p\rho_m)}{(1 + \rho_2\rho_m)^2(1 + \rho_p\rho_m)^2}.
\end{aligned} \tag{7.38}$$

If $p = 1$ these are, respectively, < 0, > 0, < 0. Conversely, if $p = 1$ they are > 0, < 0, > 0. Hence, whether $p = 1$ or $p = 3$ it is clear that $\Delta\rho_r$ is greatest if ρ_1 is large, ρ_2 is close to unity, and ρ_3 is small.

Case	ρ_1	ρ_2	ρ_3	S_1	S_2	S_3
1	10	1	0.2	1	10	0.1
2	10	1	0.2	1	10	0.01
3	100	1	0.02	1	10	0.01
4	1000	1	0.002	1	10	0.01

Table 7.1: The four cases of 3-fluid material considered.

7.5 Numerical results

7.5.1 Example of three-fluid shells

The range of possibilities for the 3-fluid metamaterials is extensive given that there are $3 \times 2 = 6$ independent variables at our disposal. We take $\rho_2 = S_1 = 1$, $\rho_3 = 2/\rho_1$ and $S_2 = 10$, which leaves two parameters: ρ_1 and S_3. Four distinct 3-fluids are considered according to the four sets of parameters in Table 7.1 with different combinations of ρ_1 and S_3. The transformation function and the concentrations of the three fluid constituents are illustrated in Figures 7.4-7.7. The curves $R = R(r)$ illustrate the transformation, which maps the original region $R_0 \le R \le 1$ to the physical domain $r_0 \le r \le 1$, and the values of the inner radii, r_0 and R_0, are given in Table 7.2. Note that $R \le r$, as expected. Also, the concentrations for the 2D shells, in Figures 7.4a, 7.5a, 7.6a and 7.7a, satisfy $\phi_3 \approx 2\phi_1$, since $\rho_1\rho_3 = 2$. The most important aspect is the relative values of r_0 and R_0, in that it is desirable to have r_0 close to unity while R_0 should be close to zero. The value of r_0 is smallest in Figure 7.4 and largest in Figure 7.7, and it appears to increase with ρ_1. In order to obtain a value of r_0 close to unity, it is necessary to have a large value of ρ_1, see Figures 7.6 and 7.7. Although only two values of S_3 are considered here, numerical experiments indicate that the value of R_0 is more sensitive to this parameter, with R_0 decreasing as S_3 is increased. It is also found that better results, i.e. smaller R_0, larger r_0, are obtained when S_2 becomes very large. For instance, $r_0 = 0.989$, $R_0 = 0.031$ is obtained in 2D with $\rho_1 = S_2 = 10^3$, $S_3 = 10^{-3}$.

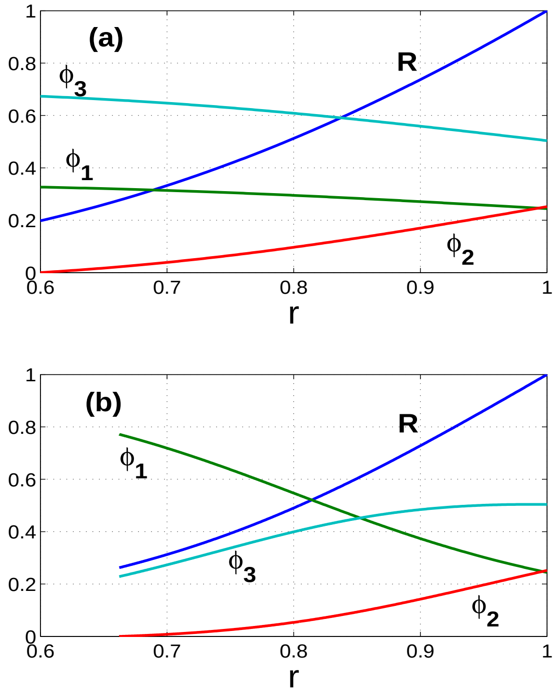

Figure 7.4: The curves show the concentrations of the three fluids and the radius R as functions of the physical radial coordinate r for the fluid parameters of Case 1 (see Table 1). (a) the 2D cylindrical configuration; (b) the 3D spherical shell.

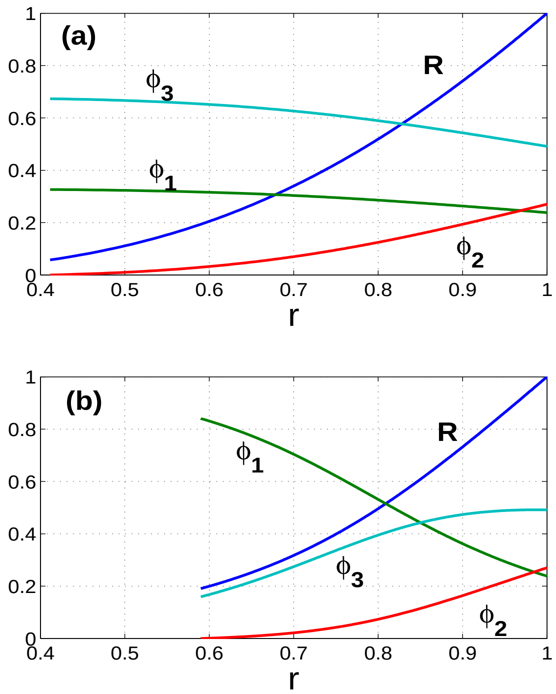

Figure 7.5: Case 2. The parameters are the same as in figure 7.4 with the exception that now $S_3 = 0.01$.

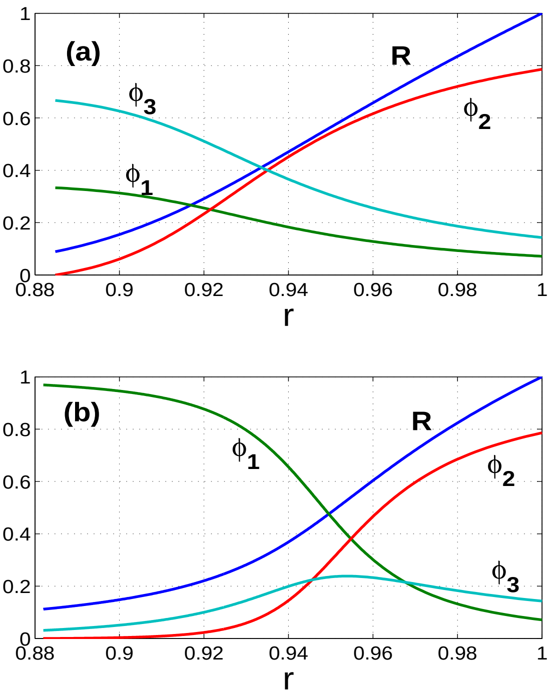

Figure 7.6: Case 3. The parameters are the same as in figure 7.5 except that $\rho_1 = 100$, $\rho_3 = 0.02$.

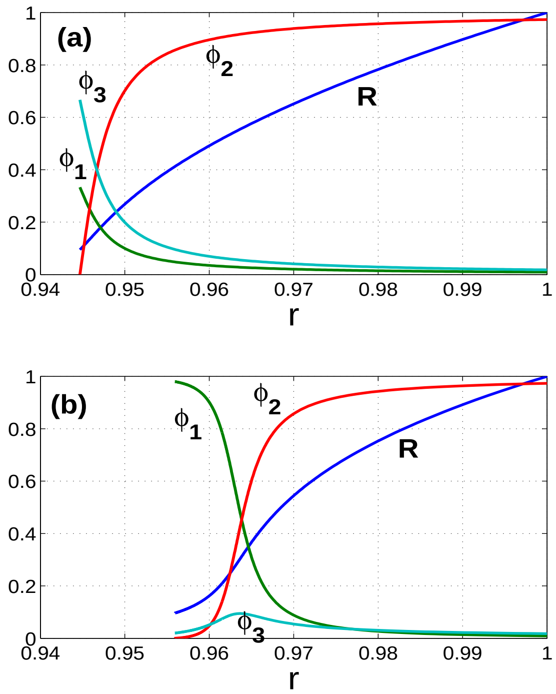

Figure 7.7: Case 4. As in figure 7.6 except that now $\rho_1 = 1000$, $\rho_3 = 0.002$.

7.5.2 Discrete layering algorithm

The inhomogeneous nature of the homogenized material is captured by layering the shell on two scales. The first scale is a fine layering of L distinct bands defined by the regions between $r_0 < r_1 < r_2 < \ldots < r_L = r_{out} = 1$. The second scale of layering defines three sub-regions between neighboring radii. Let $r_{n,1} \equiv r_n$, and define

$$r^d_{n,m} = r^d_{n,m-1} - \phi_{m-1}(r_n)\Delta_n, \quad m = 2, 3, \tag{7.39a}$$

$$\Delta_n = r^d_n - r^d_{n-1}, \quad n = 1, 2, \ldots, L, \tag{7.39b}$$

where $\frac{\pi}{3}(d+1)\Delta_n$ is the area or volume between the inner and outer radii of the band $[r_{n-1}, r_n]$. The three regions $(r_{n,2}, r_{n,1}]$, $(r_{n,3}, r_{n,2}]$ and $(r_{n-1,1}, r_{n,3}]$ have fractional volumes $\phi_1(r_n)$, $\phi_2(r_n)$ and $\phi_3(r_n)$ of the band, respectively, and are therefore occupied by the respective fluids, see Figure 7.8. The choice of the ordered set $\{r_n, n = 1, 2, \ldots, L-1\}$ is relatively arbitrary as long as it is finely spaced for large values of L. For simplicity we take Δ_n constant, independent of n, in which case $\Delta_n \equiv \Delta$

	2D				3D			
	r_0	R_0	$\bar{\rho}$	$\sigma_0(\%)$	r_0	R_0	$\bar{\rho}$	$\sigma_0(\%)$
1	0.60	0.20	3.12	25.8	0.66	0.26	5.41	4.55
2	0.41	0.06	3.13	2.37	0.59	0.19	5.69	2.20
3	0.88	0.09	19.17	0.69	0.88	0.11	57.7	.033
4	0.94	0.09	40.22	0.69	0.96	0.096	192	.012

Table 7.2: Results for the four cases of Table 7.1. $\bar{\rho}$ is the average density in the shell $r_0 \le r \le 1$. σ_0 is the relative value of the total scattering cross section at $kr_0 = 3$ of a rigid cylinder/sphere surrounded by the 3-fluid shell with 500 layers. A value of 100% corresponds to the bare rigid target.

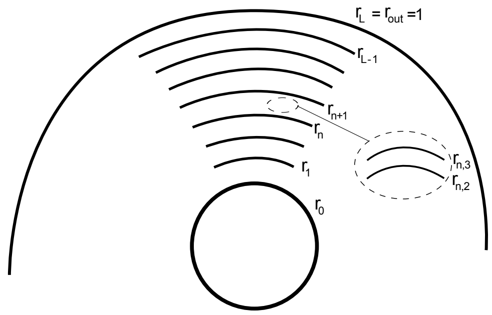

Figure 7.8: The discrete layering algorithm to reproduce the local homogenization properties of the 3-fluid shell.

and the radii become

$$r_{n,1}^d = r_0^d + n\Delta, \quad n = 1, 2, \ldots, L, \tag{7.40a}$$

$$r_{n,m}^d = r_{n,m-1}^d - \phi_{m-1}(r_{n,1})\Delta, \quad m = 2, 3, \tag{7.40b}$$

$$\Delta = (1 - r_0^d)/L. \tag{7.40c}$$

7.5.3 Numerical results

Three different numerical methods are employed to find the scattered pressure: (i) by solving for the Matricant; (ii) using a global matrix; and (iii) by solving the Matricant of the homogenized radially dependent anisotropic fluid. The code is attached in the appendix D.8. Figures 7.9 and 7.10 show the magnitude of the scattered acoustic field for an incident wave of unit amplitude. Since the radius of the object being cloaked changes for each of the four cases of Table 7.1 we take the non-dimensional

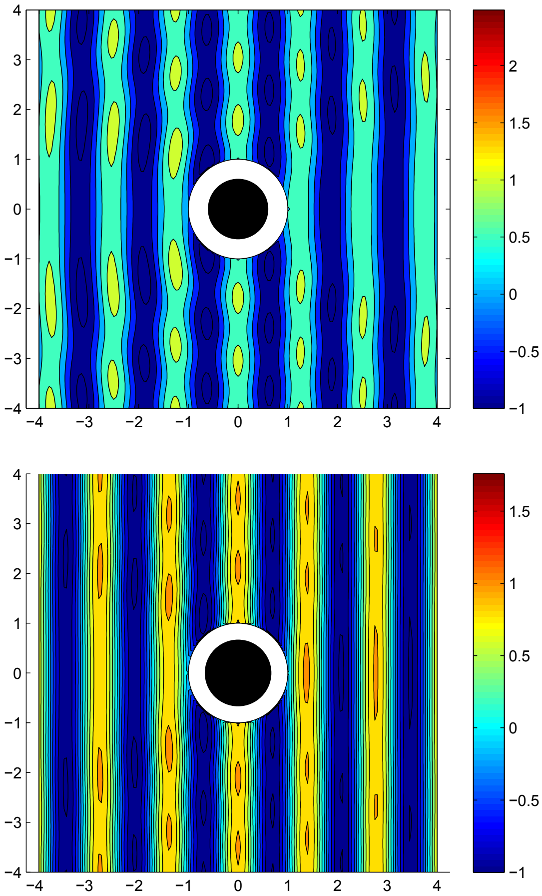

Figure 7.9: Case 1. The magnitude of the scattered pressure for an incident wave of unit amplitude for the 2D (top) and 3D (bottom) 3-fluid shells. In each case $kr_0 = 3$ and $L = 500$. The inner dark circular region depicts the rigid target of radius r_0, surrounded by the shell of unit outer radius.

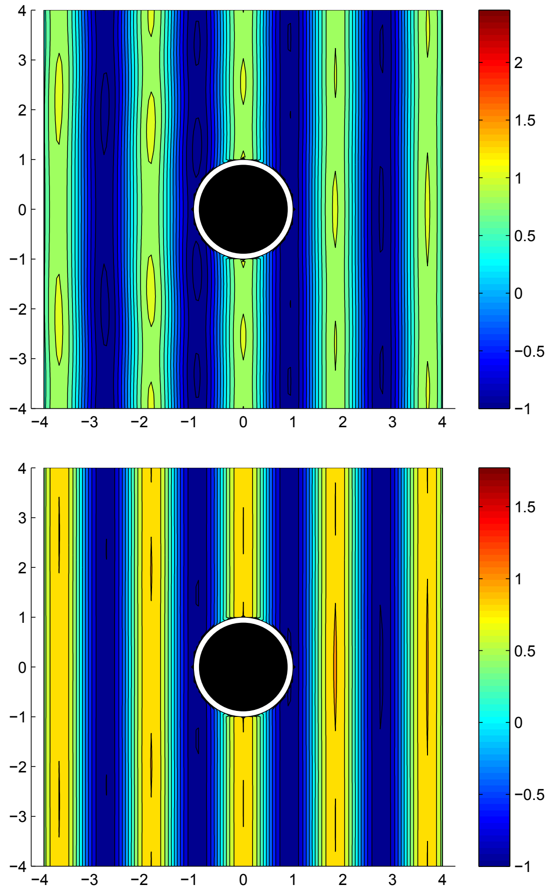

Figure 7.10: Case 3. The same as for figure 7.9: 2D and 3D simulations are in the upper and lower plots, respectively.

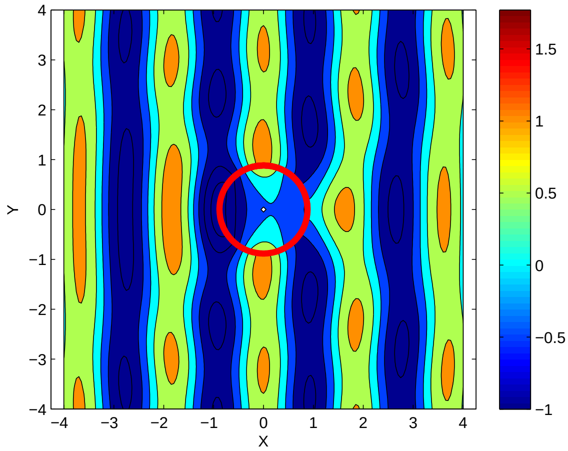

Figure 7.11: 3D pressure map solution for a rigid cylinder; $kr_0 = 3$, $r_0 = .88$.

characteristic value $kr_0 = 3$ in each scattering simulation. This allows us to compare the total scattering cross-section between the four cases even though the values of r_0 are different. Figure 7.11 shows the response of the bare 3D spherical rigid target based upon case 3 in which $r_0 = .88$. The total scattering cross-section for the "cloaked" rigid object was calculated using the coefficients A_n, and compared with the cross-section for the bare rigid object. In each case, as Table 7.2 shows, the relative cross-section satisfies $\sigma_0 < 1$. Also, the numerical methods (i) and (ii) were found to be in agreement with one another, and with method (iii) when L is very large. For instance, the cross-section found using method (iii) is 0.3% larger than that of method (i) for the 2D example in figure 7.9. Finally Figure 7.12 shows the effect of increasing the number of layers versus the relative value of the total scattering cross section, σ_0. It should be noted that Figure 7.12 shows the homogenization process at work. When there are very few layers the incident wave does not respond as if the medium were described by a cloaking medium. However as we increase the number of layers within the cloaking region and therefore decrease the thickness of each layer of individual fluid, the incident wave begins responding as if the medium contained the fluid properties of Equation 7.2. A curve fit of the power function $f(x) = ax^b + c$ was used and the results can be found in the caption of Figure 7.12.

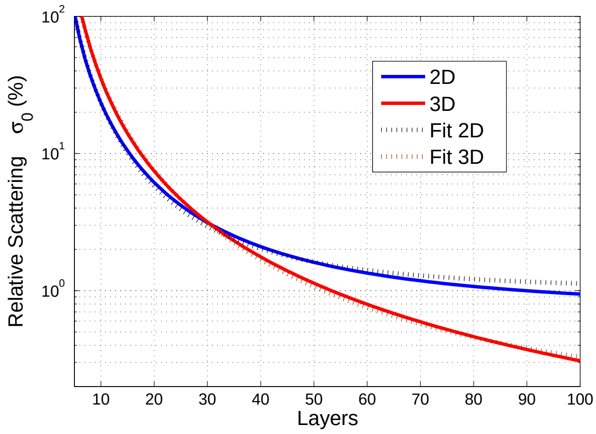

Figure 7.12: Number of three-fluid layers vs. the relative value of the total scattering cross section for case 3, in which the layers occupy $r_0 < r \leq 1$. Where $5 \leq L \leq 100$. The curve fit used was of the form $f(x) = ax^b + c$. For 2D $a = 3716, b = -2.221, c = .9924$. The root mean squared error (RMSE)=.290 and $R^2 \approx 1$. For 3D $a = 6435, b = -2.258, c = .1324$, (RMSE)=.278 and $R^2 \approx 1$.

7.6 Three fluid examples using feasible materials

Using Equation (7.28a) a plot of values for r_0 vs. R_0 using combinations of several materials was created. Ideally we want r_0 to be close to unity and R_0 to be close to zero. The list of materials considered is located in the appendix C. We considered gases, liquids, and solids. Although solids will have shear effects we consider them negligible when layering a thin strip of solid material between two fluids. Having taken all possible three-combinations of the tables in the appendix, Figure 7.13 was created. Unfortunately no combination resulted in any significant cloaking. Interestingly however is that points that lie on the 45^o line mimic the background fluid for a given volume. The three colors of Figure 7.13 correspond to which volume fraction ϕ_i went to zero first. For instance, referring to Figures 7.4-7.7, the fluids for those figures were chosen such that ϕ_2 was zero at $r = r_0$, however this is not always the case for a given random set of fluids. Ultimately a random set of fluids starts somewhere within the surface of Figure 7.2 at $r = 1$, for two dimensional structures, and transformation occurs until one $\phi_i(r = r_0) = 0$, for $i = 1, 2, 3$.

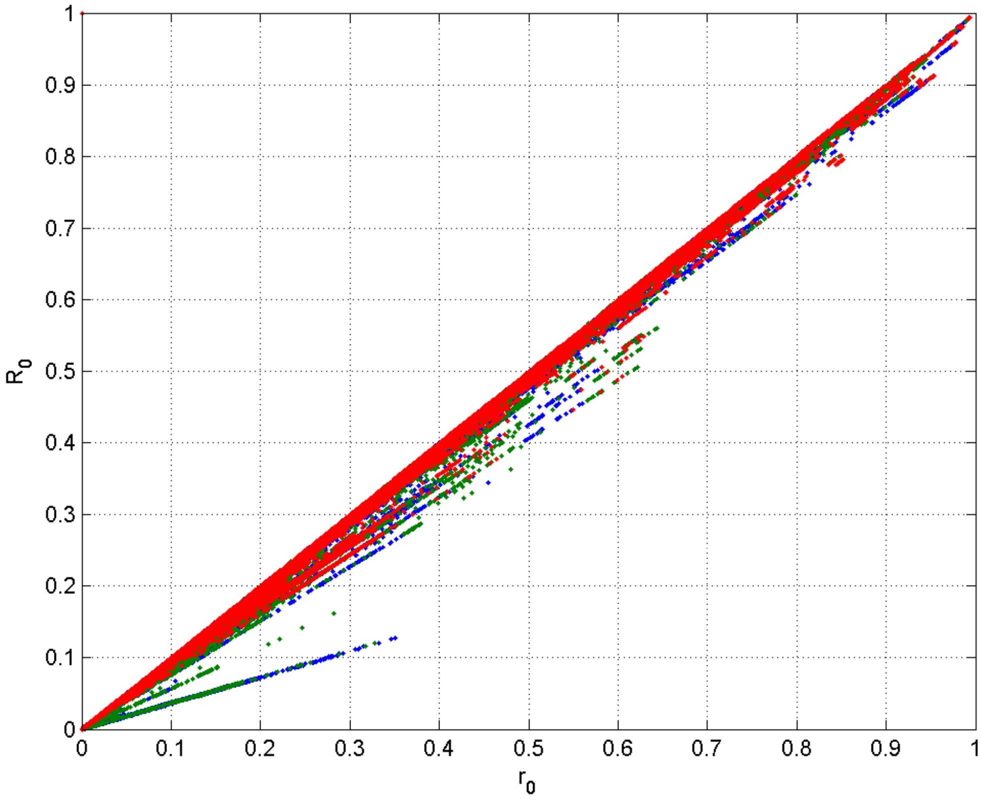

Figure 7.13: Plot of r_0 vs. R_0 made from 198 different materials constituting 1,274,196 different three-pair combinations, this is produced by the binomial coefficient n choose k written $\binom{n}{k}$. The three colors correspond to which volume fraction went to zero first, further explained in section 7.6

7.7 Conclusion

The 2 and 3-fluid shells have the effect of creating an inertially anisotropic medium however the 2-fluid shell results in constant functions for ρ_r and ρ_θ that have no radial dependence. By introducing the 3-fluid shell additional degrees of freedom are exploited and a desired radial dependent inertial medium is attained that upon layering and homogenizing has the effect of steering incident acoustic energy around the structure, and conversely, reducing the radiation strength. The overall effectiveness and the precise form of the layering depends upon the relative densities and compressibilities of the three fluids. The best results are obtained if one fluid has density equal to the background or host fluid, while the other two densities are much greater and much less than the background values, as per the discussion in Section 7.4. Future improvements in optimization of the layering of the three fluids to result in an effective homogenized medium with fewer layers may significantly improve the results of Fig. 7.12.

Chapter 8

Summary and future work

This thesis covered a somewhat extensive review of acoustic wave theory in order to review and develop acoustic cloaking theory. Chapters 3 - 5 covered one, two, and three dimensional scattering problems where solution methods were discussed and developed. In Chapters 4 and 5 the optical theorem was derived in two and three dimensions yielding the scattering cross section for later use when determining the effectiveness of a cloak. Matlab codes were written to compare solution methods and compute the effectiveness of acoustic cloaking mediums proposed by the literature. A review of Torrent and Sánchez-Dehesa in Chapter 6 considered an inertial cloak comprised of layering several hundred unique fluids. We found that only three unique fluids are required to create a cloaking medium, the main results are in Chapter 7. As discussed in the literature, mass is an issue in cloaks of the inertial type. Future work will need to consider a broader set of cloaking materials, such as pentamode elastic solids with anisotropic strength and isotropic inertia.

Appendix A

Derivation of optical theorem for section 4.7

Detailed solution for (4.47),

$$\int_0^{2\pi} \mathrm{Re}(P_{sc}^* V_{sc,r})\mathrm{d}\theta + \int_0^{2\pi} \mathrm{Re}(P_{inc}^* V_{inc,r})\mathrm{d}\theta + \int_0^{2\pi} \mathrm{Re}(P_{inc}^* V_{sc,r} + P_{sc}^* V_{inc,r}).$$

Where P_{sc} is given by Equation (4.38) and P_{inc} is given by (4.4). Determining the first term, the complex conjugate of the scattered pressure, $P_{sc}^* = P_0^* \frac{e^{-ikr}}{\sqrt{kr}} f^*(\theta)$. Using linear momentum balance and Equation (4.38), $V_{sc,r} = \frac{P_0}{i\omega\rho} f(\theta) \frac{\mathrm{d}}{\mathrm{dr}}(g(r))$, where $\frac{\mathrm{d}}{\mathrm{dr}}(g(r)) = e^{ikr} \frac{-1+2ikr}{2\sqrt{k}r^{3/2}}$. $V_{sc,r}$ is then

$$V_{sc,r} = \frac{P_0}{i\omega\rho} e^{ikr} \frac{-1+2ikr}{2\sqrt{k}r^{3/2}} f(\theta). \tag{A.1}$$

Multiplying P_{sc}^* and $V_{sc,r}$ and taking the real part, the first term of Equation (A.1) can be found, with

$$P_{sc}^* V_{sc,r} = \frac{|P_0|^2}{i\omega\rho} \frac{-1+2ikr}{2kr^2} f(\theta) f^*(\theta), \tag{A.2a}$$

$$\mathrm{Re}(P_{sc}^* V_{sc,r}) = \frac{|P_0|^2}{2i\omega\rho}(\frac{-1+2ikr}{2kr^2})|f(\theta)|^2 + \frac{|P_0|^2}{2i\omega\rho}(\frac{1+2ikr}{2kr^2})|f(\theta)|^2 = \frac{|P_0|^2}{r\omega\rho}|f(\theta)|^2. \tag{A.2b}$$

Using Equation (4.39) for $f(\theta)$, the integral may be found,

$$\int_0^{2\pi} \mathrm{Re}(P_{sc}^* V_{sc,r})\mathrm{d}\theta = \frac{4|P_0|^2}{r\omega\rho}|A_n|^2. \tag{A.3}$$

The second term of (A.1) is zero as this is the flux of the incident wave integrated over a closed region. Now we begin working on the third term where $V_{inc,r} = \frac{P_0}{Z}\cos\theta e^{ikr\cos\theta}$. Then we may find,

$$P_{inc}^* V_{sc,r} = \frac{|P_0|^2}{Z\sqrt{kr}} e^{ikr(1-\cos\theta)} f(\theta), \tag{A.4}$$

taking the real part,

$$\mathrm{Re}(P_{inc}^* V_{sc,r}) = \frac{|P_0|^2}{2Z\sqrt{kr}}[e^{ikr(1-\cos\theta)} f(\theta) + e^{ikr(\cos\theta-1)} f^*(\theta)]. \tag{A.5}$$

Similarly the next term

$$P^*_{sc}V_{inc,r} = \frac{|P_0|^2}{Z\sqrt{kr}}\cos\theta e^{ikr(\cos\theta-1)}f^*(\theta), \tag{A.6a}$$

$$\mathrm{Re}(P^*_{sc}V_{inc,r}) = \frac{|P_0|^2}{2Z\sqrt{kr}}\cos\theta[e^{ikr(\cos\theta-1)}f^*(\theta) + e^{ikr(1-\cos\theta)}f(\theta)]. \tag{A.6b}$$

Finally we may integrate over θ,

$$\int_0^{2\pi}\mathrm{Re}(P^*_{inc}V_{sc,r}+P^*_{sc}V_{inc,r}) = \frac{|P_0|^2}{2Z\sqrt{kr}}\int_0^{2\pi}e^{ikr(1-\cos\theta)}(1+\cos\theta)f(\theta)+e^{ikr(\cos\theta-1)}(1+\cos\theta)f^*(\theta)\mathrm{d}\theta$$

This is a rather complicated integral we begin with the first term, where

$$\int(1+\cos\theta)e^{ikr(1-\cos\theta)}f(\theta)\mathrm{d}\theta = \int(2+\mathbf{O}(\theta^2))e^{ikr(\frac{\theta^2}{2})}f(\theta)\mathrm{d}\theta.$$

The above is done using the series expansion of $1-\cos\theta \approx \frac{\theta^2}{2} - \frac{\theta^4}{24} + \mathbf{O}(\theta^6)$ for $\theta \approx 0$. Using the substitution, $\theta = (kr)^{-1/2}\sqrt{2}y$,

$$\int 2e^{ikr(\frac{\theta^2}{2})}f(\theta)\mathrm{d}\theta = f(0)\frac{2\sqrt{2}}{\sqrt{kr}}\int_{-\infty}^{\infty}e^{iy^2}\mathrm{dy}, \tag{A.7}$$

where, $\int_{-\infty}^{\infty}e^{iy^2}\mathrm{dy} = (1+i)\sqrt{\frac{\pi}{2}} = \sqrt{\pi}e^{\frac{i\pi}{4}}$. Finally,

$$\int(1+\cos\theta)e^{ikr(1-\cos\theta)}f(\theta)\mathrm{d}\theta = \frac{f(0)2\sqrt{2\pi}e^{\frac{i\pi}{4}}}{\sqrt{kr}} + \mathbf{O}(\frac{1}{(kr)^{3/2}}).$$

The next term to be investigated,

$$\int(1+\cos\theta)e^{ikr(\cos\theta-1)}f^*(\theta)\mathrm{d}\theta.$$

Applying the exact same maneuvers as done for the previous integral to obtain,

$$\int(1+\cos\theta)e^{ikr(\cos\theta-1)}f^*(\theta)\mathrm{d}\theta = \frac{f^*(0)2\sqrt{2\pi}e^{\frac{-i\pi}{4}}}{\sqrt{kr}} + \mathbf{O}(\frac{1}{(kr)^{3/2}}).$$

Now the entirety of Equation (A.1) can be written.

$$\int_0^{2\pi}\mathrm{Re}(P^*_{sc}V_{sc,r})\mathrm{d}\theta + \int_0^{2\pi}\mathrm{Re}(P^*_{inc}V_{inc,r})\mathrm{d}\theta + \int_0^{2\pi}\mathrm{Re}(P^*_{inc}V_{sc,r}+P^*_{sc}V_{inc,r})\mathrm{d}\theta,$$

$$= \frac{4|P_0|^2}{r\omega\rho}[\sum_{n=-\infty}^{\infty}|A_n|^2 + \sum_{n=-\infty}^{\infty}\mathrm{Re}(A_n e^{-\frac{in\pi}{2}})] = 0. \tag{A.8}$$

Appendix B

Derivation of optical theorem for section 5.4

Detailed solution for

$$\int_0^{\pi}\int_0^{2\pi}(\mathrm{Re}(P_{sc}^*V_{sc,r})+\mathrm{Re}(P_{inc}^*V_{inc,r})+\mathrm{Re}(P_{inc}^*V_{sc,r}+P_{sc}^*V_{inc,r}))\sin\theta\mathrm{d}\phi\mathrm{d}\theta = 0. \quad \text{(B.1)}$$

Working with the first term the complex conjugate of the scattered pressure is given by

$$P_{sc}^* = P_0^*\frac{e^{-ikr}}{kr}f^*(\theta). \quad \text{(B.2)}$$

The radial scattered velocity is given by,

$$V_{sc,r} = \frac{P_0}{i\omega\rho}\frac{e^{ikr}}{kr}(ik-\frac{1}{r})f(\theta). \quad \text{(B.3)}$$

Multiplying the complex conjugate of the scattered pressure and velocity and taking the real part attains

$$P_{sc}^*V_{sc,r} = \frac{|P_0|^2}{i\omega\rho}\frac{1}{(kr)^2}(ik-\frac{1}{r})f(\theta)f^*(\theta), \quad \text{(B.4)}$$

$$\mathrm{Re}(P_{sc}^*V_{sc,r}) = \frac{|P_0|^2|f(\theta)|^2}{\omega\rho kr^2}. \quad \text{(B.5)}$$

Taking the integral over θ and ϕ

$$\int_0^{\pi}\int_0^{2\pi}\mathrm{Re}(P_{sc}^*V_{sc,r})\sin\theta\mathrm{d}\phi\mathrm{d}\theta = \frac{2\pi|P_0|^2}{\omega\rho kr^2}\int_0^{\pi}|f(\theta)|^2\sin\theta\mathrm{d}\theta. \quad \text{(B.6)}$$

The above integral is done through a variable change where $\mu = \cos(\theta)$, where $f(\theta)$ is given in Equation (5.22).

$$\frac{2\pi|P_0|^2}{\omega\rho kr^2}\int_0^{\pi}|f(\theta)|^2\sin\theta\mathrm{d}\theta = \frac{2\pi|P_0|^2|A_n|^2}{\omega\rho kr^2}\int_{-1}^{1}|P_n(\mu)|^2\mathrm{d}\mu = \frac{4\pi|P_0|^2|A_n|^2}{\omega\rho kr^2(2n+1)}. \quad \text{(B.7)}$$

Where the last integral was found from the identity, $\int_{-1}^{1}P_n^m(x)P_{n'}^m(x)\mathrm{d}x = \frac{2}{2n+1}\frac{(n+m)!}{(n-m)!}\delta_{nn'}$. Next working with the second term of Equation (B.1), for which we expect the result to be zero, since the flux of incident waves over a period should be zero. Starting with

$$P_{inc}^* = P_0^* e^{-ikr\cos\theta}, \quad V_{inc,r} = \frac{P_0\cos\theta}{Z} e^{ikr\cos\theta}, \tag{B.8}$$

and multiplying the the two terms together, $P_{inc}^* V_{inc,r} = \frac{|P_0|^2}{Z}\cos\theta$. Next by taking the integral over θ and ϕ we see

$$\int_0^\pi \int_0^{2\pi} \mathrm{Re}(P_{inc}^* V_{inc,r}) \sin\theta \mathrm{d}\phi \mathrm{d}\theta = 0. \tag{B.9}$$

Next we work on the third term from Equation (B.1), where $P_{inc}^* V_{sc,r} = \frac{|P_0|^2}{\omega\rho r}[1 + \frac{i}{kr}] e^{ikr(1-\cos\theta)} f(\theta)$ and $P_{sc}^* V_{inc,r} = \frac{|P_0|^2}{\omega\rho r}\cos\theta f^*(\theta) e^{ikr(\cos\theta - 1)}$. Taking the real parts and adding the two terms

$$\mathrm{Re}(P_{inc}^* V_{sc,r} + P_{sc}^* V_{inc,r}) = \frac{|P_0|^2}{2\omega\rho r}\Big[(1+\frac{i}{kr}+\cos\theta) f(\theta) e^{ikr(1-\cos\theta)} + (1-\frac{i}{kr}+\cos\theta) f^*(\theta) e^{ikr(\cos\theta-1)}\Big].$$

Taking $\boldsymbol{O}(\frac{1}{r^2}) \approx 0$,

$$\mathrm{Re}(P_{inc}^* V_{sc,r} + P_{sc}^* V_{inc,r}) = \frac{|P_0|^2}{2\omega\rho r}\Big[(1+\cos\theta) f(\theta) e^{ikr(1-\cos\theta)} + (1+\cos\theta) f^*(\theta) e^{ikr(\cos\theta-1)}\Big].$$

Integrating over θ and ϕ, $\int_0^\pi \int_0^{2\pi} \mathrm{Re}(P_{inc}^* V_{sc,r} + P_{sc}^* V_{inc,r}) \sin\theta \mathrm{d}\phi \mathrm{d}\theta$, yields

$$\frac{\pi|P_0|^2}{\omega\rho r}\Big[\int_0^\pi (1+\cos\theta)\sin\theta f(\theta) e^{ikr(1-\cos\theta)} \mathrm{d}\theta + \int_0^\pi (1+\cos\theta)\sin\theta f^*(\theta) e^{ikr(\cos\theta-1)} \mathrm{d}\theta\Big].$$

Solutions for each integral is done by integration by parts and using the substitution $\cos\theta = \mu$, $\mathrm{d}\mu = -\sin\theta$.

$$\int_0^\pi f(\theta)(1+\cos\theta)\sin\theta e^{ikr(1-\cos\theta)} \mathrm{d}\theta = \int_{-1}^1 F(\mu)(1+\mu) e^{ikr(1-\mu)} \mathrm{d}\mu = \frac{2i}{kr} F(1) + \boldsymbol{O}[\frac{1}{(kr)^2}],$$

where $F(1) = f(0)$. Integrating the next term

$$\int_0^\pi f^*(\theta)(1+\cos\theta)\sin\theta e^{ikr(\cos\theta-1)} \mathrm{d}\theta = \int_{-1}^1 F^*(\mu)(1+\mu) e^{ikr(\mu-1)} \mathrm{d}\mu = -\frac{2i}{kr} F^*(1) + \boldsymbol{O}[\frac{1}{(kr)^2}].$$

Finally putting everything together the third term of Equation (B.1) yields

$$\int_0^\pi \int_0^{2\pi} \mathrm{Re}(P_{inc}^* V_{sc,r} + P_{sc}^* V_{inc,r}) \sin\theta \mathrm{d}\phi \mathrm{d}\theta = \frac{2\pi i|P_0|^2}{\omega\rho k r^2}[f(0) - f^*(0)]. \tag{B.10}$$

Putting every term together in Equation (B.1) we have the optical theorem for a three dimensional problem of a plane wave incident on a sphere.

$$\mathrm{Im}(f(0)) = \sum_{n=0}^{\infty} \frac{|A_n|^2}{2n+1}. \tag{B.11}$$

Appendix C

Materials used for section 7.6

Source of material parameters: mostly from Onda Corporation. Website: ondacorp.com

GASSES		
Material	$\frac{\rho}{\rho_{H_2O}}$	$\frac{C}{C_{H_2O}}$
Acetate, butyl	0.871	1.559
Acetate, ethyl, $C_4H_8O_2$	0.900	1.719
Acetate, methyl, $C_3H_6O_2$	0.934	1.602
Acetate, PROPYL	0.891	1.766
ACETONE, $(CH_3)_2CO$	0.791	2.009
ACETONITRILE, C_2H_3N	0.783	1.681
ACETONYL ACETONE, $C_6H_{10}O_2$	0.729	1.533
ACETYLENDICHLORIDE, $C_2H_2C_{12}$	1.260	1.671
ALCOHOL, BUTYL, C_3H_9OH	0.810	1.759
ALCOHOL, ETHANOL, C_2H_5OH	0.790	1.903
ALCOHOL, FURFURYL, $C_5H_4O_2$	1.135	0.918
ALCOLHOL, ISOPROPYL, 2-PROPANOL	0.786	2.036
ALCOHOL, METHANOL, CH_3OH	0.791	2.276
ALCOLHOL, PROPYL (N) C_3H_7OH	0.804	1.830
ALCOHOL, T-AMYL, C_5H_9OH	0.810	1.878
ALKAZENE 13, $C_{15}H_{24}$	0.860	1.462
ANILINE, $C_6H_5NH_2$	1.022	0.750
ARGON, LIQUID AT 87k	1.430	2.171
BENZENE, C_6H_6	0.870	1.501
BENZOL	0.878	1.410

Material	$\frac{\rho}{\rho_{H_2O}}$	$\frac{C}{C_{H_2O}}$
BENZOL, ETHYL	0.868	1.405
BROMOBENZENE, C_6H_5Br	1.522	1.057
BROMOFORM, $CHBr_3$	2.890	0.895
t-BUTYL CHLORIDE, C_4H_9Cl	0.840	2.715
BUTYRATE, ETHYL	0.877	1.825
CARBITOLTM, $C_6H_{14}O_3$	0.988	1.040
CARBON DISULPHIDE, CS_2	1.260	1.317
CARBON DISULPHIDE CS_2, 3GHz	1.221	1.045
CARBON TETRACHLORIDE, CCI_4	1.594	1.603
CESIUM	1.880	1.246
CHLORO-BENZENE, C_6H_5Cl	1.106	1.165
CHLORO-BENZEN, C_6H_5Cl	1.100	1.178
CHLOROFORM, $CHCl_3$	1.490	1.509
CYCLOHEXANOL, $C_6H_{12}O$	0.962	1.083
CYCLOHEXANONE, $C_6H_{10}O$	0.948	1.146
DIACETYL, $C_4H_6O_2$	0.990	1.439
1,3 DICHLOROISOBUTANE, $C_3H_{18}C_{l2}$	1.140	1.291
DIETHYL KETONE	0.813	1.570
DIMETHYL PHTHALATE, $C_8H_{10}O_4$	1.200	0.856
DIOXANE	1.033	1.113
ETHANOL AMIDE, C_2H_7NO	1.018	0.724
ETHYL ETHER, $C_4H_{10}O$	0.713	3.166
d-FENCHONE	0.940	1.337
FOMAMIDE, CH_3NO	1.134	0.736
FURFURAL, $C_5H_4O_2$	1.157	0.901
CARBON TETRACHLORIDE, CCI_4	1.594	1.603
CESIUM	1.880	1.246
CHLORODIMETHYL PHTHALATE, $C_8H_{10}O_4$	1.200	0.856
DIOXANFLUORINERT, FC-104	1.760	3.764
FLUORINERT, FG-43	1.850	2.760
FLUORO-BENZENE, C_6H_5F	1.024	1.536
FREON, TF	1.570	2.721

Material	$\frac{\rho}{\rho_{H_2O}}$	$\frac{C}{C_{H_2O}}$
GALLIUM	6.090	0.0437
GASOLINE	0.803	1.746
GLYCERIN	1.260	0.480
GLYCOL - 2,3 BUTYLENE	1.019	0.981
GLYCOL - DIETHYLENE $C_4G_{10}O_3$	1.116	0.786
GLYCOL - ETHYLENE 1,2-ETHANEDIOL	1.113	0.716
GLYCOL - ETHYLENE PRESTON II	1.108	0.782
GLYCOL - OLOYETHYLENE 200	1.087	0.768
GLYCOL - POLYETHYLENE 400	1.060	0.787
GLYCOL - TETRAETHYLENE $C_9H_{18}O_6$	1.120	0.783
GLYCOL, TRIETHYLENE, $C_6H_{14}O_4$	1.123	0.752
HELIUM-4, LIQUID AT .4K	0.147	263.058
HELIUM-4, LIQUID AT 2K	0.145	293.159
HELIUM-4 LIQUID AT 4.2K	0.126	519.100
n-HEXANONL, C_6H_{14}	0.659	2.732
HONEY, sue Bee orange	1.420	0.374
HYDROGEN LIQUID AT 20K	0.070	22.097
IODO-BENZENE, C_6H_5I	1.183	1.519
ISOPENTANE, C_5H_{12}	0.620	3.590
KERSONE	0.810	1.543
LINALOOL	0.884	1.264
MERCURY AT 25 ^{o}C	13.5	0.0772
MESITYLOXIDE, $C_6H_{16}O$	0.850	1.502
METHYLETHYLKETONE	0.805	1.858
METHYL NAPTHALENE, $C_{11}H_{10}$	1.090	0.881
MONOCHLOROBENZENE, C_6H_5Cl	1.107	1.227
MORPHOLINE, C_3H_9NO	1.00	1.056
NEON, LIQUID AT 27K	1.20	1.268
NICOTIN, $C_{10}H_{14}N_2$	1.01	0.977
NITROBENZENE, $C_6H_6NO_2$	1.20	0.852
NITROGEN, N_2, LIQUID AT 77K	0.80	4.215

Material	$\frac{\rho}{\rho_{H_2O}}$	$\frac{C}{C_{H_2O}}$
NITROMETHANE, CH_3NC_2	1.13	1.0958
OIL - BABY	0.821	1.305
OIL - CASTOR $C_{11}H_{10}O_{10}$	0.968	1.037
OIL - CASTOR AT 20.2C AT 4.224MHz	0.942	1.024
OIL-CORN	0.922	1.115
OIL GRAVITY FUEL AA	0.990	0.997
OIL JOJOBA	1.17	0.884
OIL LINSEED	0.940	1.093
OIL MENERAL LIGHT	0.825	1.280
OIL MINERAL HEAVY	0.843	1.219
OIL OLIVE	0.918	1.143
OIL PARRAFIN	0.835	1.301
OIL PEANUT	0.914	1.162
OIL SAE 20	0.870	0.832
OIL SAE 30	0.880	0.861
OIL-SILICON DOW 200 1 CENTISTOKE	0.818	2.906
OIL-SILICON DOW 200 10 CENTISTOKE	0.940	2.487
OIL-SILICON DOW 200 100 CENTISTOKE	0.968	2.356
OIL-SILICON DOW 200 1000 CENTISTOKE	0.972	2.299
OIL-SILICON DOW 704	1.020	1.082
OIL-SILICON DOW 705	1.150	0.896
OIL-SILICON DOW 710	1.110	1.080
OIL-SAFFLOWER	0.900	1.158
OIL SOYBEAN	0.930	1.152
OIL SPERM	0.880	1.200
OIL SUNFLOWER	0.920	1.132
OIL-TRANSFORMER	0.920	1.232
OIL WINERGREEN (METHYL SALICYLATE)	1.600	0.719
OXYGEN, O_2, AT 90K	1.110	2.436
n-PENTANE, C_5H_{12}	0.626	3.317
POTASSIUM	0.830	0.797

Material	$\frac{\rho}{\rho_{H_2O}}$	$\frac{C}{C_{H_2O}}$
PYRIDINE	0.982	1.122
SODIUM AT 300C	8.810	0.042
SOLVESSO #3	0.877	1.331
SONOTRACH COUPLANT	1.040	0.803
THALLIUM	11.90	0.0701
TRICHORETHYLENE	1.05	1.892
TURPENTINE	0.88	1.580
UNIVIS 800	0.87	1.381
WATER HEAVY,D2O	1.104	1.012
WATER LIQUID 20 ^{o}C	1.000	1.000
WATER - SEA 25^{o}C	1.025	0.912
XENON AT 166K	2.860	1.930
XYLENE HEXAFLORIDE, $C_8H_4F_6$	1.370	2.069
m-Xylol, C_8H_{10}	0.864	1.455
GASSES		
Air	0.00129	15420.159
Ammonia, NH_3	0.000771	16495.780
Argon at 0^{o}C	0.00056	38437.403
Carbon monoxide, CO	0.00125	15338.399
Carbon dioxide, CO_2	0.00198	16516.470
Chlorine	0.00321	16059.910
Deuterium	0.00019	14554.250
Ethane, C_2H_6	0.00136	17027.948
Ethylene, C_2H_4	0.00126	17299.532
Helium	0.000178	13214.441
Hydrogen at 0^{o}C	0.0000899	14778.614
Hydrogen bromide, HBr	0.0035	15645.714
Hydrogen chloride, HCl	0.00164	15253.203
Hydrogen iodide, Hi	0.00566	15700.291
Hydrogen sulfide, H_2S	0.00154	17040.766
Methane, CH_4	0.000717	16526.791
Neon at 0^{o}C	0.0009	12861.819

Material	$\frac{\rho}{\rho_{H_2O}}$	$\frac{C}{C_{H_2O}}$
Nitric oxide, NO	0.00134	15571.434
Nitrogen, $N2$ at 0^oC	0.00125	15695.429
Nitrous oxide, N_2O	0.00198	16017.888
Oxygen, O_2 at 0^oC	0.00143	15350.306
Sulfur dioxide	0.00293	16494.589
SOLIDS		
Aluminum Alloy (7075-T6)	2.710	0.0277
Brass	2.70	0.0188
Bronze, Regular	8.30	0.0175
Bronze, Manganese	8.30	0.0192
Concrete	2.50	0.0435
Copper	8.94	0.0167
Glass	2.60	0.0342
Gold	19.32	0.0211
Iron (Cast)	7.20	0.0157
Iron (Wrought)	7.60	0.0104
Magnesium, Mg	1.74	0.0465
Nickel	8.89	0.00936
Nylon, Polyamide	1.10	0.745
Platinum	21.4	0.0128
Steel	7.85	0.0200
Tin	7.30	0.0462
Titanium	4.51	0.0176
Alumina, Al_2O_3	3.90	0.00520
Beryllium alloy	2.90	0.00875
Bone, (compact)	2.0	0.127
Brass, (annealed)	8.4	0.0149
Cermets, (Co/WC)	11.5	0.00421
CFRP Laminate (graphite)	1.5	1.336
Copper Alloys	8.3	0.0141
Cork	0.18	63.689
Epoxy thermoset	1.2	0.582

Material	$\frac{\rho}{\rho_{H_2O}}$	$\frac{C}{C_{H_2O}}$
GFRP Laminate (glass)	1.8	0.0771
Glass (soda)	2.5	0.0317
Granite	2.6	0.0309
Ice, H_2O	0.92	0.220
Lead alloys	11.1	0.108
Nickel alloys	8.5	0.0109
Polyamide (nylon)	1.1	0.597
Polybutadiene elastomer	0.91	1019.022
Polycarbonate	1.2	0.663
Polyester thermoset	1.3	0.582
Polyethylene (HDPE)	0.95	2.558
Polypropylene	0.89	1.989
Polyurethane elastomer	1.2	65.217
Polyvinyl chloride (rigid PVC)	1.4	1.194
Silicon	2.3	0.0186
Silicon Carbide, Si_C	2.8	0.00472
Spruce (parallel to grain)	0.6	0.220
Steel high strength 4340	7.8	0.00948
Titanium alloy (6A14V)	4.5	0.0189
Tungsten Carbide (WC)	15.5	0.00378

Appendix D

Matlab codes

D.1 Reference codes for section 4.3.1

Matlab Code: D.1: Code used in reference to section 4.3.1.

```
global w n
w=5;   n=0;
rmin=1;
rmax=2;

options = odeset('RelTol',1e-10,'AbsTol',[1e-10 1e-10 1e-10 1e-10]);
[R,M] = ode45(@Matrivary_polar_vary_p_and_K, [rmin rmax], [1 0 0 1],
    options);
ZM2 = [M(end,1) M(end,2);M(end,3) M(end,4)];

Mb = M(size(M,1),:);
Zb = Mb(1)/Mb(3);

nmax=10000; h=(rmax-rmin)/nmax;
Mzm = eye(2);
for j = 1:nmax

    rj = rmin+ j*h*(rmax-rmin);
    p= rj;
    K= rj;
    c=sqrt(K/p); z=p*c; k=w/c;

Mcheck = [besselj(n,k*(h+rj)) bessely(n,k*(h+rj)); (((h+rj))/(1i*z))*...
    (.5*(besselj(n-1,k*(h+rj))-besselj(n+1,k*(h+rj))))...
```

```
    ((h+rj)/(1i*z))*(.5*(bessely(n-1,k*(h+rj))-bessely(n+1,k*(h+rj))))
        ]*...
    inv([besselj(n,k*rj) bessely(n,k*rj);...
    ((rj)/(1i*z))*(.5*(besselj(n-1,k*rj)-besselj(n+1,k*rj)))...
    ((rj)/(1i*z))*(.5*(bessely(n-1,k*rj)-bessely(n+1,k*rj)))]);
Mzm=Mcheck*Mzm;
end
```

Matlab Code: D.2: Function used for code D.1

```
function dM = Matrivary_polar_vary_p_and_K(r,M)
global w n

p=r;
K=r;
Q = (1i*w/r)*[0 p ;(((r^2)/K) - ((n^2)/((w^2)*p))) 0];
dM = zeros(4,1);
dM(1) = Q(1,2)*M(3); %using rigid at r=a so Vr(a) = 0;
dM(2) = Q(1,2)*M(4);
dM(3) = Q(2,1)*M(1) + Q(2,2)*M(3);
dM(4) = Q(2,1)*M(2) + Q(2,2)*M(4);
```

Matlab Code: D.3: Check on $\boldsymbol{M}$ using code D.1

```
>>ZM2-Mzm
ans =
   1.0e-004 *

  -0.0629              0 - 0.3497i
   0 + 0.3497i         0.0629
```

D.2 Reference codes for section 6.2

Matlab Code: D.4: Torrent and Sánchez-Dehesa comparison, reference for section 6.2

```
global w n Ksub psub
w=3;  P_0 = 1;  p0 =1;  c0=1;
R2 = 1;  r(1)=R2;
```

```
layers = 400;
R1 = R2/2;
dr = (R2-R1)/(layers);
for n=1:layers+1
      r(n) = R2-(dr*(n-1));
      if mod(n,2)==1
      p(n) = (r(n)+sqrt(2*r(n)*R1 - R1^2))/(r(n)-R1);
      end
      if mod(n,2)==0
      p(n) = (r(n)-R1)/(r(n)+sqrt(2*r(n)*R1 - R1^2));
      end
      c(n) = ((R2-R1)/R2)*((r(n))/(r(n)-R1));
end
p(layers+1)=10000;  %%% MOST inner cylinder properties.
c(layers+1)=10000;  %%% MOST inner cylinder properties.
k0=w/c0; z0 = p0*c0; ka=k0*r(1) k = w./c;
K = p.*c.^2; z=p.*c;
[x,y] = meshgrid([-4:.05:4]);
[theta,rad] = cart2pol(x,y);
siz=5+ka
cnt = 1;
for n = 0:siz
      %GLOBAL MATRIX
      Hk0r1 = besselh(n,1,k0*r(1));
      Jk1r1 = besselj(n,k(1)*r(1));
      Yk1r1 = bessely(n,k(1)*r(1));
      GM(1,:) = [Hk0r1 -Jk1r1 -Yk1r1];
      dHk0r1=.5*((besselh(n-1,1,k0*r(1))-besselh(n+1,1,k0*r(1))));
      dJk1r1=.5*(besselj(n-1,k(1)*r(1))-besselj(n+1,k(1)*r(1)));
      dYk1r1=.5*(bessely(n-1,k(1)*r(1))-bessely(n+1,k(1)*r(1)));
      GM(2,:)=[-(z0^-1)*dHk0r1 (z(1)^-1)*(dJk1r1) (z(1)^-1)*(dYk1r1)];
      for m = 1:layers-1
                Jkrn = besselj(n,k(m)*r(m+1));
                Ykrn = bessely(n,k(m)*r(m+1));
                Jkrn1 = -besselj(n,k(m+1)*r(m+1));
                Ykrn1 = -bessely(n,k(m+1)*r(m+1));

```

```
            dJkrn=.5*(besselj(n-1,k(m)*r(m+1))-besselj(n+1,k(m)*r(m+1)));
            dYkrn=.5*(bessely(n-1,k(m)*r(m+1))-bessely(n+1,k(m)*r(m+1)));
            dJkrn1=-.5*(besselj(n-1,k(m+1)*r(m+1))-besselj(n+1,k(m+1)*r(m+1)));
            dYkrn1=-.5*(bessely(n-1,k(m+1)*r(m+1))-bessely(n+1,k(m+1)*r(m+1)));
            b = 2*m;
            GM(b+1,b:b+3)=[Jkrn Ykrn Jkrn1 Ykrn1];
            GM(b+2,b:b+3)=[(z(m)^-1)*dJkrn (z(m)^-1)*dYkrn (z(m+1)^-1)*dJkrn1 (z(m+1)^-1)*dYkrn1];
    end
    m=layers;
            Jkrn = besselj(n,k(m)*r(m+1));
            Ykrn = bessely(n,k(m)*r(m+1));
            Jkrn1 = -besselj(n,k(m+1)*r(m+1));
            Ykrn1 = -bessely(n,k(m+1)*r(m+1));
            dJkrn=.5*(besselj(n-1,k(m)*r(m+1))-besselj(n+1,k(m)*r(m+1)));
            dYkrn=.5*(bessely(n-1,k(m)*r(m+1))-bessely(n+1,k(m)*r(m+1)));
            dJkrn1=.5*(besselj(n-1,k(m+1)*r(m+1))-besselj(n+1,k(m+1)*r(m+1)));
            dYkrn1=.5*(bessely(n-1,k(m+1)*r(m+1))-bessely(n+1,k(m+1)*r(m+1)));
            b = 2*m;
            GM(b+1,b:b+2)=[Jkrn Ykrn Jkrn1];
            GM(b+2,b:b+2)=[-(z(m)^-1)*dJkrn -(z(m)^-1)*dYkrn (z(m+1)^-1)*dJkrn1];
            vec = zeros(2*(layers+1),1);
            vec(1) = -P_0*besselj(n,k0*r(1));
            vec(2) = (z0^-1)*P_0*.5*(besselj(n-1,k0*r(1))-besselj(n+1,k0*r(1)));
            Coef=GM\vec;
            An(cnt)=Coef(1);
            if n==0
                Pout(:,:,cnt) = (An(cnt)*besselh(n,1,k0.*rad));
            else
                Pout(:,:,cnt) = (1i^n)*2*cos(n*theta).*((An(cnt)*besselh(n,1,k0.*rad)));
```

```
                end
                GMs{cnt}=GM;  Coefs{cnt}=Coef;
clear GM

%MATRICANT
H1k0sumr = besselh(n,1,k0*R2);
dH1k0sumr = .5*(besselh(n-1,1,k0*R2)-besselh(n+1,1,k0*R2));
Jk1r1 = besselj(n,k(end)*R1);
Jk0sumr = besselj(n,k0*R2);
dJk0sumr = .5*(besselj(n-1,k0*R2)-besselj(n+1,k0*R2));
dJk1r1 = .5*(besselj(n-1,k(end)*R1)-besselj(n+1,k(end)*R1));
M = eye(2);
for jk = 1:layers
          psub=p((layers+1)-jk);
          Ksub=K((layers+1)-jk);
options = odeset('RelTol',1e-10,'AbsTol',[1e-5 1e-5 1e-5 1e-5]);
[R12,M1] = ode45(@Matrivary_polar1, [r((layers+1)-jk+1) r((layers+1)-jk)],
      [1 0 0 1], options);
ZM1 = [M1(end,1) M1(end,2);M1(end,3) M1(end,4)];
M = ZM1*M;
end
zin = [Jk1r1;(r(end)/(1i*z(end)))*dJk1r1];
Zb = M*zin;
Zb = R2*Zb(1)/Zb(2);
Anm(cnt) = P_0*(Jk0sumr - (Zb/(1i*z0))*dJk0sumr) / ((Zb/(1i*z0))*dH1k0sumr
      - H1k0sumr);
if n==0
Poutm(:,:,cnt) = (Anm(cnt)*besselh(n,1,k0.*rad));
else
Poutm(:,:,cnt) = (1i^n)*2*cos(n*theta).*((Anm(cnt)*besselh(n,1,k0.*rad)));
end
cnt=cnt+1;
end
Pot = sum((Pout),3);
Pot=Pot + P_0*exp(1i.*k0.*rad.*cos(theta));
Potm = sum((Poutm),3);
Potm=Potm + P_0*exp(1i.*k0.*rad.*cos(theta));
```

```
[row_ot, col_ot] = find(x.^2+y.^2 <= (R2^2));
for j = 1:size(row_ot,1)
     Pot(row_ot(j),col_ot(j))=0;
     Potm(row_ot(j),col_ot(j))=0;
end
hold on;
j=sqrt(-2);
df=360;
for i=1:df
     circle(i)=R2*exp(2*j*i*pi/df);
end
maxed=abs(max(max([max(max(Pot)),max(max(Potm))])));
mini=(min(min([min(min(Pot)),min(min(Potm))])));
mini=mini-1;
subplot(2,1,1);
contourf(x,y,real(Pot));
caxis manual
caxis([mini maxed]);
colorbar;
hold on
plot(circle,'r','LineWidth',4); xlabel('X'); ylabel('Y'); zlabel('Z');
     axis('equal')
subplot(2,1,2)
contourf(x,y,real(Potm));
caxis manual
caxis([mini maxed]);
colorbar;
hold on
plot(circle,'r','LineWidth',4); xlabel('X'); ylabel('Y'); zlabel('Z');
     axis('equal')
```

Matlab Code: D.5: Function used for code D.4

```
function dM1 = Matrivary_polar1(R,M1)
global w n Ksub psub
Q = (1i*w/R)*[0 psub;(((R^2)/Ksub)-((n^2)/((w^2)*psub))) 0];
dM1 = zeros(4,1);
dM1(1) = Q(1,2)*M1(3);
```

```
dM1(2) = Q(1,2)*M1(4);
dM1(3) = Q(2,1)*M1(1);
dM1(4) = Q(2,1)*M1(2);
```

D.3 Reference codes for section 7.2.2

Matlab Code: D.6: Code used in reference to section 7.2.2 to construct figure 7.1.

```
global w n C_1 pr1
w=10;
theta=[0:.01:2*pi];
p2=9999; %density of most inner cylinder
c2=9999; %speed of sound most inner cylinder
r2=.5; %inner most cylinder radius
z2=p2*c2;
pr1=20;%outer cylinder  C_* = pr
C_1=pr1;
r1=1; %outer radius of surrounding cylinder
p0=1; %outer medium surrounding concentric cylinders.
c0=1;
z0=p0*c0;
P_0=1; %magnitude of incident wave
siz=40; %maximum number of n (Code has been optimized to stop when besselj
    (n,k0*r1)<1e-4)
cntn=1;
for n=0:siz
k0=w/c0; k1=w*sqrt(C_1*pr1); k2 = w/c2;
zr=1;
N=n*pr1;
if abs(besselj(n,k0*r1))>1e-3
H1k0r1 = besselh(n,1,k0*r1);
H1k1r1 = besselh(n,1,k1*r1);
H1k1r2 = besselh(n,1,k1*r2);
H1k1r1N = besselh(N,1,k1*r1);
dH1k0r1 = .5*(besselh(n-1,1,k0*r1)-besselh(n+1,1,k0*r1));
dH1k0r2 = .5*(besselh(n-1,1,k0*r2)-besselh(n+1,1,k0*r2));
dH1k1r1 = .5*(besselh(n-1,1,k1*r1)-besselh(n+1,1,k1*r1));
```

```
dH1k1r2 = .5*(besselh(n-1,1,k1*r2)-besselh(n+1,1,k1*r2));
dH1k1r1N=.5*(besselh(N-1,1,k1*r1)-besselh(N+1,1,k1*r1));
dH1k1r2N=.5*(besselh(N-1,1,k1*r2)-besselh(N+1,1,k1*r2));
Jk2r2 = besselj(n,k2*r2);
Jk1r2 = besselj(n,k1*r2);
Jk1r2N = besselj(N,k1*r2);
Jk1r1 = besselj(n,k1*r1);
Jk0r1 = besselj(n,k0*r1);
Jk1r1N = besselj(N,k1*r1);
dJk0r1 = .5*(besselj(n-1,k0*r1)-besselj(n+1,k0*r1));
dJk0r2 = .5*(besselj(n-1,k0*r2)-besselj(n+1,k0*r2));
dJk1r1 = .5*(besselj(n-1,k1*r1)-besselj(n+1,k1*r1));
dJk1r2 = .5*(besselj(n-1,k1*r2)-besselj(n+1,k1*r2));
dJk2r2 = .5*(besselj(n-1,k2*r2) - besselj(n+1,k2*r2));
dJk1r1N = .5*(besselj(N-1,k1*r1) - besselj(N+1,k1*r1));
dJk1r2N = .5*(besselj(N-1,k1*r2) - besselj(N+1,k1*r2));
Yk1r1 =bessely(n,k1*r1);
Yk1r2 =bessely(n,k1*r2);
Yk1r2N =bessely(N,k1*r2);
Yk1r1N =bessely(N,k1*r1);
dYk1r1 = .5*(bessely(n-1,k1*r1)-bessely(n+1,k1*r1));
dYk1r2 = .5*(bessely(n-1,k1*r2)-bessely(n+1,k1*r2));
dYk1r1N = .5*(bessely(N-1,k1*r1)-bessely(N+1,k1*r1));
dYk1r2N = .5*(bessely(N-1,k1*r2)-bessely(N+1,k1*r2));
A_r(cntn) = -((1i)^n) * dJk0r2/dH1k0r2;

%Global Matrix 4X4
AM1my =[-H1k0r1 Jk1r1N Yk1r1N 0;...
    (-1/z0)*dH1k0r1 (1/zr)*dJk1r1N (1/zr)*dYk1r1N 0;...
    0 Jk1r2N Yk1r2N -Jk2r2;...
    0 (1/zr)*dJk1r2N (1/zr)*dYk1r2N (-1/z2)*dJk2r2];
AM2my =[P_0*Jk0r1;(1/z0)*P_0*dJk0r1;0;0];
Bmy = AM1my\AM2my;
An(cntn) = Bmy(1);
C1n = Bmy(2);
D1n = Bmy(3);
C2n = Bmy(4);
```

```

%Matricant solution
options = odeset('RelTol',1e-10,'AbsTol',[1e-5 1e-5 1e-5 1e-5]);
[R1,M1] = ode45(@Matrivary_polar1, [r2 r1], [1 0 0 1], options);
ZM1 = [M1(end,1) M1(end,2);M1(end,3) M1(end,4)];
zin = [Jk2r2;(r2/(1i*z2))*dJk2r2];
Zb = ZM1*zin;
Zb = r1*Zb(1)/Zb(2);
Anm(cntn) = P_0*(Jk0r1 - (Zb/(1i*z0))*dJk0r1) / ((Zb/(1i*z0))*dH1k0r1 - H1k0r1);

if n==0
ftA_r(1:size(theta,1),1:size(theta,2),cntn)= exp(-1i*pi/4)*sqrt(2/pi).*(A_r(cntn));
ftAn(1:size(theta,1),1:size(theta,2),cntn)= exp(-1i*pi/4)*sqrt(2/pi).*(An(cntn));
else
ftA_r(1:size(theta,1),1:size(theta,2),cntn) = 2*exp(-1i*n*pi/2)*exp(-1i*pi/4)*sqrt(2/pi).*(A_r(cntn)).*cos(n.*theta);
ftAn(1:size(theta,1),1:size(theta,2),cntn) = 2*exp(-1i*n*pi/2)*exp(-1i*pi/4)*sqrt(2/pi).*(An(cntn)).*cos(n.*theta);
end
cntn=cntn+1;
end
end
ftA_rsum = sum(ftA_r,3);
subplot(2,1,1)
polar(theta,abs(ftA_rsum(:,:,1)).^2)
ftAnsum = sum(ftAn,3);
subplot(2,1,2)
polar(theta,abs(ftAnsum(:,:,1).^2))
sum_A_r = sum(abs(A_r).^2)
sum_Anm=sum(abs(Anm).^2)
sum_An =sum(abs(An).^2)
```

Matlab Code: D.7: Function used for code D.6

```
function dM1 = Matrivary_polar1(r,M1)
```

```
global w n C_1 pr1
Q = (1i*w/r)*[0 pr1;(((r^2)*C_1)-((n^2)/((w^2)*(pr1^(-1))))) 0];
dM1 = zeros(4,1);
dM1(1) = Q(1,2)*M1(3);
dM1(2) = Q(1,2)*M1(4);
dM1(3) = Q(2,1)*M1(1);
dM1(4) = Q(2,1)*M1(2);
```

D.4 Reference codes for chapter 7

Matlab Code: D.8: Code used in reference to section 7.5.1 to construct figures from chapter 7.

```
clear;clc;clf;
tic
global w n Ksub psub lam mu rvs
reso = 500;
r=[100 1 2/100]; r(3)=2/r(1);
S=[1 ; 10; .01];
p=r;
C = S./r' ;
rr = [ (r(2)+r(3))/(1+r(2)*r(3)) (r(3)+r(1))/(1+r(3)*r(1)) (r(1)+r(2))/(1+r(1)*r(2))];
M = inv( [ones(1,3) ;r ;1./r] );
eb = M(:,1); rb = M(:,2); rb1 = M(:,3);
al = C'*eb; b1 = C'*rb; b2 = C'*rb1; b = b1+b2;
lam = S(1)*(1-r(2))*(1-r(3)) / (r(1)-r(2))/(r(1)-r(3)) ...
      +S(2)*(1-r(3))*(1-r(1)) / (r(2)-r(3))/(r(2)-r(1)) ...
      +S(3)*(1-r(1))*(1-r(2)) / (r(3)-r(1))/(r(3)-r(2)) ;
mu = ( S(1)*(r(2)^2-r(3)^2)/rr(1) + S(2)*(r(3)^2-r(1)^2)/rr(2) +S(3)*(r(1)^2-r(2)^2)/rr(3) ) ...
/ ( S(1)*(r(2)^2-r(3)^2) + S(2)*(r(3)^2-r(1)^2) +S(3)*(r(1)^2-r(2)^2) ) ;
phir2 = rr(2)/(r(1)^2-r(3)^2)*[ r(1)*(1-r(3)^2); 0; r(3)*(r(1)^2-1) ];
R0 = ( (lam-1)*(1/rr(2)-mu)/(1-1/rr(2)) )^( 1/(2*(1-mu)) ) + eps;
r0 = R0/sqrt( lam*(1/rr(2)-mu)/(1-mu) ) + eps;
r0a = 1-0.5/S(2); R0a = sqrt( S(3)+S(1)/r(1)^2);
r0, (r0a-r0), R0, R0a/R0
```

```
rbar = (1-R0^2 + (lam-1)/mu*(1-R0^(2*mu)) )/(1-r0^2 )/lam ;
rbara = (1-R0^(2*mu))/mu;
mu2 = 1+ (r(1)-1)*(1-r(3))*(r(1)-r(3))*S(2)/ ( (1-r(3)^2)*S(1)+(r(1)^2 -1)*S(3) -(r(1)^2 -r(3)^2)*S(2) ) ;
R0r0= ( (1-r(3)^2)*S(1)+(r(1)^2 -1)*S(3) )/ (r(1)^2 -r(3)^2);
R02 = ( ( S(2)-1)/( S(2)/R0r0 -1) )^( 1/2/(1-mu));
r02 = R02/sqrt( R0r0 );
Rv = linspace(1,R0,reso);
rv = sqrt( (Rv.^2 + (lam-1)*Rv.^(2*mu) )/lam );
rrv = al./( (Rv./rv).^2 - b);
phi1 = eb*ones(size(rrv))+ (rb+rb1)*rrv;
phi1=phi1(:,1:size(phi1,2)-1);
phi111 = phi1(1,:);
phi222 = phi1(2,:);
phi333 = phi1(3,:);
r = rv;
rvss=linspace(1,r0,reso);
for i=1:reso
    rvs=rvss(i);
x00 = 1.5;           % Make a starting guess at the solution
options=optimset('TolFun',1e-12,'MaxIter',1000);   % Option to display output
[rfv,fval] = fzero(@asdf,[0 1.1]);  % Call optimizer
rfvs(i)=rfv;
fvals(i)=fval;
end
plot(rvss,rfvs,rv,Rv);legend('Rfsolvs','R')
Rv=rfvs;
rv=rvss;
r=rv;
rrv = al./( (rfvs./rvss).^2 - b);
phi = eb*ones(size(rrv))+ (rb+rb1)*rrv;
phi=phi(:,1:size(phi,2));
phi11 = phi(1,:);
phi22 = phi(2,:);
phi33 = phi(3,:);
[x,y] = meshgrid([-4:.05:4]);
```

```
[theta,rad] = cart2pol(x,y);
p0=1; %%MOST OUTER PROPERTIES BACKGROUND
c0=1;
w=3/r(end);
P_0=1;
R2 = 1;
R1 = r(end)
fend=Rv(end)
pin = 10000;%%% MOST inner cylinder properties.
cin=10000;
k0=w/c0;
z0 = p0*c0;
ka=k0*R1
siz=5+ka;
layers = size(phi11,2)
rz=r;
r(1)=R2;
rho(1) = p(1);
c(1) = sqrt(S(1)^-1);
cnt=2;
for n=1:layers-1
    drz(n)=pi*((rz(n)^2)-rz(n+1)^2);
    r(cnt) = sqrt(r(cnt-1)^2 -(drz(n)*phi11(n)/pi));
    rho(cnt) = p(2);
    c(cnt) = sqrt(S(2)^-1);
    r(cnt+1) = sqrt(r(cnt)^2 -(drz(n)*phi22(n)/pi));
    rho(cnt+1) = p(3);
    c(cnt+1) = sqrt(S(3)^-1);
    r(cnt+2) = sqrt(r(cnt+1)^2 -(drz(n)*phi33(n)/pi));
    rho(cnt+2) = p(1);
    c(cnt+2) = sqrt(S(1)^-1);
    cnt=cnt+3;
end
rho(end)=pin;  %%% MOST inner cylinder properties.
c(end)=cin;
k = w./c;
K = rho.*c.^2;
```

```
z=rho.*c;
cnt = 1;
for n = 0:siz
    %GLOBAL MATRIX
    Hk0r1 = besselh(n,1,k0*r(1));
    Jk1r1 = besselj(n,k(1)*r(1));
    Yk1r1 = bessely(n,k(1)*r(1));
    GM(1,:) = [Hk0r1 -Jk1r1 -Yk1r1];
    dHk0r1 = .5*((besselh(n-1,1,k0*r(1))-besselh(n+1,1,k0*r(1))));
    dJk1r1 = .5*(besselj(n-1,k(1)*r(1))-besselj(n+1,k(1)*r(1)));
    dYk1r1 = .5*(bessely(n-1,k(1)*r(1))-bessely(n+1,k(1)*r(1)));
    GM(2,:) = [-(z0^-1)*dHk0r1 (z(1)^-1)*(dJk1r1) (z(1)^-1)*(dYk1r1)];
    for m = 1:size(r,2)-2
            Jkrn = besselj(n,k(m)*r(m+1));
            Ykrn = bessely(n,k(m)*r(m+1));
            Jkrn1 = -besselj(n,k(m+1)*r(m+1));
            Ykrn1 = -bessely(n,k(m+1)*r(m+1));
            dJkrn = .5*(besselj(n-1,k(m)*r(m+1))-besselj(n+1,k(m)*r(m+1)))
                ;
            dYkrn = .5*(bessely(n-1,k(m)*r(m+1))-bessely(n+1,k(m)*r(m+1)))
                ;
            dJkrn1 = -.5*(besselj(n-1,k(m+1)*r(m+1))-besselj(n+1,k(m+1)*r(
                m+1)));
            dYkrn1 = -.5*(bessely(n-1,k(m+1)*r(m+1))-bessely(n+1,k(m+1)*r(
                m+1)));
            b = 2*m;
            GM(b+1,b:b+3)=[Jkrn Ykrn Jkrn1 Ykrn1];
            GM(b+2,b:b+3)=[(z(m)^-1)*dJkrn (z(m)^-1)*dYkrn (z(m+1)^-1)*
                dJkrn1 (z(m+1)^-1)*dYkrn1];
    end
    m=size(r,2)-1;
            Jkrn = besselj(n,k(m)*r(m+1));
            Ykrn = bessely(n,k(m)*r(m+1));
            Jkrn1 = -besselj(n,k(m+1)*r(m+1));
            Ykrn1 = -bessely(n,k(m+1)*r(m+1));
            dJkrn = .5*(besselj(n-1,k(m)*r(m+1))-besselj(n+1,k(m)*r(m+1)))
                ;
```

```
            dYkrn = .5*(bessely(n-1,k(m)*r(m+1))-bessely(n+1,k(m)*r(m+1)));
            dJkrn1 = .5*(besselj(n-1,k(m+1)*r(m+1))-besselj(n+1,k(m+1)*r(m+1)));
            dYkrn1 = .5*(bessely(n-1,k(m+1)*r(m+1))-bessely(n+1,k(m+1)*r(m+1)));
            b = 2*m;
            GM(b+1,b:b+2)=[Jkrn Ykrn Jkrn1];
            GM(b+2,b:b+2)=[-(z(m)^-1)*dJkrn -(z(m)^-1)*dYkrn (z(m+1)^-1)*dJkrn1];
            vec = zeros(2*(size(r,2)),1);
            vec(1) = -P_0*besselj(n,k0*r(1));
            vec(2) = (z0^-1)*P_0*.5*(besselj(n-1,k0*r(1))-besselj(n+1,k0*r(1)));
            Coef=GM\vec;
            Angm(cnt)=Coef(1);
            if n==0
                Pout(:,:,cnt) = (Angm(cnt)*besselh(n,1,k0.*rad));
            else
                Pout(:,:,cnt) = (1i^n)*2*cos(n*theta).*((Angm(cnt)*besselh(n,1,k0.*rad)));
            end
            GMs{cnt}=GM;
            Coefs{cnt}=Coef;
clear GM

%MATRICANT
H1k0sumr = besselh(n,1,k0*R2);
dH1k0sumr = .5*(besselh(n-1,1,k0*R2)-besselh(n+1,1,k0*R2));
Jk1r1 = besselj(n,k(end)*R1);
Jk0sumr = besselj(n,k0*R2);
dJk0sumr = .5*(besselj(n-1,k0*R2)-besselj(n+1,k0*R2));
dJk1r1 = .5*(besselj(n-1,k(end)*R1)-besselj(n+1,k(end)*R1));
M = eye(2);
for jk = 1:size(r,2)-1
        psub=rho((end)-jk);
        Ksub=K((end)-jk);
```

```
options = odeset('RelTol',1e-10,'AbsTol',[1e-5 1e-5 1e-5 1e-5]);
[R12,M1] = ode45(@Matrivary_polar1, [r((end)-jk+1) r((end)-jk)], [1 0 0
    1], options);
ZM1 = [M1(end,1) M1(end,2);M1(end,3) M1(end,4)];
M = ZM1*M;
end
zin = [Jk1r1;(r(end)/(1i*z(end)))*dJk1r1];
Zb = M*zin;
Zb = R2*Zb(1)/Zb(2);
Anm(cnt) = P_0*(Jk0sumr - (Zb/(1i*z0))*dJk0sumr) / ((Zb/(1i*z0))*dH1k0sumr
    - H1k0sumr);
if n==0
Poutm(:,:,cnt) = (Anm(cnt)*besselh(n,1,k0.*rad));
else
Poutm(:,:,cnt) = (1i^n)*2*cos(n*theta).*((Anm(cnt)*besselh(n,1,k0.*rad)));
end
cnt=cnt+1;
end
 global prv pthetv Kv
 K=Cstar.^-1;
 pr=pr11;
 r=rz;
 k1=w/cin;
 z1 = cin*pin;
 cnt = 1;
 for n = 0:siz

%MATRICANT RADIAL
 H1k0sumr = besselh(n,1,k0*R2);
 dH1k0sumr = .5*(besselh(n-1,1,k0*R2)-besselh(n+1,1,k0*R2));
 Jk1r1 = besselj(n,k1*R1);
 Jk0sumr = besselj(n,k0*R2);
 dJk0sumr = .5*(besselj(n-1,k0*R2)-besselj(n+1,k0*R2));
 dJk1r1 = .5*(besselj(n-1,k1*R1)-besselj(n+1,k1*R1));
 M = eye(2);
 for jk = 1:size(r,2)-1
      prv=pr(end-jk);
```

```
        pthetv=pthet(end-jk);
        Kv = K(end-jk);
  options = odeset('RelTol',1e-10,'AbsTol',[1e-5 1e-5 1e-5 1e-5]);
  [R12,M1] = ode45(@Matricant_pr_pthet, [r((end)-jk+1) r((end)-jk)], [1 0 0
      1], options);
 ZM1 = [M1(end,1) M1(end,2);M1(end,3) M1(end,4)];
 M = ZM1*M;
 end
 zin = [Jk1r1;(1/(1i*z1))*dJk1r1];
 Zb = M*zin;
 Zb = Zb(1)/Zb(2);
 Anmpr(cnt) = P_0*(Jk0sumr - (Zb/(1i*z0))*dJk0sumr) / ((Zb/(1i*z0))*
     dH1k0sumr - H1k0sumr);
 if n==0
 Poutmpr(:,:,cnt) = (Anmpr(cnt)*besselh(n,1,k0.*rad));
 else
 Poutmpr(:,:,cnt) = (1i^n)*2*cos(n*theta).*((Anmpr(cnt)*besselh(n,1,k0.*
     rad)));
 end
 cnt=cnt+1;
 end
toc

%COMPARISON WITH SINGLE CYLINDER WITHOUT ANY CLOAKING.
k1 = w/c(end);
z1=rho(end)*c(end);
cnt = 1;
for n = 0:siz;
H1k0 = besselh(n,1,k0*R1);
dH1k0 = .5*(besselh(n-1,1,k0*R1)-besselh(n+1,1,k0*R1));
Jk1 = besselj(n,k1*R1);
Jk0 = besselj(n,k0*R1);
dJk0 = .5*(besselj(n-1,k0*R1)-besselj(n+1,k0*R1));
dJk1 = .5*(besselj(n-1,k1*R1)-besselj(n+1,k1*R1));
An(cnt) = ((1i^n)*Jk0/H1k0)*((dJk1/(z1*Jk1)) - (dJk0/(z0*Jk0)))/((dH1k0/(
    z0*H1k0)) - (dJk1/(z1*Jk1)));
if n==0
```

```
    Pout(:,:,cnt) = (An(cnt)*besselh(n,1,k0.*rad));
else
    Pout(:,:,cnt) = (1i^n)*2*cos(n*theta).*(An(cnt)*besselh(n,1,k0.*rad));
end
    cnt=cnt+1;
end
toc
Pot = sum((Pout),3);
Pot=Pot + P_0*exp(1i.*k0.*rad.*cos(theta));
Potm = sum((Poutm),3);
Potm=Potm + P_0*exp(1i.*k0.*rad.*cos(theta));
[row_ot,col_ot] = find(x.^2+y.^2 <= (R2^2));
[row_otin,col_otin] = find(x.^2+y.^2 <= (R1^2));
for j = 1:size(row_otin,1)
    Pot(row_otin(j),col_otin(j))=0;
end
for j = 1:size(row_ot,1)
    Potm(row_ot(j),col_ot(j))=0;
end
hold on;
j=sqrt(-2);
df=360;
for i=1:df
    circle1(i)=R2*exp(2*j*i*pi/df);
end
for i=1:df
    circle2(i)=R1*exp(2*j*i*pi/df);
end
maxed=abs(max(max([max(max(Pot)),max(max(Potm))])));
mini=(min(min([min(min(Pot)),min(min(Potm))])));
mini=mini-1;
contourf(x,y,real(Potm));
caxis manual
caxis([mini maxed]);
colorbar;
hold on
radius = R2*2;
```

```
w123 = radius;
h123 = radius;
x123 = -R2;
y123 = -R2;
rectangle('Position',[x123,y123,w123,h123],'Curvature',[1,1],'FaceColor'
    ,[1,1,1])
radius = R1*2;
w123 = radius;
h123 = radius;
x123 = -R1;
y123 = -R1;
rectangle('Position',[x123,y123,w123,h123],'Curvature',[1,1],'FaceColor'
    ,[0,0,0])
axis('equal')
```

Matlab Code: D.9: Function used for code D.6

```
function dM1 = Matrivary_polar1(R,M1)
global w n Ksub psub
Q = (1i*w/R)*[0 psub;(((R^2)/Ksub)-((n^2)/((w^2)*psub))) 0];
dM1 = zeros(4,1);
dM1(1) = Q(1,2)*M1(3);
dM1(2) = Q(1,2)*M1(4);
dM1(3) = Q(2,1)*M1(1);
dM1(4) = Q(2,1)*M1(2);
```

Matlab Code: D.10: Function used for code D.6

```
function dM1 = Matricant_pr_pthet(R,M1)
global w n Kv prv pthetv
Q = [0 1i*w*prv;...
    (1i*w/Kv)-(1i*n^2)/(w*pthetv*R^2) -1/R];
dM1 = zeros(4,1);
dM1(1) = Q(1,2)*M1(3);
dM1(2) = Q(1,2)*M1(4);
dM1(3) = Q(2,1)*M1(1) + Q(2,2)*M1(3);
dM1(4) = Q(2,1)*M1(2) + Q(2,2)*M1(4);
```

References

[1] D. Schurig J.B. Pendry and D.R. Smith. Controlling electromagnetic fields. *Science*, 312:1780, 2006.

[2] M. Lassas A. Greenleaf and G. Uhlman. Anisotropic conductivities that cannot be detected by eit. *Physiol. Meas.*, 24:413, 2003.

[3] D.A. Roberts S.A. Cummer M. Rahm, D. Schurig and D.R. Smith. Design of electromagnetic cloaks and concentrators using form-invariant coordinate transformations of maxwells equations. *Photon. Nanostruct.: Fundam. Appl.*, 6:87–95, 2008.

[4] D. Schurig J.B. Pendry M. Rahm, S.A. Cummer and D.R. Smith. Optical design of reflectionless complex media by finite embedded coordinate transformations. *Phys. Rev. Lett.*, 100:063903, 2008.

[5] S.A. Cummer and D. Schurig. One path to acoustic cloaking. *New J. Phys.*, 9(3):45, 2007.

[6] B.J. Justice S.A. Cummer J.B. Pendry A.F. Starr D. Schurig, J.J. Mock and D.R. Smith. Metamaterial electromagnetic cloak at microwave frequencies. *Science*, 314:977–980, 2006.

[7] M. Briane G.W. Milton and J.R. Willis. On cloaking for elasticity and physical equations with a transformation invariant form. *New J. Phys.*, 8:248, 2006.

[8] J.R. Willis. The non-local influence of density variations in a composite. *Int. J. Solids Struct.*, 21:80517, 1985.

[9] A.N. Norris. Acoustic cloaking theory. *Proc. R. Soc. A*, 464:2411–2434, 2008.

[10] D. Torrent and J. Sánchez-Dehesa. Acoustic cloaking in two dimensions: a feasible approach. *New J. Phys.*, 10(6):063015, 2008.

[11] J.E. Boisvert C.L. Scandrett and T.R. Howarth. Acoustic cloaking using layered pentamode materials. *J. Acoust. Soc. Am.*, 127(5):2856–2864, 2010.

[12] A.N. Norris and A.J. Nagy. Acoustic metafluids made from three acoustic fluids. *J. Acoust. Soc. Am.*, 128(4):1606–1616, 2010.

[13] J. Jin. *Theory and Computation of Electromagnetic Fields*. John Wiley & Sons, Inc, New Jersey, 2010.

[14] M.D. Greenberg. *Advanced Engineering Mathematics (Second Edition)*. Prentice Hall, New Jersey, 1998.

[15] Abramowitz and Stegun. *Handbook of Mathematical Functions*. U.S. Government Printing Office, Washington D.C., 1972.

[16] L.E. Kinsler. *Fundamentals of Acoustics*. John Wiley & Sons, Inc, New York, 2000.

[17] M.C. Pease. *Methods of Matrix Algebra*. Academic Press, New York, 1965.

[18] Fran Ihlenburg. *Finite Element Analysis of Acoustic Scattering*. Springer-Verlag, Inc, New York, 1998.

[19] J.J. Faran. Sound scattering by solid cylinders and spheres. *J. Acoust. Soc. Am.*, 23(4):405–418, 1951.

[20] A.N. Norris and A.L. Shuvalov. Wave impedance matrices for cylindrically anisotropic radially inhomogeneous elastic solids. *Q J Mechanics Appl Math.*, 63 (4):401–435, 2010.

[21] A.N. Norris. Acoustic metafluids. *J. Acoust. Soc. Am.*, 125(2):839–849, 2009.

[22] M. Schoenberg and P.N. Sen. Properties of a periodically stratified acoustic half-space and its relation to a Biot fluid. *Acoust. Soc. Am.*, 73(1):61–67, 1983.

Vita

Adam J. Nagy

2001-05 Bridgewater Raritan High School, Bridgewater, New Jersey

2005-09 B. Sc. in Mechanical & Aerospace Engineering, Rutgers University

2009 J. J. Slade Scholar.

2010 Presentation:"Radiation reduction using layers of three fluids", Acoustical Society of America, 159^{th} Meeting, Baltimore, April.

2010 PASS, Physical Acoustics Summer School, Student, Sunrise Springs, La Cienega, New Mexico, May.

2010 Presentation: "Acoustic metafluids made from three acoustic fluids. (Acoustic Inertial Cloaks)", Rutgers School of Engineering, Mechanical and Aerospace, October.

2009-2010 Graduate assistant, Department of Mechanical & Aerospace Engineering, Rutgers University